

**Mitochondrial genome assembly and population genetics of the
common smoothhound shark, *Mustelus mustelus***

by

Kelvin Lloyd Hull

*Thesis presented in partial fulfilment of the requirements for the degree of Master of Science in the
Faculty of Natural Science at Stellenbosch University*



UNIVERSITEIT
iYUNIVESITHI
STELLENBOSCH
UNIVERSITY

Supervisor: Dr A.E. Bester van-der Merwe

Department of Genetics
1918 - 2018

December 2018

Declaration

By submitting this thesis electronically, I declare that the entirety of the work contained therein is my own, original work, that I am the sole author thereof (save to the extent explicitly otherwise stated), that reproduction and publication thereof by Stellenbosch University will not infringe any third-party rights and that I have not previously in its entirety or in part submitted it for obtaining any qualification.

Date: **December 2018**

Summary

Knowledge of evolutionary history and population genetic structuring in economically important marine species are integral factors for a more comprehensive fisheries management approach in order to preserve regional and global biodiversity. The common smoothhound, *Mustelus mustelus*, is a vulnerable species of shark overexploited by numerous fisheries across its wide-spread distribution range, from the Mediterranean Sea and north-east Atlantic to the south-west Indian Ocean. Although previous studies have assessed the genetic diversity and population structure along the South African coast, genetic resources are scarce, and little is known about the genetic variation across its wider distribution. This study aimed to assemble and annotate the complete mitochondrial genome of the species from available next-generation sequencing data, and assess historical and contemporary patterns of genetic diversity and population structure across three ocean basins, using a 571 bp fragment of the non-coding mitochondrial control region (mtCR) and nine species-specific microsatellite markers. The complete mitogenome of *M. mustelus* and the phylogenetic reconstruction of two other mitogenomes for the genus illustrated a closer relationship with the placental *M. griseus*, and validated the previously hypothesised correlation of reproductive mode with the phylogenetic placement within the *Mustelus* genus. Furthermore, the mtCR displayed higher levels of variability in comparison to other species assessed in the Carcharhiniformes order, and was therefore considered a suitable marker to be utilised in conjunction with nuclear markers to assess intraspecific patterns of diversity and structure on a global scale. Overall, *M. mustelus* was characterised by low to moderate genetic diversity ($h = 0.867$; $\pi = 0.00437$; $A_R = 2.5$, $H_E = 0.375$), with the Mediterranean populations appearing to exhibit the lowest mitochondrial diversity ($h = 0.443$; $\pi = 0.00083$), while the southern north-east Atlantic populations displayed the lowest nuclear diversity ($A_R = 2.6$, $H_E = 0.325$). For the mtCR sequences, a total of 18 haplotypes, and two main haplogroups representing the northern and southern hemispheres, were identified (mean $h = 0.861$;

mean $\pi = 0.0042$), with a high degree of population divergence ($\Phi_{ST} = 0.658$, $P < 0.01$). The microsatellite analyses including F-statistics (F_{ST} : 0.070 – 0.556, $P < 0.01$), multivariate and Bayesian clustering confirmed genetic differentiation between the three ocean regions investigated, with finer-scale population structure in each ocean basin. No correlation between genetic and geographical distance was observed ($R^2 = 0.0034$, $P = 0.415$), however this was most likely due to the inclusion of island populations and a stepping stone model of connectivity between collections. In conclusion, a cautious approach to the management of the species should be taken, as some regions appear to have a degree of connectivity despite being significantly differentiated. In areas with limited fisheries data, finer-scale analyses should be performed in order to develop a more comprehensive management strategy to conserve this threatened species.

Opsomming

Kennis van die evolusionêre geskiedenis en populasie genetiese struktuur van ekonomiese belangrike mariene spesies is belangrike faktore vir 'n meer omvattende benadering tot visserybestuur met die doel om plaaslike en globale biodiversiteit te behou. Die hondhaai, *Mustelus mustelus*, is 'n kwesbare haai spesie wat oorbenut word deur baie visserye oor hul verspreidingsgebied wat strek vanaf die Mediterreense See en die noordoostelike Atlantiese Oseaan tot die suidwes Indiese Oseaan. Alhoewel vorige studies die genetiese diversiteit en populasie struktuur langs die Suid-Afrikaanse kus ondersoek het is genetiese hulpbronne skaars vir hierdie spesie, en min inligting is beskikbaar rakende die genetiese variasie vir *M. mustelus*. Hierdie studie het daarom gepoog om beskikbare hoëdeurset volgordebepalings data te gebruik om die volledige mitokondriale genoom van die spesie te bepaal en te annoteer. Historiese en hedendaagse patrone van genetiese diversiteit en populasie struktuur oor drie oseaanbekkens was geëvalueer, met die gebruik van 'n 571 bp fragment van die nie-koderende mitokondriale beheerstreek (mtBS) en nege spesies-spesifieke mikrosatelliet merkers. Die volledige mitogeenom van *M. mustelus* en die filogenetiese rekonstruksie met twee ander mitogeenome vir die genus het 'n nader verwantskap met die plasentale *M. griseus* geïllustreer en die vorige hipotetiese korrelasie van reprodutiewe modus met die filogenetiese plasing binne die *Mustelus* genus bevestig. Die mtBS het hoër vlakke van variasie in die Carcharhiniformes orde vertoon, en is daarom beskou as 'n geskikte merker om gebruik te word in samewerking met nukleêre merkers om intraspesifieke patrone van diversiteit en struktuur op 'n wêreldwye skaal te evalueer. 'n Lae tot matige genetiese diversiteit ($h = 0.867$; $\pi = 0.00437$; $A_R = 2.5$, $H_E = 0.375$) was waargeneem, met die Mediterreense populasies met die laagste mitokondriale diversiteit ($h = 0.443$; $\pi = 0.00083$), terwyl die suidelike noordoostelike Atlantiese populasies die laagste nukleêre diversiteit ($A_R = 2.6$, $H_E = 0.325$) gehad het. Die mtBS belyning het bestaan uit 'n totaal van 18 haplotipes en twee kern haplogroepe, wat die noordelike en suidelike hemisfeer respektiewelik verteenwoordig (gemiddelde

$h = 0.861$; gemiddelde $\pi = 0.0042$), met 'n hoë graad van populasie differensiasie ($\Phi_{ST} = 0.658$, $P < 0.01$). Die mikrosatelliet analyses wat F-statistieke (F_{ST} : 0.070 - 0.556, $P < 0.01$), multivariate en Bayesiese groepering ingesluit het, het bevestig dat genetiese differensiasie tussen die drie oseaan gebiede bestaan, met fyner populasie struktuur in elke oseaanbekken. Geen korrelasie tussen genetiese en geografiese afstand was waargeneem nie ($R^2 = 0.0034$, $P = 0.415$), maar dit was waarskynlik as gevolg van die eiland populasies wat ingesluit was en 'n “stepping-stone” model van konnektiwiteit tussen die steekproef populasies. 'n Versigtige benadering vir die bestuur van die spesie moet aangewend word, aangesien sommige gebiede gedeeltelik verbind is, alhoewel daar 'n aansienlike hoeveelheid differensiasie is. In gebiede met beperkte vissery data moet fyner skaal studies uitgevoer word om 'n meer omvattende bestuurstrategie te ontwikkel met die doel om hierdie bedreigde spesies te bewaar.

Acknowledgements

I wish to express my gratitude to the following institutions for their financial and travel support during my MSc studies; the National Research Foundation of South Africa, Stellenbosch University, and the Department of Genetics. I would like to thank all collaborators, both domestic and international, for their contributions to the project, including Charlene da Silva (Department of Agriculture, Forestry and Fisheries, Republic of South Africa), Matthew Dicken (KwaZulu-Natal Sharks Board, South Africa), Ana Veríssimo (Research Center for Biodiversity and Genetic Resources, Portugal), Edward Farrell (University College Dublin, Ireland), Stefano Mariani (University of Salford, England), Carlotta Mazzoldi, Ilaria Marino and Lorenzo Zane (University of Padova, Italy). The staff at the Central Analytical Facility (CAF) at Stellenbosch University should also be commended for the vital work they conduct for the Department of Genetics.

To my supervisor, Dr Aletta Bester-van der Merwe, I wish to thank you for your mentorship, guidance, and the trust you placed in me. Your direct input in driving my tertiary education has allowed me to grow as a young researcher, and the countless opportunities you gave me to become independent are invaluable. I would also like to extend my appreciation and gratitude to the Molecular Breeding and Biodiversity (MBB) research group, particularly Ms Jessica Vervalle, Dr Clint Rhode, Dr Barbara van Asch and Professor Rouvay Roodt-Wilding, for providing countless pieces of advice throughout the duration of my project. Furthermore, I would like to thank Dr Simo Maduna, for helping to shape me into the scientist I am today. Finally, without the love and support of my friends and family, especially my partner Marissa Brink, I doubt this thesis would have come to fruition, and for that, I thank you.

Preface

Scientific contributions during Masters degree (2017 – 2018):

1. Published or submitted papers directly emanating from the work presented in this thesis:

Hull KL, Maduna SN, Bester-van der Merwe AE. (2018) Characterization of the complete mitochondrial genome of the common smoothhound shark, *Mustelus mustelus* (Carcharhiniformes: Triakidae). Mitochondrial DNA Part B **3**: 964–965.

Hull KL, Asbury TA, da Silva C, Dicken M, Verissimo A, Farrell ED, Mariani S, Mazzoldi C, Marino IAM, Zane L, Maduna SN, Bester-van der Merwe AE. Strong genetic isolation despite wide distribution in a commercially exploited coastal shark. Hydrobiologia (submitted 27 October 2018).

2. Submitted papers with indirect relevance to the work presented in this thesis:

Maduna SN, **Hull KL** Wintner S, Mariani S, da Silva C, Farrell ED, Mazzoldi C, Zane L, Bester-van der Merwe AE, Verissimo A, Boomer J, Marino IAM, Chesalin M, Gubili C. (in review) Phylogeny, character evolution and statistical historical biogeography of *Mustelus* Linck, 1790 (Chondrichthyes: Triakidae) with reference to species from southern Africa. Molecular Phylogenetics and Evolution.

Contributions: Provided data and contributed to the preparation of the manuscript.

3. Local conference presentations:

Hull KL*, Maduna SN, da Silva C, Dicken M, Marino IAM, Zane L, Bester-van der Merwe AE. Oral presentation: Global population structure and mitogenome assembly of the common smoothhound shark, *Mustelus mustelus*. Southern African Shark and Ray Symposium. September 2017. Hermanus, South Africa: 15.

(*Presenting author)

4. *International conference presentations:*

Hull KL*, Asbury TA, Maduna SN, da Silva C, Dicken M, Veríssimo A, Marino IAM, Zane L, Bester-van der Merwe AE. Oral presentation: Global population structure of the common smoothhound, *Mustelus mustelus*: Implications for conservation and fisheries management. Sharks International. July 2018. João Pessoa, Brazil: 1.

(*Presenting author)

Table of contents

Declaration	i
Summary	ii
Opsomming	iv
Acknowledgements.....	vi
Preface	vii
1. Published or submitted papers directly emanating from the work presented in this thesis	vii
2. Submitted papers with indirect relevance to the work presented in this thesis.....	vii
3. Local conference presentations	vii
4. International conference presentations	viii
Table of contents	ix
List of figures.....	xiv
List of tables	xvii
List of abbreviations	xx
Literature review, research aims and objectives, and thesis outline	1
1.1 Elasmobranchs: An overview of one of the oldest extant vertebrates in the world, with focus on the common smoothhound shark, <i>Mustelus mustelus</i>	1
1.2 Is the elasmobranch fishing industry sustainable?.....	6
1.2.1 History of the global elasmobranch fishing industry.....	6
1.2.2 Mediterranean fishing industry	7

1.2.3	West African fishing industry	9
1.2.4	Southern African fishing industry	11
1.3	Molecular resources and applications in population genetic studies of elasmobranchs	14
1.3.1	Mitochondrial DNA.....	15
1.3.2	Microsatellite markers	16
1.4	Implementation of molecular markers for genetic assessment of elasmobranch species	18
1.4.1	Species identification and phenotypic plasticity	18
1.4.2	The stock problem: what and where are they?	19
1.4.3	Site specificity and philopatric behaviour.....	22
1.5	Aims and objectives	23
Characterisation of the complete mitochondrial genome of the common smoothhound shark, <i>Mustelus mustelus</i>, and its phylogenetic placement among the main orders of modern sharks		
	25
	Abstract	25
2.1	Introduction	26
2.2	Materials and methods	28
2.2.1	Sample collection, DNA extraction and next-generation sequencing data preparation ..	28
2.2.2	Isolation of mitochondrial sequences, mitogenome assembly and annotation	28
2.2.3	Phylogenomic placement of <i>Mustelus mustelus</i>	29
2.2.4	Sequence variation within the Carcharhiniformes order	29
2.3	Results	30
2.4	Discussion	36

2.5	Conclusion.....	38
Population structure of the common smoothhound shark, <i>Mustelus mustelus</i>, based on mtDNA sequence data 39		
	Abstract	39
3.1	Introduction	40
3.2	Materials and methods	42
3.2.1	Sample collection and DNA extraction	42
3.2.2	Mitochondrial control region amplification and genetic diversity analyses	44
3.2.3	Phylogenetic analysis.....	45
3.2.4	Spatial patterns of population divergence.....	45
3.2.5	Historical demographic analysis	46
3.3	Results	46
3.3.1	Global genetic diversity	46
3.3.2	Phylogenetic placement of <i>Mustelus mustelus</i> haplotypes	52
3.3.3	Population divergence.....	55
3.3.4	Demographic analyses of global <i>Mustelus mustelus</i> sampling population.....	57
3.4	Discussion	59
3.4.1	Genetic diversity.....	59
3.4.2	Patterns of genetic divergence.....	60
3.4.3	Historical demography.....	64
3.5	Conclusions	64

Contemporary population structure and demographics of <i>Mustelus mustelus</i> inferred from nuclear markers	66
Abstract	66
4.1 Introduction	67
4.2 Materials and methods	69
4.2.1 Sample collection and DNA extraction	69
4.2.2 Microsatellite amplification	71
4.2.3 Genetic diversity analyses.....	71
4.2.4 Genetic structuring analyses	72
4.2.5 Demographic analyses	73
4.3 Results	74
4.3.1 Global genetic diversity	74
4.3.2 Spatial patterns of genetic differentiation	77
4.3.3 Demographic assessment of <i>Mustelus mustelus</i>	84
4.4 Discussion	89
4.4.1 Genetic composition of <i>Mustelus mustelus</i> : cause for concern?	89
4.4.2 Inter-oceanic population stratification of <i>Mustelus mustelus</i>	90
4.4.3 Demography of <i>Mustelus mustelus</i>	93
4.5 Conclusion.....	95
Concluding remarks and future perspectives	97
5.1 Introduction	97
5.2 Summary of research results	98

5.3	Limitations and future prospects	101
5.4	Final remarks	103
	References	105
	Appendix A Supplementary information for Chapter II	129
	Appendix B Supplementary Information for Chapter III.....	131
	Appendix C Supplementary information for Chapter IV	133
	Appendix D Published papers	138

List of figures

Figure 1.1 Graphical representation of several anatomical features of <i>Mustelus mustelus</i> . Adapted from Shark Trust (https://www.sharktrust.org/en/factsheets).	4
Figure 1.2 Distribution range of <i>Mustelus mustelus</i> . Adapted from the IUCN Red List of Threatened Species (http://www.iucnredlist.org/details/links/39358/0).	4
Figure 1.3 Map of the Mediterranean Sea, with the Strait of Gibraltar and entrance to the sea encircled in red.	8
Figure 1.4 Graphical representation of Sub-Regional Fisheries Commission (SRFC) established area of competence and member countries along the coast of west Africa. Adapted from www.fao.org/fishery/rfb/srhc	10
Figure 1.5 Map of South Africa, with circles indicating the fishing locations where elasmobranchs are harvested. Adapted from da Silva <i>et al.</i> (2015).	13
Figure 1.6 Traditionally recognised marine biogeographic barriers: EPB – Eastern Pacific Barrier; IPB – Isthmus of Panama Barrier; AB – Amazon Barrier; MAB – Mid-Atlantic Barrier; BB – Benguela Barrier; OWB – Old World Barrier; SSB – Sunda Shelf Barrier.	21
Figure 2.1 Graphical representation of the complete mitochondrion of the common smoothhound, <i>Mustelus mustelus</i>	33
Figure 2.2 Phylogenetic relationships between the eight orders of modern sharks constructed using Bayesian Inference from 31 whole mitogenome sequences, with the thorny skate (<i>Raja radiata</i>) mitogenome included as an outgroup. Numbers at nodes indicate posterior probabilities. Genbank accession numbers are given adjacent to the species name, and scale bar indicates groupings of species into orders.	34
Figure 2.3 Sequence comparison of coding and non-coding regions of the mitochondrial genome of <i>Mustelus mustelus</i> to six species of the Carcharhiniformes order, in decreasing order of sequence	

similarity. Yellow bars – rRNA genes; blue bars – protein-coding genes; orange bar – control region.	
.....	35
Figure 3.1 Global sampling sites of <i>Mustelus mustelus</i> in the Mediterranean (circles), southern north-east Atlantic (diamonds) and south-east Atlantic/south-west Indian Oceans (triangles) populations, with sample size (<i>n</i>) and oceans indicated. MS – Mediterranean Sea; SNEAO – southern north-east Atlantic Ocean; SEAO – south-east Atlantic Ocean; SWIO – south-west Indian Ocean.....	43
Figure 3.2 Median Joining haplotype network based on mitochondrial control region sequence data for global sampling populations of <i>Mustelus mustelus</i> , with mutations separating haplotypes indicated as slashes.	51
Figure 3.3 Bayesian Inference (BI) tree based on global sampling populations of <i>Mustelus mustelus</i> , with numbers on the tree indicating posterior probability. Red branches indicate haplotypes from the Mediterranean (MED), blue branches indicate haplotypes from north-east Atlantic (NEA), and green branches indicate haplotypes from south-east Atlantic/south-west Indian (SAI) populations.	53
Figure 3.4 Maximum Likelihood (a) and Maximum Parsimony (b) phylogenies of global sampling populations of <i>Mustelus mustelus</i> based on a 571 bp fragment of the mitochondrial DNA control region. Both methods employed the Hasegawa, Kishino and Yano model of nucleotide substitution model with a number of invariable sites (HKY+I) to allow for non-uniformity of rates among sites. The reliability of the trees was tested using bootstrap analysis with 1,000 replicates (bootstrap values given at branching points).	54
Figure 3.5 Isolation by distance assessment of global <i>Mustelus mustelus</i> sampling populations, (a) including all sampling populations, and (b) excluding island locations.	57
Figure 4.1 Global sampling sites of the common smoothhound in the Mediterranean (circles), southern north-east Atlantic (diamonds) and south-east Atlantic/south-west Indian Oceans (triangles) populations, with sample size and oceans indicated. MS – Mediterranean Sea; SNEAO – southern north-east Atlantic Ocean; SEAO – south-east Atlantic Ocean; SWIO – south-west Indian Ocean.	70

Figure 4.2 Graphical representation of mean genetic diversity estimates for each sampling population using nine microsatellite loci. A_N = number of alleles; A_R = allelic richness (rarefied); I = Shannon-Weaver Information Content; A_P = private alleles; H_E = expected heterozygosity.....	77
Figure 4.3 Isolation by distance (IBD) scatter plots using geographic distance in 1,000 km and genetic distance measured by linearised pairwise F_{ST} estimates, with (a) all sampling populations and (b) excluding island populations.	80
Figure 4.4 Discriminant Analysis of Principal Components (DAPC) analysis of global <i>Mustelus mustelus</i> populations. (a) Inference of the number of genetic clusters based on BIC statistic. (b) Assignment of individuals from their respective populations to genetic clusters, with the size of the square correlated to number of individuals assigned to a cluster. (c) Scatterplot illustrating clustering patterns on a global scale, with the colour and shape of each data point representing a genetic cluster as defined in (b).	82
Figure 4.5 Genetic structure of <i>Mustelus mustelus</i> based on Bayesian clustering analyses for $K = 3$ to $K = 7$, using six analytical methods [(a) $K = 3$ – Delta K (Evanno <i>et al.</i> 2005); (b) $K = 5$ – <i>MedMedK</i> , <i>MedMeaK</i> ; (c) $K = 6$ – <i>MaxMedK</i> , <i>MaxMeaK</i> (Puechmaille 2016); (d) $K = 7$ – $\text{Ln Pr}(X K)$ (Evanno <i>et al.</i> 2005)].	83

List of tables

Table 1.1 Fisheries catch for Sub-Regional Fisheries Commission (SRFC) countries from 2003 to 2006. Adapted from Diop and Dossa (2011).....	11
Table 2.1 List of mitochondrial genomes utilised in the current study, separated into the eight higher orders of modern sharks.	31
Table 3.1 Polymorphic nucleotide positions in <i>Mustelus mustelus</i> mtCR haplotypes. A dot indicates that the base at that position is the same as the base in haplotype 1.....	48
Table 3.2 Geographic distributions of <i>Mustelus mustelus</i> haplotypes and the number of individuals from each sampling location	49
Table 3.3 Genetic diversity indices for <i>Mustelus mustelus</i> based on a 571 bp fragment of the mitochondrial control region. N – sample size; H – number of haplotypes; h – haplotype diversity; π – nucleotide diversity, k – average number of nucleotide changes.	50
Table 3.4 Genetic differentiation between eight sampling populations of <i>Mustelus mustelus</i> based on the mitochondrial control region. Φ_{ST} estimates below the diagonal, P -values above the diagonal..	55
Table 3.5 Hierarchical analysis of molecular variance (AMOVA) for different grouping hypotheses of <i>Mustelus mustelus</i> based on separate sampling populations and broad oceanic regions.....	56
Table 3.6 Demographic analysis parameters for mtCR sequences for global sampling populations and oceanic regions of <i>Mustelus mustelus</i>	58
Table 4.1 Genetic diversity indices for global sampling populations of <i>Mustelus mustelus</i> based on nine microsatellite loci. n – sample size; A_N – mean number of alleles per locus; A_R – allelic richness; H_E – expected heterozygosity; F_{IS} – inbreeding coefficient.....	76
Table 4.2 Genetic differentiation estimates for global sampling locations of <i>Mustelus mustelus</i> . F_{ST} estimates below the diagonal, corresponding P values above the diagonal.....	79

Table 4.3 Hierarchical analysis of molecular variance (AMOVA) results for different structuring hypotheses of <i>Mustelus mustelus</i> based on separate sampling populations and different ocean basins.	81
Table 4.4 Bottleneck test (Wilcoxon) of global <i>Mustelus mustelus</i> sampling populations under three mutational models; infinite allele model (IAM), two-phase model (TPM), and stepwise mutational model (SMM).	85
Table 4.5 Log Bayes Factor (LBF) using thermodynamic integration of different gene flow models <i>Mi</i> compared with Model 1 for three sampling regions of <i>Mustelus mustelus</i> within the Mediterranean Sea (A: Adriatic Sea; S: Strait of Sicily; B: Balearic Islands); p_{Mi} - model choice probability; $\ln L$ - log marginal likelihood.	86
Table 4.6 Log Bayes Factor (LBF) using thermodynamic integration of different gene flow models <i>Mi</i> compared with Model 3 for three sampling populations of <i>Mustelus mustelus</i> within the southern north-east Atlantic Ocean (V: Cape Verde; B: Guinea Bissau; C: Guinea); p_{Mi} – model choice probability; $\ln L$ – log marginal likelihood.	87
Table 4.7 Log Bayes Factor (LBF) using thermodynamic integration of different gene flow models <i>Mi</i> compared with Model 1 for two sampling populations of <i>Mustelus mustelus</i> within the south-east Atlantic/south-west Indian oceans (A: Angola; S: South Africa); p_{Mi} – model choice probability; $\ln L$ – log marginal likelihood.	88
Table S2.1 BLAST results for <i>Mustelus mustelus</i> sequence comparison of mitochondrial regions with six species within the Carcharhiniformes order.....	129
Table S3.1 Mean pairwise genetic distance between global sampling populations of <i>Mustelus mustelus</i>	131
Table S3.2 Pairwise D_{est} estimates between global sampling populations of <i>Mustelus mustelus</i> . D_{est} values below the diagonal, corresponding P -value above the diagonal	131

Table S3.3 Genetic differentiation between sampling populations grouped into broad oceanic regions. Φ_{ST} estimates below the diagonal, P -values above the diagonal. MED – Mediterranean Sea; SNEA – southern north-east Atlantic; SAI – south-east Atlantic/south-west Indian	132
Table S4.1 Multiplex assay characterisation. MP – multiplex number; SSR – repeat motif; T_A – annealing temperature.	133
Table S4.2 Genetic diversity indices per microsatellite marker for <i>Mustelus mustelus</i> sampling populations at eight collection sites along its global distribution: polymorphic information content (PIC); average number of alleles (A_N); effective number of alleles (A_E); Shannon’s information index (I); observed heterozygosity (H_O); fixation index (F) and null allele frequencies ($Fr_{(Null)}$), as well as the standard error (SE) for each mean estimate. An asterisk (*) indicates deviation from Hardy-Weinberg equilibrium ($P < 0.01$).....	134
Table S4.3 Pairwise F_{ST} estimates between oceanic regions. F_{ST} estimates below diagonal, corresponding P value above diagonal. MED – Mediterranean Sea; SNEA – southern north-east Atlantic; SAI – south-east Atlantic/south-west Indian.	137

List of abbreviations

%	Percentage
<	Less than
>	Greater than
®	Registered Trademark
\$	United States Dollar
µl	Micro-litre
µM	Micro-mole
3'	Three prime
5'	Five prime
A	Adenine
Accession No.	GenBank Accession Number at www.ncbi.nlm.nih.gov
A_E	Effective number of alleles
AFLP	Amplified Fragment Length Polymorphism
AMOVA	Analysis of Molecular Variance
A_N	Number of alleles
AN	Angola population
A_R	Allelic richness
AS	Adriatic Sea population
ATP	Adenosine triphosphate
B-H	Benjamini-Hochberg correction

BI	Balearic Island population
BLAST	Basic Local Alignment Search Tool
bp	Base pair
°C	Degrees Celsius
C	Cytosine
CI	Confidence Interval
cm	Centimetre
<i>COI</i>	<i>Cytochrome c Oxidase subunit I</i>
CTAB	Cetyltrimethylammonium Bromide $[(C_{16}H_{33})N(CH_3)_3Br]$
<i>Cytb</i>	<i>Cytochrome b</i>
CV	Cape Verde population
DAFF	Republic of South Africa Department of Agriculture, Forestry and Fisheries
DAPC	Discriminant Analysis of Principal Components
ddH ₂ O	Distilled deionised water
DNA	Deoxyribonucleic Acid
dNTP	Deoxyribonucleotide Triphosphate
E	East
ESU	Evolutionary Significant Unit
FAM	Blue (R100); 5-carboxyfluorescein (ABI-fluorescent label)
F_{CT}	Derivative of Wright's Fixation Index adapted for hierarchical AMOVA (group of populations relative to the total population)

F_{IS}	Wright's Fixation Index (individual relative to the sub-population, equal to the inbreeding coefficient)
$Fr_{(NULL)}$	Null allele frequency
F_{SC}	Derivative of Wright's Fixation Index adapted for hierarchical AMOVA (sub-population relative to the group of populations)
F_{ST}	Wright's Fixation Index (subpopulation relative to total population)
G	Guanine
GB	Guinea Bissau population
GC	Guinea population
H	Number of haplotypes
h	Haplotype diversity
H_O	Observed heterozygosity
H_E	Expected heterozygosity
H_R	Harpending's raggedness index
I	Shannon's information index
IAM	Infinite Allele Model
IBD	Isolation by Distance
IUCN	International Union for the Conservation of Nature
K	Number of genetic clusters
k	Average number of nucleotide changes
km	Kilometers
LD	Linkage Disequilibrium
LMPA	Langebaan Marine Protected Area
L_T	Total length
M	Molar (Moles per litre)
m	Meters

MED	Mediterranean Sea region
mg/ml	Milligram per millilitre
MgCl ₂	Magnesium Chloride
min	Minutes
ml	Millilitre
mM	Millimole
mm	Millimeter
MP	Multiplex
MPA	Marine Protected Area
mtCR	Mitochondrial control region
mtDNA	Mitochondrial DNA
MU	Management Unit
MYA	Million Years Ago
ng	Nanograms
<i>ND2</i>	<i>NADH dehydrogenase subunit 2</i>
<i>ND4</i>	<i>NADH dehydrogenase subunit 4</i>
NED	Yellow (Tamra) (ABI-fluorescent label)
NGS	Next-generation sequencing
PCR	Polymerase Chain Reaction
PET	Red (ABI-fluorescent label)
PIC	Polymorphism Information Content
<i>P</i> -value	Probability value (as a statistically significant threshold)
<i>RAG1</i>	<i>Recombination-activating gene 1</i>
rRNA	Ribosomal ribonucleic acid
S	South
SA	South Africa population

SAI	South-east Atlantic/south-west Indian oceanic region
SMM	Stepwise Mutation Model
SNP	Single Nucleotide Polymorphism
SNEA	Southern north-east Atlantic oceanic region
SS	Strait of Sicily population
SSD	Sum of squared deviations
SSG	IUCN Shark Specialist Group
SSR	Simple Sequence Repeat
STR	Short Tandem Repeat
T	Thymine
T _A	Annealing temperature
tRNA	Transfer ribonucleic acid
Taq	<i>Thermus aquaticus</i> DNA polymerase
™	Trademark
U	Units (enzyme)
VIC	Green (ABI-fluorescent label)
w/v	Weight per Volume

CHAPTER I

Literature review, research aims and objectives, and thesis outline

1.1 Elasmobranchs: An overview of one of the oldest extant vertebrates in the world, with focus on the common smoothhound shark, *Mustelus mustelus*

Chondrichthyes, the class that cartilaginous fish belong to, is divided into two subclasses, namely elasmobranchs and holocephalans. All modern sharks, rays and skates belong to the elasmobranch subclass, and are among the oldest extant vertebrate species on the planet, with the oldest jawed vertebrate fossil dating back 455 million years ago (MYA) to the Late Ordovician period (Arratia *et al.* 2005). The first fossil record of chondrichthyans finds its origin approximately 443 MYA in the early Silurian Period (Predtechenskyj and Karatajute-Talimaa 1995). There is some contention between sources regarding the first ‘true’ chondrichthyan fossil, however, findings in the last decade provided the universally accepted oldest chondrichthyan fossil, originating in the Early Devonian Period (~400 MYA) (Coates and Friedman 2010). However, these ancient chondrichthyans bear little resemblance to their descendants that currently inhabit the world’s oceans, and it was only through millennia of evolution that these prehistoric fish developed into the known apex predators today. These animals have survived five mass extinction events in the past 439 million years and morphological and molecular data suggests that the modern orders of elasmobranchs are a result of divergent events that occurred approximately 100 - 200 MYA (Kriwet *et al.* 2012).

Sharks play an integral role in sustaining the ecological balance in marine systems as keystone species. However, many species are experiencing declines in population numbers on a global scale due to anthropogenic effects, such as exploitation and degradation of marine and coastal habitats either through overfishing or pollution (Dulvy *et al.* 2014; Davidson *et al.* 2015). Population declines have an impact on lower trophic species, thereby altering the balance between species and overall biodiversity of the seas (Dudgeon *et al.* 2012). Species that are categorised by *r*-selected life history characteristics can recover from population declines due to their high fecundity. Conversely, most

sharks are characterised by *K*-selected like history traits, such as late maturity, slow growth and low reproductive outputs (Compagno 1984; Ebert *et al.* 2013) and the ability of these fish to recover from overexploitation is limited.

In recent years, these anthropogenic threats have garnered wide-spread concern, with the increasing impact of both direct and indirect human influences on marine diversity over the past 500 years being particularly noticeable (Jackson 2010). Jackson (2010) highlights similarities between past extinction events, such as climate change, ocean acidification, and global-scale loss of biodiversity, and present trends, with human impacts being the driving factor. Furthermore, a recent study by Dulvy *et al.* (2014) illustrates that the majority of our understanding of changes in marine biodiversity is limited to charismatic species, commercially important fisheries and coral reef systems. This ‘snapshot’ of marine biodiversity is impaired even further with studies under-representing the global effect of humans on marine ecosystems, with most of the inferences made originating from data-rich northern hemisphere seas (Worm *et al.* 2009). This results in a false perception regarding the state of global marine biodiversity, as areas in the southern hemisphere often lack data on marine diversity or clear management strategies for many species.

Sharks have been caught and consumed for centuries, mainly by artisanal fisheries. However, recent increases in demand have seen the emergence of a global market for shark related products. Currently, traditional Asian markets are supplied with shark fins from numerous sources on a global scale (Clarke *et al.* 2006). An increasing demand coupled with numerous anti-finning regulations, which intended to encourage the full utilisation of carcasses, has caused the market for shark meat to expand further (Clarke *et al.* 2007). Commercial fisheries that previously targeted more valuable line-fish species now consider sharks and other elasmobranchs as commercially viable, thus resulting in increased fishing pressure, often at unsustainable levels (Clarke *et al.* 2006, 2007). Not surprisingly, this has led to an increased risk of extinction for many elasmobranch species, with a recent assessment placing 18% of elasmobranch species as vulnerable, endangered, or critically endangered by the

International Union for the Conservation of Nature (IUCN) Shark Specialist Group (SSG) (Dulvy *et al.* 2014, 2017). The majority of these species are found along the coast, which exposes these species to a wider variety of fishing practices, including recreational and artisanal fisheries (Chapman *et al.* 2005; da Silva *et al.* 2013; Oliver *et al.* 2015). Therefore, it is important to assess these threatened fish, particularly those species that are considered “non-charismatic” or are under-studied, such as the common smoothhound, *Mustelus mustelus*.

Broadly, the *Mustelus* genus belongs to the order Carcharhiniformes (“ground sharks”) and the family Triakidae (houndsharks). As the nomenclature of the order suggests, houndsharks or smoothhounds are demersal sharks that commonly occur on the shelves and uppermost slopes of tropical and temperate continental seas, at depths ranging from 5 m to 1,463 m (Weigmann 2016). Smoothhounds are ecologically important meso-predators, and are often exposed to recreational, artisanal and commercial fishing practices (Heemstra 1997; Gardner and Ward 2002). The *Mustelus* genus currently comprises 27 extant species, which are globally distributed (Ebert *et al.* 2013; Weigmann 2016; Maduna and Bester-van der Merwe 2017).

In this study, the focus is on the common smoothhound, *Mustelus mustelus* (Linnaeus, 1758), a demersal species of shark that is slender bodied with flattened ventral surfaces on the head and body (Smale and Compagno 1997). Furthermore, they are grey to grey-brown in colour, mostly spotless, characterised by a short head and rounded snout, and possess teeth with low blunt cusps arranged in multi-serial rows (Compagno 1984; Smale and Compagno 1997) (**Figure 1.1**). This species occurs in warm and temperate coastal waters, and is distributed across the north-east Atlantic Ocean, the Mediterranean Sea, the south-east Atlantic Ocean, and the south-west Indian Ocean (**Figure 1.2**).

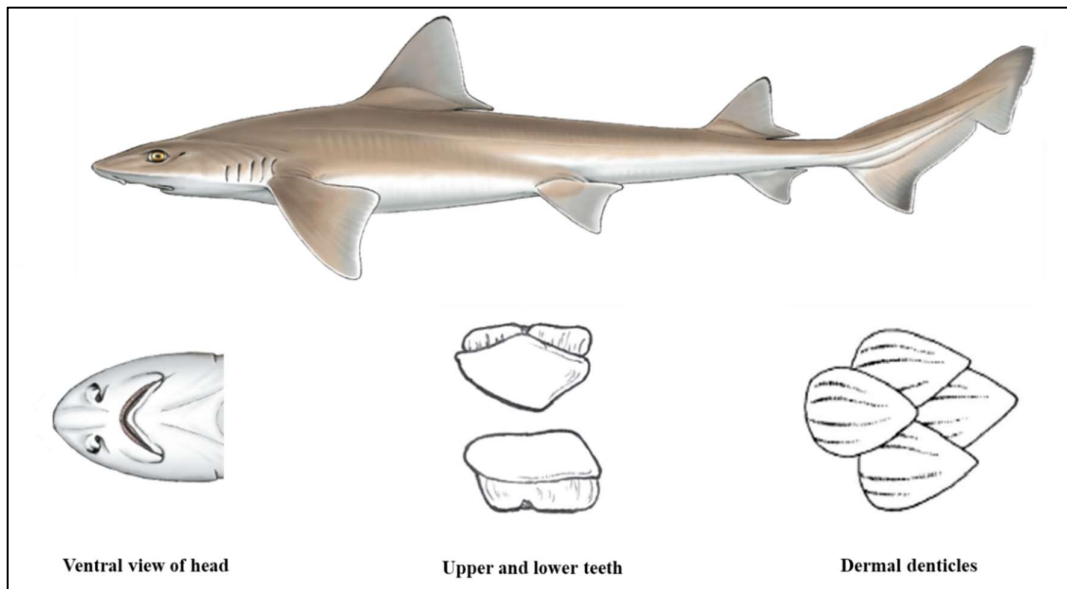


Figure 1.1 Graphical representation of several anatomical features of *Mustelus mustelus*. Adapted from Shark Trust (<https://www.sharktrust.org/en/factsheets>).



Figure 1.2 Distribution range of *Mustelus mustelus*. Adapted from the IUCN Red List of Threatened Species (<http://www.iucnredlist.org/details/links/39358/0>).

The common smoothhound ranges in size from 390 to 1,650 mm total length (L_T). Males are typically the smaller sex, ranging from ~391 – 1,450 mm, whereas females range from 390 – 1,650 mm (Smale and Compagno 1997; Saidi *et al.* 2008). The size at maturity also varies with gender, with males maturing between 950 – 1,300 mm and females maturing between 1,250 – 1,400 mm (Smale and Compagno 1997; Saidi *et al.* 2008). The lengthy maturation period, when coupled with a gestation period of 7 – 12 months (Smale and Compagno 1997; Saidi *et al.* 2008) and increasing fishing pressure limits the rate that these natural populations may grow over generations, making the species particularly vulnerable to exploitation (Stevens *et al.* 2000; Barker and Schluessel 2005; Dulvy *et al.* 2014). Additionally, a recent study illustrated that they exhibit a high degree of residency and site-fidelity within a small area (34 km²), with occasional movements into outlying areas, at least for Langebaan Lagoon on the west coast of South Africa (da Silva *et al.* 2013). Although this region falls within an area closed to fishing, similar residency in other regions close inshore make them vulnerable to fishing activities, and may have drastic effects on population recovery.

There is a need for sound conservation and management practices of coastal sharks in particular, as continued pressure from the fishery industry may cause irrevocable harm to many species. As such, *Mustelus mustelus* has been classified as Vulnerable by the IUCN Red List in 2009 (Serena *et al.* 2009), which warrants reassessments and improvements to current management strategies of this species as the classification nears the 10 year mark. In a regional context, a preliminary stock assessment of South African *M. mustelus* was completed last year, which was suggestive of a 50 – 60% probability that the stock is overfished (Charlene da Silva pers comms), again illustrating the need for reforms to current management practices for the species. However, to establish these management practices, fisheries data are required, which in many countries are currently unavailable (Velez-Zuazo *et al.* 2015). Furthermore, as many elasmobranch species (including *M. mustelus*) are widely distributed, the conservation of these fish is complicated by the movement potential of these animals, as they could potentially migrate through or out of a country's jurisdiction zone or management area. Although limited data are available regarding their migration range, it stands to

reason that different countries will utilise marine resources in alternate ways, and thus, it is crucial to understand the manner in which they are being exploited locally and internationally.

1.2 Is the elasmobranch fishing industry sustainable?

1.2.1 History of the global elasmobranch fishing industry

The technological advancements within the fishing industry during the 1920s saw an increased harvesting of elasmobranchs in general, with global catches reaching approximately 270,000 tons in the 1950s (Food and Agriculture Organisation, FAO 2005). This trend continued to increase over time, with the global elasmobranch catch tripling between 1950 and the end of the century, finally peaking at 893,000 tons in 2000 (FAO 2014). However, a downward trend has been observed since this time, with catches 15% lower at 766,000 tons in 2011 (FAO 2014). Most elasmobranch-based fisheries are characterised by two main phases, namely a historical overharvesting followed by stock declines with limited recovery (Bonfil 1994). However, there are cases of sustainable harvesting, especially where targeted species were resilient to fishing pressure or where timely management interventions were introduced (Stevens *et al.* 2000).

The management of chondrichthyans as a whole remains complex and has been plagued by negligent fishing practices or mismanagement of certain species. This can be attributed to three main factors. Firstly, as discussed previously, these fish are characterised by *K*-selected life-history traits (Cortés 2000; Frisk *et al.* 2001), which renders these species particularly vulnerable to overfishing. Secondly, the economic value of these animals is lower than teleost species, with an estimated global value of ~ US\$1 billion per year for elasmobranch fisheries, in comparison to teleost fisheries with an estimated US\$ 129.8 billion global value in 2012 (FAO 2014). This results in a lack of baseline landing and catch data necessary for basic resource assessments. Finally, accurate species identification protocols are not always in place, meaning that elasmobranch catch data are frequently

reported by family or by grouping of morphologically similar species, with only 20% of landed elasmobranch catches identified to the species level globally (FAO 2011).

All of the above-mentioned factors applies directly to the common smoothhound, *M. mustelus*. As the common smoothhound is one of the more widely distributed *Mustelus* species (Serena *et al.* 2009), the species is exposed to severe fishing pressure, from both target and non-target fisheries, driven by varying degrees of demand for shark related products (fins, meat, liver oil and cartilage) in different areas (da Silva and Bürgener 2007; Dulvy *et al.* 2014; Davidson *et al.* 2015). For this study, the fishing customs and pressure on *M. mustelus* within three broad oceanic regions will be discussed, namely the Mediterranean Sea (MED), the southern north-east Atlantic (SNEA) along the coast of west Africa, and finally the southern African coast, spanning the south-east Atlantic/south-west Indian Oceans (SAI).

1.2.2 Mediterranean fishing industry

The Mediterranean Sea covers an area of approximately 2,5 million km², with a coastline extending for 4,600 km, bordered by 21 countries (Zenetos *et al.* 2002). While it is termed a semi-enclosed sea, the chondrichthyan fauna found within the area is relatively diverse, hosting an estimated 80 species of chondrichthyan fish, comprised of 45 shark species from 17 families, 34 batoid species from nine families and one species of chimaera (Compagno 2001). However, evidence seems to suggest a general decline in abundance, diversity and range for many species (Walker *et al.* 2005; Cavanagh and Gibson 2007). Common factors that can be attributed to these declines are *K*-selected life-history traits, overfishing and pollution. Additionally, the semi-enclosed nature of the sea, with the only entrance and exit being located at the Strait of Gibraltar (**Figure 1.3**) means that the supplementation of marine populations from external sources will be limited, resulting in a further decrease in the recovery potential for most species.



Figure 1.3 Map of the Mediterranean Sea, with the Strait of Gibraltar and entrance to the sea encircled in red.

Commercially, chondrichthyans are less valuable than teleost fish and shellfish, representing 0.78% of the total landings in the Mediterranean Sea (FAO 2005). Between 1970 and 1985, landings of chondrichthyans increased from 10,000 tons to 25,000 tons. Thereafter, reported landings declined to 1,000 tons by 2004 (Cavanagh and Gibson 2007), although it remains unclear whether this can be attributed to improved management, decreased demands, or a lower overall abundance.

Benthic trawl efforts have increased in the shelf and slope area of the Mediterranean Sea over the past 50 years, as several demersal species are utilised commercially in countries such as Turkey, Tunisia, Greece, Italy and Spain (Walker *et al.* 2005). The species most commonly taken in coastal fisheries of these areas are: smoothhounds *Mustelus* spp., skates *Rajids*, catsharks *Scyliorhinus* spp., dogfish *Squalus* spp., eagle rays *Myliobatids*, and whiptail stingrays *Dasyatids* (Walker *et al.* 2005). However, as is true for many chondrichthyan fisheries, catch data are incomplete due to landings of various species with similar morphological features being reported under a single group. Although

directed fisheries have caused stock collapses for some species, more significant threats to elasmobranchs are mortality in mixed species fisheries and bycatch in fisheries targeting more valuable species (Bonfil 2005; Walker *et al.* 2005).

1.2.3 West African fishing industry

Records of shark fisheries in west African countries extend just about 30 years into the past, and are mainly limited to members of the Sub-Regional Fisheries Commission (SRFC) (Diop and Dossa 2011). The SRFC is a coalition of several countries including Cape Verde, Gambia, Guinea Bissau, Guinea, Mauritania, Senegal and Sierra Leone (**Figure 1.4**). Prior to the establishment of international markets for shark products, the degree to which sharks were harvested was at manageable levels, with shark catches only being used for local markets (Diop and Dossa 2011). However, during the 1970s, an export market was established in response to high demands for shark fins in Asian countries that offered lucrative means of employment for many, previously subsistence, fisheries (Ducrocq *et al.* 2005; Diop and Dossa 2011). Along the western coast of Africa, the shark trade originated in Gambia (Diop and Dossa 2011), with a rapid and consistent increase in fishing pressure, mainly in the form of artisanal fishing in the SRFC zone.

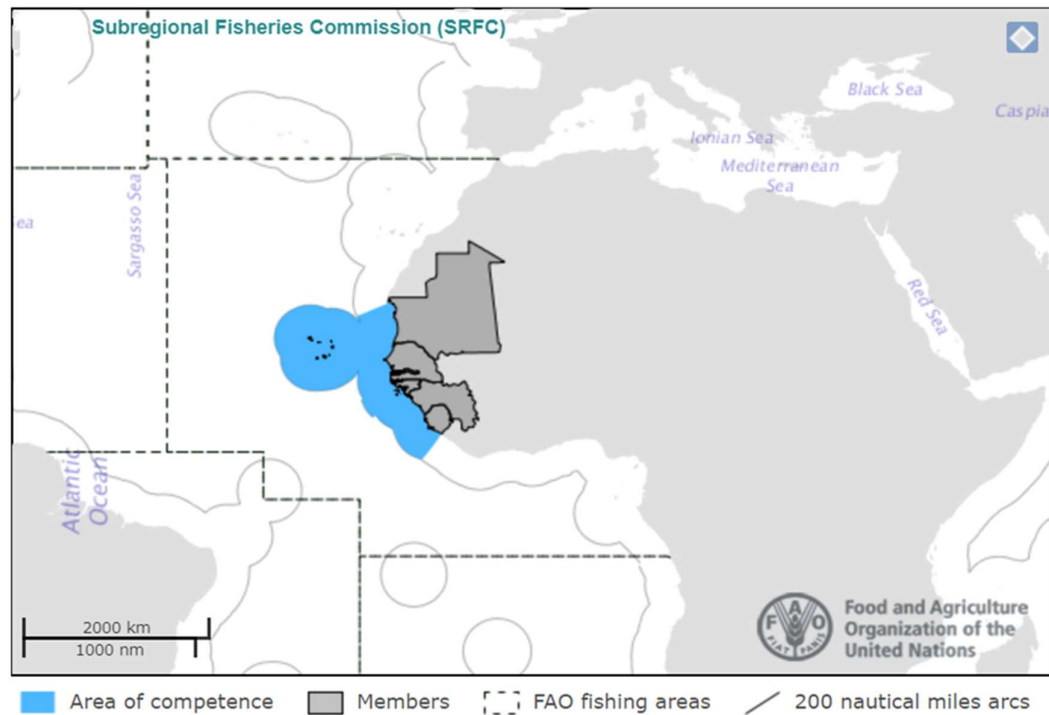


Figure 1.4 Graphical representation of Sub-Regional Fisheries Commission (SRFC) established area of competence and member countries along the coast of west Africa. Adapted from www.fao.org/fishery/rfb/srhc

However, this form of fishing resulted in lower yields, thus limiting the net profit that could be made from a single region. Therefore, many fisherman began to move seasonally towards other fishing zones (Diop and Dossa 2011), leading to unsustainable levels of harvesting of many species in the region. The seasonal migratory patterns of many shark species, either to breed or to locate other feeding sources, meant that if fishermen were to follow these migrations, eventual depletion of stocks will be inevitable. This led the SRFC member states to formalise and develop a management program within the sub-region, termed the Sub-Regional Plan of Action for the Conservation and Management of Sharks (SRPOA-Sharks). Subsequently, one of the main findings is the similar amounts of total catch for both artisanal and industrial fisheries (709,708 and 965,620 tons, respectively) (**Table 1.1**) in 2003 (Diop and Dossa 2011). This suggests that it is difficult to control the artisanal fishing sectors in these countries, with the catch of artisanal fisheries exceeding that of industrial fisheries in some

countries, possibly as it serves as a primary source of income for many households in the SRFC. More so, these figures do not give an indication as to the number of sharks caught in these areas, and chondrichthyan fishing records are difficult to find and validate due to frequent species misidentification or seafood mislabelling. A more recent study investigated the harvesting of sharks in the Bijagós Archipelago, off the coast of Guinea Bissau (Cross 2015). Out of the 9,214 kg of catch, elasmobranchs comprised 10% (Cross 2015). If this percentage of catch composition is comparable to the rest of the countries in the SRFC, that would result in approximately 167,500 tons total elasmobranch catch from 2003 to 2006. Without some form of intervention, this level of fishing and suboptimal management may lead to overexploitation of species and collapse of elasmobranch populations in the region.

Table 1.1 Fisheries catch for Sub-Regional Fisheries Commission (SRFC) countries from 2003 to 2006. Adapted from Diop and Dossa (2011).

Countries	Cape Verde	Gambia	Guinea	Guinea-Bissau	Mauritania	Senegal	Sierra Leone	Total
Sector	Catches (tons)							
Total artisanal fishing	4,200	30,000	57,000	26,306	89,700	385,902	116,600	709,708
Total industrial fishing	3,800	10,000	42,000	44,720	807,300	42,000	15,800	965,620
Total catch	8,000	40,000	99,000	71,026	897,000	427,902	132,400	1,675,328

1.2.4 Southern African fishing industry

The 1930s saw the beginning of commercial-scale exploitation of chondrichthyans in South Africa (von Bonde 1934). These fisheries targeted several species, most notably the tope shark, *Galeorhinus galeus*, which was fished heavily in the Western Cape. This industry was driven by the increased demand for natural sources of vitamin A, which was sourced from shark liver (van Zyl 1993). Although the synthesis of vitamin A in 1967 resulted in decreased demand for shark related products, catches of the tope shark were already declining by the late 1940s (Kroese and Sauer 1998). After many decades, renewed interest in sharks occurred and a shark-focused longline fishery was

established in 1992 (Kroeze and Sauer 1998). This fishery initially targeted demersal and pelagic sharks when further industrialisation and motorisation enabled fisheries to increase the range and duration to which fishermen could travel, shifting the focus to pelagic fishing. Annual landings have fluctuated severely since the fishery's establishment, due to both variations in demand and price (da Silva and Bürgener 2007).

Conforming to the global trend, research in South Africa has focused on the distribution, abundance and movement patterns of several charismatic, non-harvested species, such as the great white shark, *Carcharodon carcharias*, the bull shark, *Carcharhinus leucas*, and the ragged-tooth shark, *Carcharias taurus* (McCord and Lamberth 2009; Smale *et al.* 2012; Towner *et al.* 2013). A recent study by da Silva *et al.* (2015), which utilised catch data from a wide distribution of fishery locations (**Figure 1.5**), revealed that 99 of 204 chondrichthyan species that occur in southern African waters are regularly targeted or taken as bycatch. These species include the common smoothhound, *M. mustelus*; the white-spotted smoothhound, *M. palumbes*; the tope shark, *Galeorhinus galeus*; the copper shark, *Carcharhinus brachyurus*; the shortfin mako, *Isurus oxyrinchus*; and the blue shark, *Prionace glauca* (da Silva *et al.* 2015). Furthermore, total reported catch data for the years 2010, 2011 and 2012 was estimated to be 3,375 tons, 3,241 tons and 2,527 tons, respectively; two thirds of which was bycatch (da Silva *et al.* 2015). While this decline in total catch could be indicative of population declines due to overharvesting, it should be noted that when compared to most developing countries, South African shark fishing is relatively well controlled and managed (da Silva *et al.* 2015). Furthermore, the country designed and implemented shark-specific management actions, via the National Plan of Action for Sharks (NPOA-Sharks), which may have resulted in the declines in catch levels previously reported (Department of Agriculture, Forestry and Fisheries, DAFF 2013).

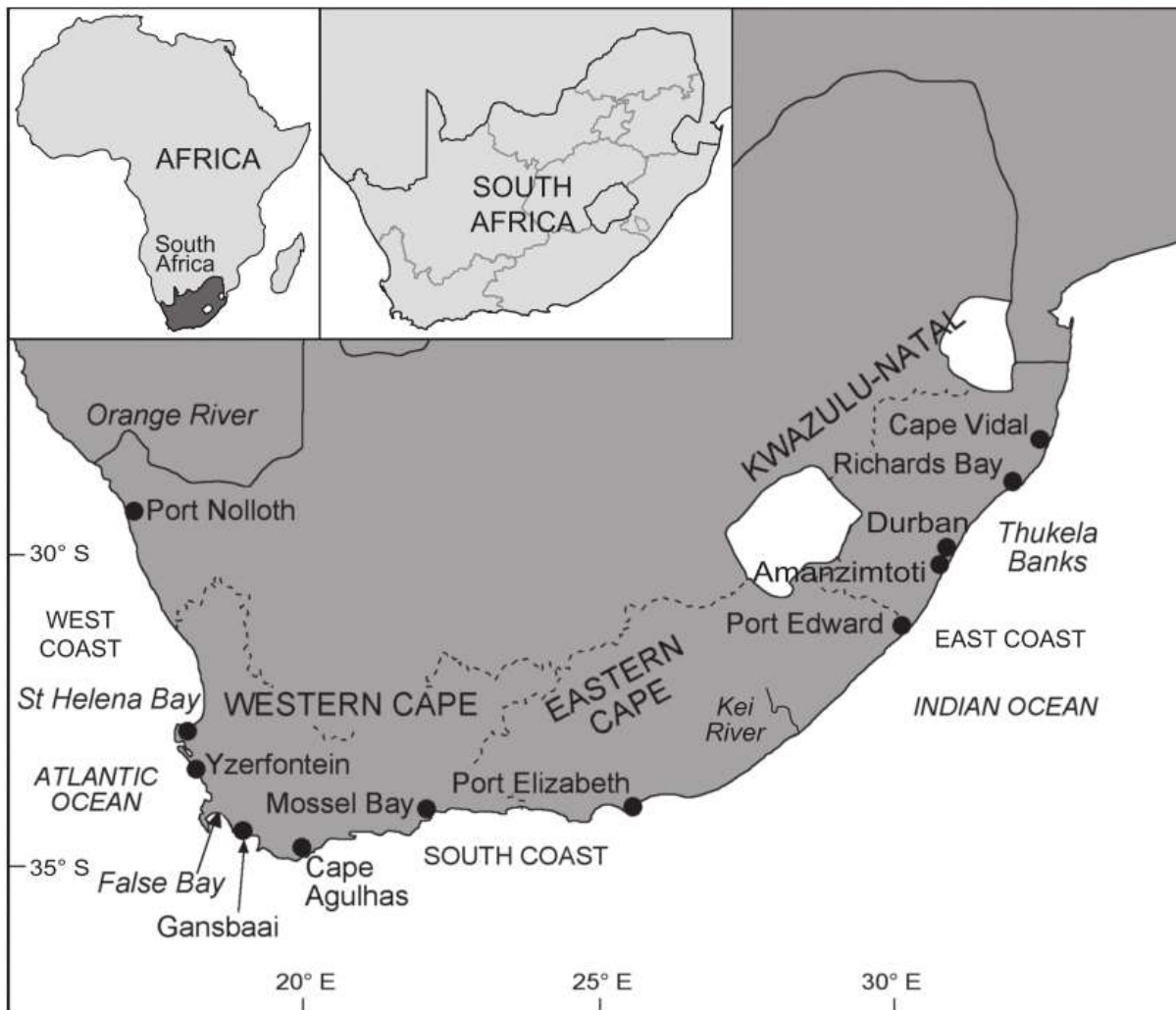


Figure 1.5 Map of South Africa, with circles indicating the fishing locations where elasmobranchs are harvested. Adapted from da Silva *et al.* (2015).

In contrast to the relatively well-managed industry in South Africa, Angolan fisheries are not nearly as well managed. In broad terms, the fishing industry can be separated into two main areas, namely the pelagic longline fisheries, and the artisanal line fisheries. Pelagic fisheries generally target tuna, swordfish and pelagic sharks, although it has been observed that foreign fishing vessels frequently operate in Angolan waters (Basson *et al.* 2007). These vessels do not report their catch to Angolan authorities, and Angolan fisheries are not required to report on bycatch levels, and thus no species-specific data exists for the region (Basson *et al.* 2007). Additionally, the subsistence artisanal fisheries that mainly target line fish such as grouper occasionally catch sharks, with sampling surveys

conducted in 2002 and 2003 identifying 6% of this incidental catch as houndsharks, although it was not possible to determine the catch rates of this fishery due to lack of data (Basson *et al.* 2007). To address this lack of information on Angolan catch data, the Angola Elasmobranch Project (<http://www.gulfelasmobranchproject.com/angola-project.html>) was launched in 2016 to assess the impact of artisanal fisheries on elasmobranch diversity in Angolan waters, although no data are currently available. Clearly, the fishing sector in Angola requires urgent attention, as the continued, undocumented nature in which species are targeted could have dire consequences to the diversity of the region.

1.3 Molecular resources and applications in population genetic studies of elasmobranchs

Various molecular markers and analytical methods have been used to study population dynamics amongst marine populations. The most commonly used markers include mitochondrial DNA (mtDNA) genes, microsatellite markers, amplified fragment length polymorphisms (AFLPs) and single nucleotide polymorphisms (SNPs). Marine species are frequently characterised by weak or low levels of population structure, due to the high dispersal ability aided by ocean currents that facilitate gene flow (Ovenden 2013). However, in the case of widely distributed species, physical distance and ocean currents between populations can serve as barriers to gene flow, resulting in significant population structuring (Ovenden 2013). Therefore, polymorphic DNA markers can provide fisheries researchers with new insights into the behaviour, ecology and genetic structure of fish populations, levels of inbreeding, and the intensity of natural and sexual selection (Ferguson and Danzmann 1998; Abdul-Muneer 2014).

A significant short-coming in many studies is the inferences made regarding genetic diversity and population structuring using a single marker type (Keeney *et al.* 2003; Benavides *et al.* 2011). This limits the depth to which many biological questions can be investigated, as different marker types behave in different ways in terms of mutation rate, inheritance patterns and sequence conservation

within and between taxa. It is also well known that the power to detect population stratification could vary between marker types. The use of SNPs in population genetic studies have increased in recent years, due to several technical advantages over the popular microsatellite markers (Morin *et al.* 2009). However, due to the bi-allelic nature of SNPs, substantially larger numbers of SNPs are needed to achieve the same statistical power of a smaller panel of microsatellite markers (Morin *et al.* 2009), which inflates the cost of the analyses performed.

Molecular markers can be divided into two categories: type I markers, which are markers associated with known genes or coding regions, and type II markers, which are situated within non-coding regions (O'Brien 1991). Type I markers are firstly not that polymorphic, as genic or coding regions are generally highly conserved, and secondly, usually in violation of several assumptions made by models utilised in population genetic analyses (O'Brien 1991). For instance, the Hardy-Weinberg model of genetic equilibrium assumes that there is no selection, which does not hold for coding regions. The genic region is transcribed for a specific protein with a designated function, and thus would be selected for and passed on to subsequent generations. This is not to say type I markers are not without merit, but their use in various analytical pipelines for population genetic inferences have limited functionality. Type II markers, on the other hand, are highly polymorphic and considered to be selectively neutral (generally) (O'Brien 1991). The type II markers most frequently used in population genetics are microsatellites, and due to the marker properties and inheritance patterns, this marker type is ideal for assessing both fine- and broad-scale contemporary population structure across many geographical ranges.

1.3.1 Mitochondrial DNA

Mitochondrial DNA (mtDNA) represents a small portion of organismal DNA, yet it has been extremely popular in the study of molecular diversity in animals for many years (Galtier *et al.* 2009). This can be attributed to the ease at which regions within mtDNA can be amplified, as numerous copies occur in a cell, and sequence variation accumulates faster in mtDNA than in nuclear DNA,

due to a faster mutation rate (Galtier *et al.* 2009). The mitochondrial genome of animals consists of 13 protein coding genes, 22 tRNA genes, 2 rRNA genes and a non-coding control region. This control region exhibits greater levels of variation in comparison to the coding genes, due to reduced functional constraints and relaxed selection pressure (Lui and Cordes 2004). Furthermore, the use of mtDNA is quite popular in studies aiming to differentiate between species using the barcoding gene, *cytochrome c oxidase subunit I (COI)* (Greig *et al.* 2001; Hebert *et al.* 2003; Ward *et al.* 2005), as well as to infer phylogeographic patterns and historical population structure (Keeney *et al.* 2003; Duncan *et al.* 2006; Kousteni *et al.* 2015). The disadvantages of mtDNA include back mutations, where positions that have undergone a mutation are returned to their original state through a subsequent substitution event; parallel substitution, where mutations occur at the same position in different lineages; and mutational hot spots, where some sites undergo mutation at a faster rate than other sites in the same region (Lui and Cordes 2004)

In recent years, and with the advancement of modern sequencing technologies, numerous studies have been conducted to assemble the complete mitochondrial genome of individual species, including elasmobranchs (Alam *et al.* 2014; Chang *et al.* 2015a, b; Chai *et al.* 2016; Kemper and Naylor 2016; Santaquiteria *et al.* 2017). The sequence data generated from these studies can be used to elucidate the evolutionary relationships between the orders of modern shark species, with a higher degree of statistical power as opposed to using a single gene or only a few genes.

1.3.2 Microsatellite markers

Microsatellites are also known as Short Tandem Repeats (STRs) (Edwards *et al.* 1991) or Simple Sequence Repeats (SSRs) (Tautz 1989). These markers are tandemly arrayed di-, tri-, or tetranucleotide repeat sequences, with repeat sizes ranging from 1 – 6 base pairs repeated numerous times, and are flanked by non-repetitive unique DNA sequences (Ellegren 2004). Microsatellites are incredibly useful for genetic diversity studies, due to their high polymorphism levels, high abundance throughout most genomes and prevalence throughout the entire genome of all organisms (Liu and

Cordes 2004; Hoffman and Nichols 2011). Microsatellite markers allow for the quantification of genetic diversity parameters, such as number of alleles (A_N), effective number of alleles (A_E), and observed and expected heterozygosities (H_O and H_E , respectively), which can be an indication of the genetic variability of a population, and once genotyped, can be used in the detection of population stratification, whilst models of gene flow can be assessed to determine migration rates between populations (Liu *et al.* 2005). Despite the advantages of this marker type, SSRs are prone to technical difficulties with genotyping, such as null alleles, allelic stuttering or dropout (Hoffman and Nichols 2011).

Furthermore, genotyping of non-model organisms, sharks in particular, has been achieved predominantly through the use of cross-species amplification of microsatellite markers (Morin *et al.* 2010; Seeb *et al.* 2011; Maduna *et al.* 2014; Marino *et al.* 2014). This can be attributed to the length-slippage mode of mutation of microsatellites (Dieringer and Schlötterer 2003), which means that microsatellite loci amplified in one species would almost always be polymorphic in another (Chen and Dorn 2010; Seeb *et al.* 2011), if amplification is successful. Furthermore, the success rate of the amplification of microsatellite markers is dependent on the evolutionary relationship between the target species and the species in which the markers were developed for. A recent study observed a higher cross-amplification success rate when markers (previously designed for species in the Triakidae family) were amplified in more closely related species than in distantly related taxa (Maduna *et al.* 2014).

The use of SSRs in genetic surveys has contributed to the knowledge of contemporary processes driving elasmobranch distribution patterns (Vignaud *et al.* 2013; Dudgeon and Ovenden 2015). This research enables the definition of reproductively isolated stocks, quantifying genetic diversity, and assessing demographic factors of populations, across smaller (Bitalo *et al.* 2015; Maduna *et al.* 2016) and larger geographic ranges (Karl *et al.* 2011; Verissimo *et al.* 2017).

1.4 Implementation of molecular markers for genetic assessment of elasmobranch species

While taxonomic assessments have been employed to manage a variety of fishery aspects, there is some concern as to only using phenotypic information for species identification in catch data and stock assessments. Genetic data may provide a more comprehensive picture regarding population dynamics of various species, and marrying stock assessments with molecular methods of assessing population genetic parameters could result in a more integrated approach to stock management. Furthermore, molecular methods of species assessment could in future prove to be faster than traditional methods of tracking species, such as telemetry or mark/recapture practices (Farrell *et al.* 2009; Marino *et al.* 2014; Maduna *et al.* 2017).

1.4.1 Species identification and phenotypic plasticity

Many houndshark species exhibit similar morphological characteristics that impede the identification of individuals to the species level (Heemstra 1997; López *et al.* 2006). This is compounded by overlapping distribution ranges of different species, as well as the method by which sharks are processed by fisheries (Marino *et al.* 2014). These methods involve the removal of the head and fins of the shark, which are the areas that possess the most distinct morphological features that allow for species differentiation. This means that one cannot rely solely on phenotypic methods of identification, but instead should place greater importance on the development of molecular means. A study on the Mediterranean houndsharks that aimed to differentiate between two houndsharks, *M. mustelus* and *M. punctulatus*, found that the amplification of a panel of microsatellite markers, and the subsequent identification of private alleles, allowed for the differentiation between the study species (Marino *et al.* 2014). Similarly, a study conducted on four houndshark species along the South African coast implemented a similar method, and successfully differentiated between the four species (Maduna *et al.* 2017). This lends credence to the inclusion of a microsatellite marker panel to

supplement existing species identification methods to successfully identify an individual shark to the species level, regardless of the degree to which the shark has been processed.

This ties in directly with the monitoring of trade of shark products in various markets. In a recent study that utilised DNA barcoding methods to investigate several Italian fish markets that sold *Mustelus* products, it was found that lucrative *Mustelus* species were substituted with less attractive species, such as the spiny dogfish, shortfin mako and blue shark in 77% of samples tested (Barbuto *et al.* 2010). On a regional scale, a 31% incidence of seafood mislabelling was found in South African commercial fish products using the *COI* barcoding gene, although this did not include shark related products (Cawthorn *et al.* 2012). This highlights the importance of molecular methods of species identification, both in the management of fisheries, and in the detection of seafood fraud.

1.4.2 *The stock problem: what and where are they?*

The goal of many population genetic studies centred on natural populations of fish is to identify and characterise ‘stocks’ to manage a species adequately i.e. to conserve diversity and sufficient individuals for the population to be self-sustaining in the long-term. However, the exact definition of what constitutes a marine stock is a multi-faceted concept, considering the biological, practical and political realms of interest in a particular species of fish (Carvalho and Hauser 1995). The most common definition is that a stock is a group of fish that are exploited in a specific area by a specific method (Smith 1990). While practical, this concept discounts several biological aspects that are integral for the continued management of a species, such as whether a stock consists of different species, are abundant in sufficient numbers to be self-sustaining, or whether this stock is spatially or temporally structured. Therefore, a more biological classification of groups of organisms can be defined, termed a genetic stock, which is a reproductively isolated unit with significant genetic differentiation from other stocks (Jamieson 1974; Ovenden 1990), and considers migrants between populations as significant events that can alter the genetic composition of a genetic stock. This concept feeds directly into the definition of two additional concepts, namely Evolutionary Significant

Units (ESUs) and Management Units (MUs). Evolutionary Significant Units are groups of historically-isolated populations that are characterised by unique lineages, and a specific potential to adapt to a particular area or environment (Moritz 1994; Funk *et al.* 2012). Evolutionary Significant Units can be viewed as long-term conservation units that are designated to conserve a species within a particular area. Finally, and perhaps a more short-term conservation goal, is the identification of MUs, which are considered as populations with statistically significant differences in allele frequencies at nuclear or mitochondrial loci (Moritz 1994).

In marine species, there are several factors that drive the genetic differentiation of populations from one another. This differentiation is a result of the interaction between evolutionary processes, life history characteristics of the species in question, and the oceanographic features of the areas they inhabit (Ovenden 2013). Therefore, the genetic structuring of natural populations can be assessed by comparing the genetic profiles of several spatially separated sampling locations across the distribution range of the species (Waples and Gaggiotti 2006; Dudgeon *et al.* 2012; Ovenden 2013), which allows for the evaluation of various hypotheses of population structure. For instance, isolation by distance (IBD) proposes that gene flow is likely to occur between populations in closer proximity than distant populations, although connectivity can occur between remote populations in a stepping stone fashion (Wright 1943). Alternatively, genetic discontinuity can result between adjacent populations if separated by a biogeographic barrier, with several studies showing that traditionally recognised oceanographic barriers (**Figure 1.6**) effect gene flow and population connectivity in marine species, and therefore impact phylogeographic patterns of a species (Keeney and Heist 2006; Schultz *et al.* 2008).

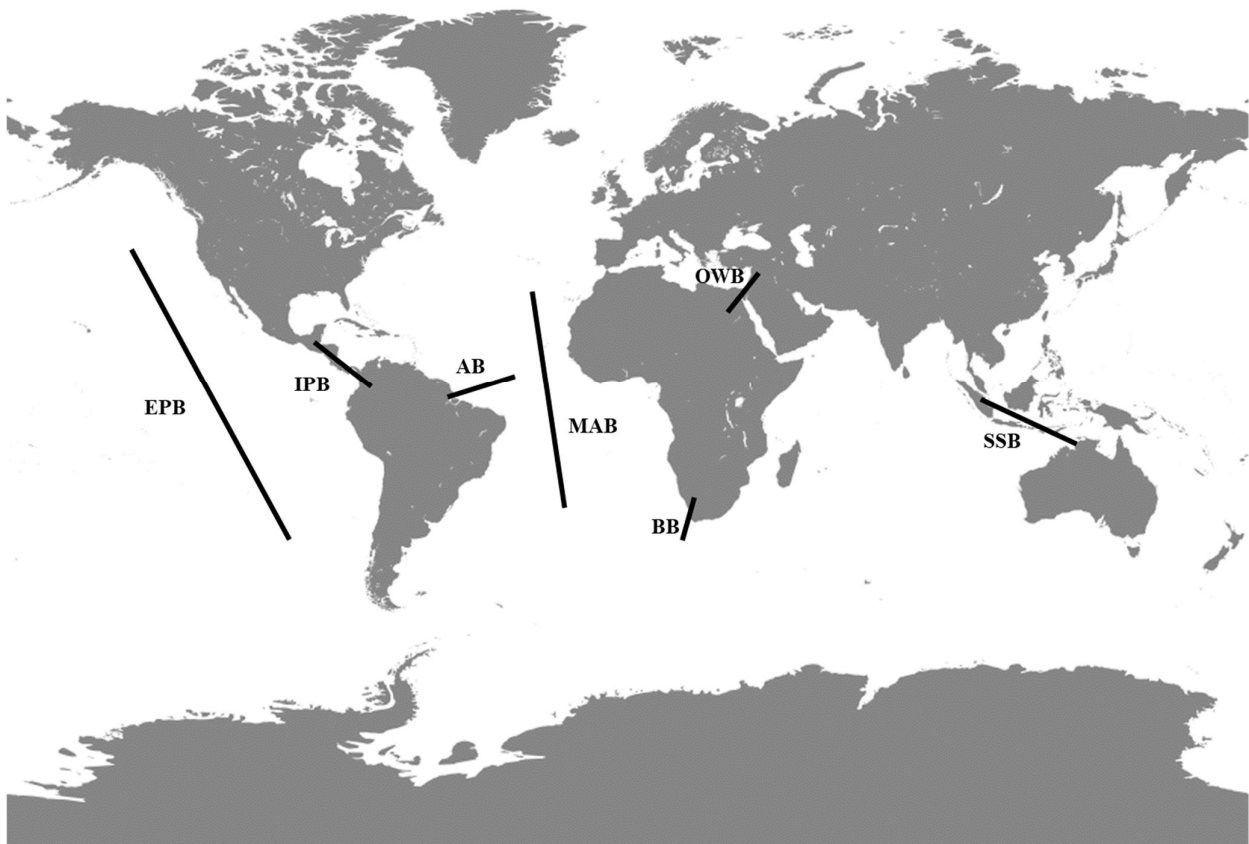


Figure 1.6 Traditionally recognised marine biogeographic barriers: EPB – Eastern Pacific Barrier; IPB – Isthmus of Panama Barrier; AB – Amazon Barrier; MAB – Mid-Atlantic Barrier; BB – Benguela Barrier; OWB – Old World Barrier; SSB – Sunda Shelf Barrier.

In recent years, the implementation of molecular markers (such as DNA sequence information or microsatellite markers) has been used to elucidate historical and contemporary processes that result in patterns of genetic differentiation in elasmobranch species over small and large spatial scales (Benavides *et al.* 2011; Vignaud *et al.* 2013; Bernard *et al.* 2016; Bester-van der Merwe *et al.* 2017; Bailleul *et al.* 2018). For cosmopolitan marine species with fragmented distributions, the general assumption is that these species are genetically heterogenous, in contrast to species characterized by a continuous distribution pattern (Graves 1998; Chabot and Allen 2009). This hypothesis is a popular avenue of investigation in many species of shark, with studies assessing genetic diversity and

population structure in both coastal sharks (scalped hammerhead, *Sphyrna lewini*, Duncan *et al.* 2006; blacktip shark, *Carcharhinus limbatus*, Keeney *et al.* 2005; brown smoothhound, *Mustelus henlei*, Chabot *et al.* 2015), and pelagic sharks (blue shark, *Prionace glauca*, Verissimo *et al.* 2017; whale shark, *Rhincodon typus*, Schmidt *et al.* 2009). From these studies, it was generally found that species that are capable of travelling long distances will display genetic connectivity, whether it is along the coast or across ocean basins, while less vagile species will exhibit genetically distinct populations, and constitute separate genetic stocks.

1.4.3 Site specificity and philopatric behaviour

The establishment of conservation and fisheries management programs may stem the tide of overexploitation of stocks, but the main problem of population declines is still to be addressed. The life history characteristics displayed by sharks means that the production of offspring to supplement declining population numbers is infrequent, and thus inadequate, placing importance on the survival of these juveniles to maturity (Dudgeon *et al.* 2012). Thus, extra focus should be placed on managing these species from a nursery perspective. In a study by da Silva *et al.* (2013), it was shown that *M. mustelus* displayed site fidelity to the Langebaan Lagoon along the west coast of South Africa, an area that was declared a Marine Protected Area (MPA). This study found that these sharks spent, on average, 79% of their time over a one-year period within the MPA. Specifically, this species pupped in the lagoon during spring months, and displayed residency during the summer months, before briefly moving out of the lagoon for the autumn and winter months. Fishing mainly occurs during the summer months, thus the high degree of residency may offer protection during these heightened fishing periods (barring poaching) (da Silva *et al.* 2013). This lends credence to the establishment of MPAs in known nursery areas of threatened animals, as it limits the impact of anthropogenic effects on recovering populations to some degree.

This high degree of site specificity is suggestive of reproductive philopatric behaviour, which explains the return of adult individuals to specific areas or nurseries to mate or give birth (Feldheim

et al. 2004; Hueter *et al.* 2005). This behaviour has important implications regarding the continued management of a species, as these nursery sites may have a direct impact on the level of genetic differentiation and divergence among geographic regions of a species (Hueter *et al.* 2005). Molecular data can be used in confirming whether particular areas serve as suspected nursery grounds (identified through tagging or observational datasets) by identifying site-specific haplotypes or by observing different structuring patterns based on mitochondrial and nuclear DNA, termed mito-nuclear discordance, which is suggestive of sex-biased dispersal (Keeney *et al.* 2005; Ovenden *et al.* 2009).

1.5 Aims and objectives

As the access to sequence information continues to increase for both model and non-model organisms, the ability to develop additional molecular markers improves. This allows for more in depth analyses of non-model organisms, such as the study species *M. mustelus*. To complicate the assessment of this shark, a lack of fisheries and ecological data in many countries, particularly along the western coast of Africa, limits the degree to which this marine resource can be evaluated and protected. Therefore, the aim of this study was to isolate, assemble and annotate the complete mitochondrial genome of *M. mustelus* from available NGS data, and to assess global structuring patterns, both historically and contemporarily, of the threatened common smoothhound shark, *M. mustelus*. These data, if married to traditional stock assessments methods, could aid in fisheries management in the three oceanic basins investigated, as the data may serve as a baseline assessment of the species in these areas.

In the first experimental chapter, chapter II, NGS sequence data was used to identify, isolate and assemble the complete mitochondrial genome of the common smoothhound shark. Once assembled, the complete mitogenome was annotated using available web services MitoFish and MitoAnnotator (Iwasaki *et al.* 2013). This complete mitogenome was used to investigate evolutionary relationships within the *Mustelus* genus in order to evaluate if the alternate modes of reproduction of the different *Mustelus* species are correlated to their phylogenetic relationship (López *et al.* 2006), as well as the

phylogenetic relationships between the broader orders of modern sharks. Additional comparisons between mitogenomes within the Carcharhiniformes order were performed to determine variable regions for subsequent analyses within this order of sharks.

Chapter III determined historical population genetic dynamics of the species using a fragment of the mitochondrial DNA control region. This chapter aimed to determine the historical population structure of *M. mustelus* across the global distribution of the species, as well as to validate the phylogeographic patterns determined in a recent study (Maduna *et al.* in review), from the Mediterranean Sea to the south-west Indian Ocean.

Chapter IV determined contemporary global population structure of the common smoothhound shark from the northern reaches of the Adriatic Sea, along the west coast of Africa to the eastern coast of South Africa. This chapter focused on the utility of species-specific microsatellite markers to determine contemporary patterns of genetic diversity, population structuring and migration rates of *M. mustelus* along the distribution range of the species.

Finally, chapter V tied all findings together to better understand the population ecology of the species, as well as the impact of fisheries on population health. This dual marker approach provides novel insight into both historical and contemporary population dynamics of this species on a global scale, and may serve to improve current practices that aim to preserve or protect this vulnerable species. The findings of this study could prove valuable for conservation and fisheries management, in terms of population genetic structuring and the species' propensity to overcome exploitation on a global scale.

CHAPTER II

Characterisation of the complete mitochondrial genome of the common smoothhound shark, *Mustelus mustelus*, and its phylogenetic placement among the main orders of modern sharks

Abstract

This chapter presents the first complete mitochondrial genome sequence of the common smoothhound shark, *Mustelus mustelus*, generated from Illumina next-generation sequence data. The complete mitochondrial genome is 16,755 bp in length, contains 13 protein-coding genes, 22 tRNA genes, 2 rRNA genes, and the non-coding control region. The order and contents of the genes display synteny with other sharks and broader vertebrates. Almost all protein-coding genes begin with the ATG start codon, except for the *COI* gene, which begins with GTG codon. Six protein-coding genes terminated with the TAA stop codon, and six with incomplete stop codons, T or TA. The *cytb* gene ended with the AGG codon. Phylogenetic reconstruction shows placement of the *M. mustelus* mitogenome within the genus *Mustelus*, with the closest relationship to the placental species, the spotless smoothhound *M. griseus*. Additional comparisons of sequence variability in coding genes and regions of the mitogenome of *M. mustelus* with other mitogenomes within the broader order of Carcharhiniformes revealed that the non-coding control region (mtCR) generally displayed the greatest sequence variation amongst the Carcharhiniformes examined in this chapter, and may be a suitable region to further investigate micro-evolutionary processes in this order of sharks. This mitogenome provides valuable information to further unravel the evolution of alternate reproduction modes in the genus *Mustelus*, and evolutionary processes in the Carcharhiniformes order.

2.1 Introduction

Recent advances in sequencing technologies have given access to new avenues of investigation in molecular research, providing greater insight into various genetic aspects of model organisms. Model organisms, in this case, can be described as those with reference genomes readily available for analysis. While this is clearly beneficial to further the understanding of these organisms, research into non-model organisms has lagged behind due to the scarcity of DNA sequence and marker data available for analysis (Seeb *et al.* 2011). However, the introduction of next-generation sequencing (NGS) has addressed this problem to some degree, as it facilitates the sequencing of entire genomes and the identification of thousands of potential markers. Therefore, a range of biological questions with regards to non-model organisms can now be addressed, enabling a transition from molecular ecology to ecological genomics (Tautz *et al.* 2010). Sharks in general can be classified as non-model organisms, as there is only a fraction of the 517 extant species (Weigmann 2017) with available sequence information. More so, as approximately 16% of shark species are threatened with extinction by the IUCN Red List's Shark Specialist Group (Dulvy *et al.* 2014, 2017), it has become crucial to generate genetic resources for these species. The application of high-throughput genetic data could contribute greatly to a better understanding of the genetic diversity and population structure of these animals, especially for genera that are currently experiencing increased levels of exploitation on a global scale.

The species-rich shark genus *Mustelus*, or smoothhounds, is one of the more commercially important groups of sharks in the world's oceans. Species of *Mustelus* are small to medium-sized (57 – 185 cm total length, L_T) demersal sharks abundant in temperate and tropical nearshore habitats, from shallow waters to a maximum reported depth of about 1,463 m (Weigmann 2016). All species of *Mustelus* are viviparous (live-bearing) with two discrete reproductive modes; some species provide additional nutrients to their offspring through a placental attachment (placental species); and other species do not form such a placental attachment whereby nutrients for their offspring are solely

provided by the yolk-sac (aplacental species) (Heemstra 1973). Molecular phylogenetic studies of the genus *Mustelus* based on four protein-coding gene sequences (*cytochrome b*, *cytb*; *NADH dehydrogenase subunit 2* and *-4*, *NADH-2* and *NADH-4*; *recombination-activating gene 1*, *RAG1*) and the non-coding mitochondrial control region (mtCR), provide compelling evidence that the genus is paraphyletic i.e. comprised of two subsidiary groupings of extant species of the genus (López *et al.* 2006; Boomer *et al.* 2012; Naylor *et al.* 2012). However, the genus constitutes a single monophyletic group when *Scylliogaleus queckettii* and *Triakis megalopterus*, two other houndshark species, are included (López *et al.* 2006; Naylor *et al.* 2012). Consequently, López *et al.* (2006) and Boomer *et al.* (2012) suggested that species of *Mustelus* could be divided into two clades representing different modes of reproduction, placental vs. aplacental species, coupled to the presence or absence of white spots on the dorsal surface, respectively.

The common smoothhound shark *Mustelus mustelus* (Linnaeus 1758) is a medium-sized ($L_T < 1,7$ m) epibenthic member of the houndshark family Triakidae, order Carcharhiniformes (Weigmann 2016), with the reproduction mode being placental viviparity (Saidi *et al.* 2008). This species is widely distributed, ranging from the north-east Atlantic Ocean and Mediterranean Sea, to the south-west Indian Ocean along the coast of South Africa. *Mustelus mustelus* is heavily exploited across its distribution and is currently classified as Vulnerable in the IUCN Red List of Threatened Species (Serena *et al.* 2009). The development of genomic resources for the genetic assessment of this species is crucial for this resource's continued management and long-term conservation. However, only two complete mitochondrial genomes are available for the *Mustelus* genus as a whole, namely the aplacental species *Mustelus manazo* (Cao *et al.* 1998) and the placental species *Mustelus griseus* (Chen *et al.* 2016). Therefore, the aim of this chapter was to assemble and annotate the complete mitochondrion sequence of *Mustelus mustelus*, which will allow for a more thorough assessment of the evolutionary processes that may have driven speciation events in the past, as well as determine variable genes or regions for future analysis within the Carcharhiniformes order.

2.2 Materials and methods

2.2.1 Sample collection, DNA extraction and next-generation sequencing data preparation

A single specimen was collected by the Department of Agriculture, Forestry and Fisheries (DAFF), South Africa during tagging surveys off the south-west coast of South Africa (Langebaan Lagoon, Western Cape, latitude: 33°06' S, longitude: 18°01' E). Total genomic DNA was extracted from a fin clip sample (LL5MM) using a modified cetyltrimethylammonium bromide (CTAB) extraction protocol of Sambrook and Russell (2001) and sent to the Agricultural Research Council Biotechnology Platform, South Africa for next-generation sequencing. One microgram of genomic DNA was used for paired-end library preparation (2×250 bp) with a mean insert size of 400 bp using the Illumina TruSeq® DNA library preparation kit (Illumina). The library was sequenced on two lanes of an Illumina HiSeq™ 2000 sequencer. A quality control (QC) step was performed on the generated reads to remove artificial duplicates or reads that contained any sequence ambiguities using PRINSEQ v0.20.4 (Schmieder and Edwards 2011). Reads were quality filtered and trimmed to remove all sequences shorter than 35 bp and Nextera adapters using TRIMMOMATIC v0.33 (Bolger *et al.* 2014) with default settings. A Phred quality threshold of 15 was selected and sequences were filtered to contain at least 90% of the individual bases above this quality score. Subsequently, sequence quality was visualized using the software FASTQC v0.11.4 (Andrews 2010) to ensure that primer-, barcode-, and adapter sequences had been adequately trimmed, resulting in 181,361,000 reads for further analysis.

2.2.2 Isolation of mitochondrial sequences, mitogenome assembly and annotation

To determine which of the two available *Mustelus* mitogenomes to use as a reference for the isolation and mapping of mitochondrial reads, a *COI* sequence of *M. mustelus* (Accession Number: JF493920) was used in a BLASTn search against the complete mitogenomes of *M. manazo* and *M. griseus*, with *M. griseus* having a higher percentage identity than *M. manazo*. Therefore, the reads were used in a BLASTn search against the *M. griseus* mitogenome (Accession Number:

NC_023527.1) in GENEIOUS v10.1 (Kearse *et al.* 2012) with a maximum E-value of $1e-20$ specified, in order to isolate the mitochondrial sequences from the total NGS dataset. These putative mitochondrial sequences were mapped against the mitogenome of *M. griseus* using the Geneious Read Mapper algorithm, with default parameters. The mapped sequences were then annotated using the MITOFISH and MITOANNOTATOR web service (Iwasaki *et al.* 2013), resulting in the annotated mitochondrial genome of *Mustelus mustelus*.

2.2.3 Phylogenomic placement of *Mustelus mustelus*

A total of 31 mitogenome sequences obtained from GenBank (see **Table 2.1** for accession numbers) representing the eight orders of modern sharks were aligned using MAFFT v7.402 (Katoh and Standley 2013), with default parameters. The nucleotide substitution model that best fit the multi-sequence alignment was determined in JMODELTEST v2.0 (Darriba *et al.* 2012) according to the Bayesian Information Criterion (BIC). Based on this statistic, the General Time Reversible with a proportion of invariable sites and gamma distribution rate variation among sites (GTR+I+G) model was identified as the best fit model for the dataset. Bayesian inference of the phylogenetic relationships among mitogenomes was performed in MRBAYES v3.2.6 (Ronquist *et al.* 2012) with 2,000,000 MCMC generations, sampling every 1,000 generations, and the first 500,000 generations discarded as burn-in. These analyses were performed through the CIPRES Science Gateway (Miller *et al.* 2010) and the consensus tree was visualized in FIGTREE v1.4.3 (<http://tree.bio.ed.ac.uk/software/figtree>).

2.2.4 Sequence variation within the *Carcharhiniformes* order

To investigate micro-evolutionary processes at work within the broader order of *Carcharhiniformes*, protein-coding genes, *rRNA* genes and the non-coding control region were isolated from the complete mitogenome of *M. mustelus*. The complete sequences of these regions were used in a MEGABLASTn search against the six *Carcharhiniformes* mitogenome sequences utilised throughout the study in BLAST2GO v5.0 (Conesa *et al.* 2005). Each mitogenome sequence

was used to create separate BLAST databases, and MEGABLASTn searches of each gene or region of *M. mustelus* was performed against these databases. Default parameters were used to perform the search, with the word size of the search set to 15.

2.3 Results

The complete mitogenome consensus sequence for *M. mustelus* is 16,755 bp in length (**Figure 2.1**), including 13 protein-coding genes, 22 tRNA genes, 2 rRNA genes, and a non-coding mitochondrial control region (mtCR). The majority of protein-coding genes begin with the ATG start codon, except for the *cytochrome oxidase subunit 1* (*COI*) gene, which begins with the GTG codon. Six protein-coding genes terminated with the TAA stop codon, and six with incomplete stop codons, T or TA. However, the *cytochrome b* (*cytb*) gene ended with the AGG codon. Furthermore, phylogenetic analysis separated all shark species into eight orders with a high degree of statistical support and clear differentiation between the orders of modern sharks (**Figure 2.2**).

Furthermore, the analysis of sequence variation revealed that the mtCR and *NADH dehydrogenase* genes generally displayed the most sequence variation relative to the reference mitogenomes, whereas the *12S* and *16S rRNA* genes were the most conserved within the broader Carcharhiniformes order (**Figure 2.3, Table S2.1**).

Chapter II

Mitochondrial genome

Table 2.1 List of mitochondrial genomes utilised in the current study, separated into the eight higher orders of modern sharks.

Order	Scientific name	mtDNA size (bp)	Accession no.	Reference
Carcharhiniformes	<i>Carcharhinus amblyrhynchoideus</i>	16,705	NC_023948.1	Feutry <i>et al.</i> (2016)
	<i>Galeocerdo cuvier</i>	16,703	KX858829.1	Unpublished
	<i>Mustelus griseus</i>	16,754	NC_023527.1	Chen <i>et al.</i> (2016)
	<i>Mustelus manazo</i>	16,707	AB015962.1	Cao <i>et al.</i> (1998)
	<i>Mustelus mustelus</i>	16,755	MH559351	This study
	<i>Prionace glauca</i>	16,705	NC_022819.1	Chen <i>et al.</i> (2015a)
	<i>Sphyrna lewini</i>	16,726	JX827259.1	Chen <i>et al.</i> (2015b)
Heterodontiformes	<i>Heterodontus zebra</i>	16,720	NC_021615.1	Chen <i>et al.</i> (2014)
Hexanchiformes	<i>Chlamydoselachus anguineus</i>	17,313	KU159431.1	Bustamante <i>et al.</i> (2016)
	<i>Heptranchias perlo</i>	18,909	NC_022730.1	Tanaka <i>et al.</i> (2013)
	<i>Hexanchus griseus</i>	17,405	KF894491.1	Unpublished
	<i>Hexanchus nakamurai</i>	18,605	AB560491.1	Tanaka <i>et al.</i> (2013)
	<i>Notorynchus cepedianus</i>	16,990	NC_022731.1	Tanaka <i>et al.</i> (2013)
Lamniformes	<i>Alopias pelagicus</i>	16,692	KF020876.1	Unpublished
	<i>Carcharias taurus</i>	16,773	NC_023520.1	Chang <i>et al.</i> (2015a)
	<i>Carcharodon carcharias</i>	16,744	KC914387.1	Chang <i>et al.</i> (2014)
	<i>Isurus oxyrinchus</i>	16,701	KF361861.1	Chang <i>et al.</i> (2015b)
	<i>Mitsukurina owstoni</i>	17,743	EU528659.1	Unpublished

Chapter II

Mitochondrial genome

Orectolobiformes	<i>Chiloscyllium griseum</i>	16,755	NC_017882.1	Direct Submission
	<i>Chiloscyllium plagiosum</i>	16,726	NC_012570.1	Unpublished
	<i>Orectolobus japonicus</i>	16,706	NC_022148.1	Direct Submission
	<i>Rhincodon typus</i>	16,875	NC_023455.1	Alam <i>et al.</i> (2014)
Pristiophoriformes	<i>Pristiophorus japonicus</i>	18,430	NC_024110.1	Unpublished
Squaliformes	<i>Cirrhigaleus australis</i>	16,544	NC_024059.2	Yang <i>et al.</i> (2016)
	<i>Etmopterus pusillus</i>	16,729	NC_031810.1	Chen <i>et al.</i> (2016)
	<i>Somniosus microcephalus</i>	16,730	KY513709.1	Santaquiteria <i>et al.</i> (2017)
	<i>Squaliolus aliae</i>	16,717	NC_031508.1	Direct Submission
	<i>Squalus montalbani</i>	16,555	NC_028537.1	Kemper and Naylor (2016)
Squatiniiformes	<i>Squatina formosa</i>	16,690	KM084865.1	Corrigan <i>et al.</i> (2016)
	<i>Squatina japonica</i>	16,689	NC_024276.1	Chai <i>et al.</i> (2016)
	<i>Squatina nebulosa</i>	16,698	NC_025578.1	Gao <i>et al.</i> (2016)
Rajiformes	<i>Raja radiata</i>	16,783	AF106038.1	Rasmussen and Arnason (1999)

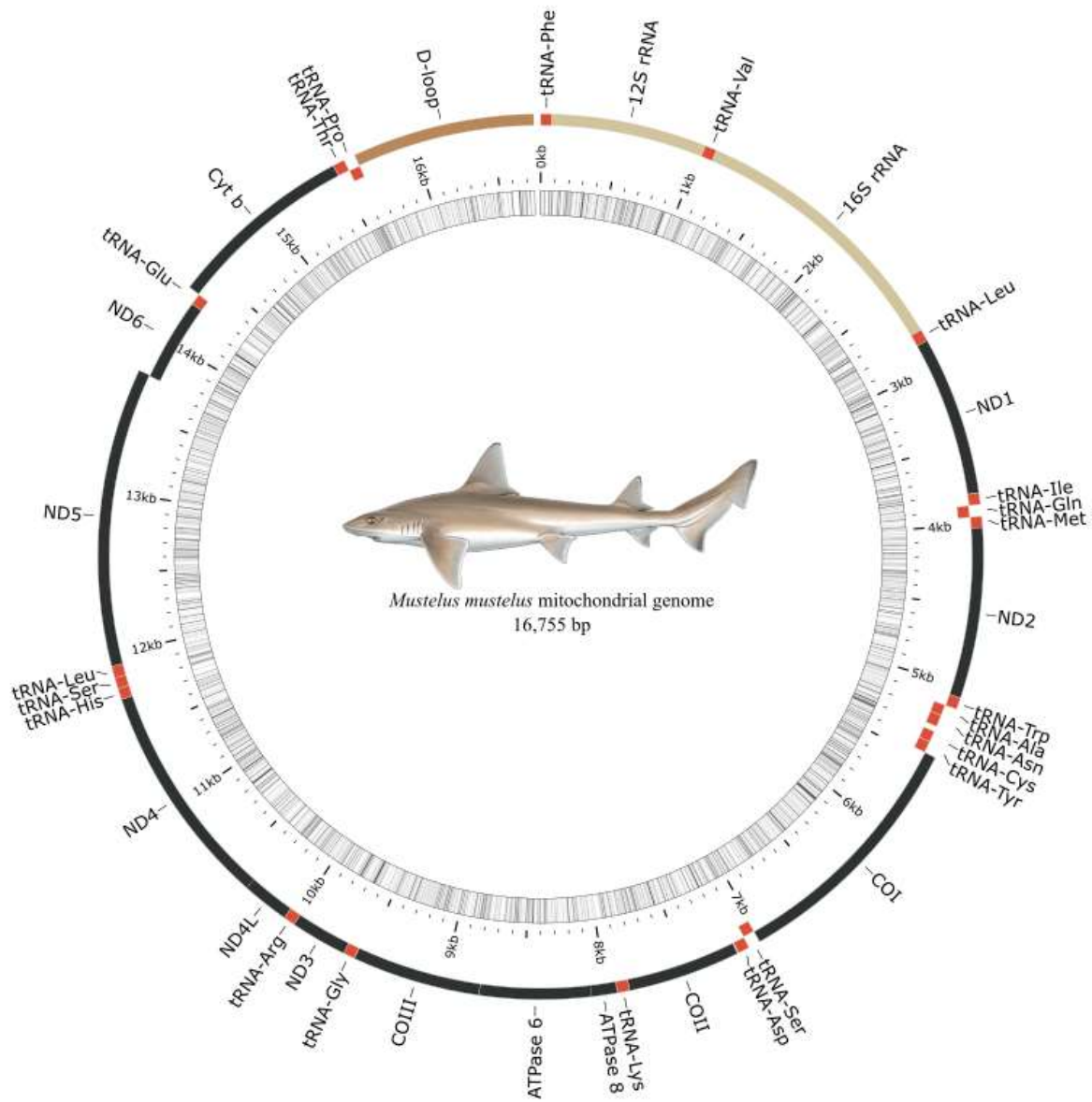


Figure 2.1 Graphical representation of the complete mitochondrion of the common smoothhound shark, *Mustelus mustelus*.

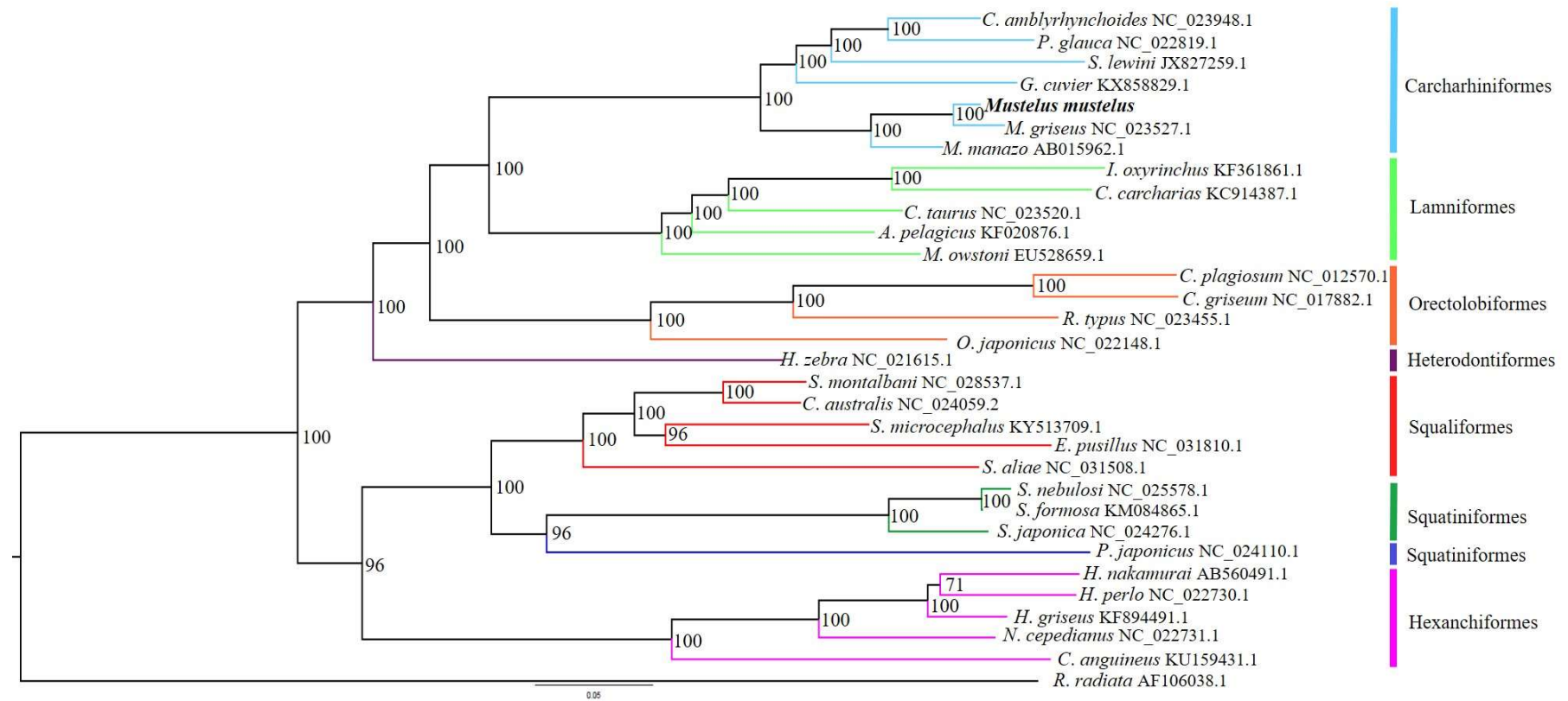


Figure 2.2 Phylogenetic relationships between the eight orders of modern sharks constructed using Bayesian Inference from 31 whole mitogenome sequences, with the thorny skate (*Raja radiata*) mitogenome included as an outgroup. Numbers at nodes indicate posterior probabilities. Genbank accession numbers are given adjacent to the species name, and scale bar indicates groupings of species into orders.

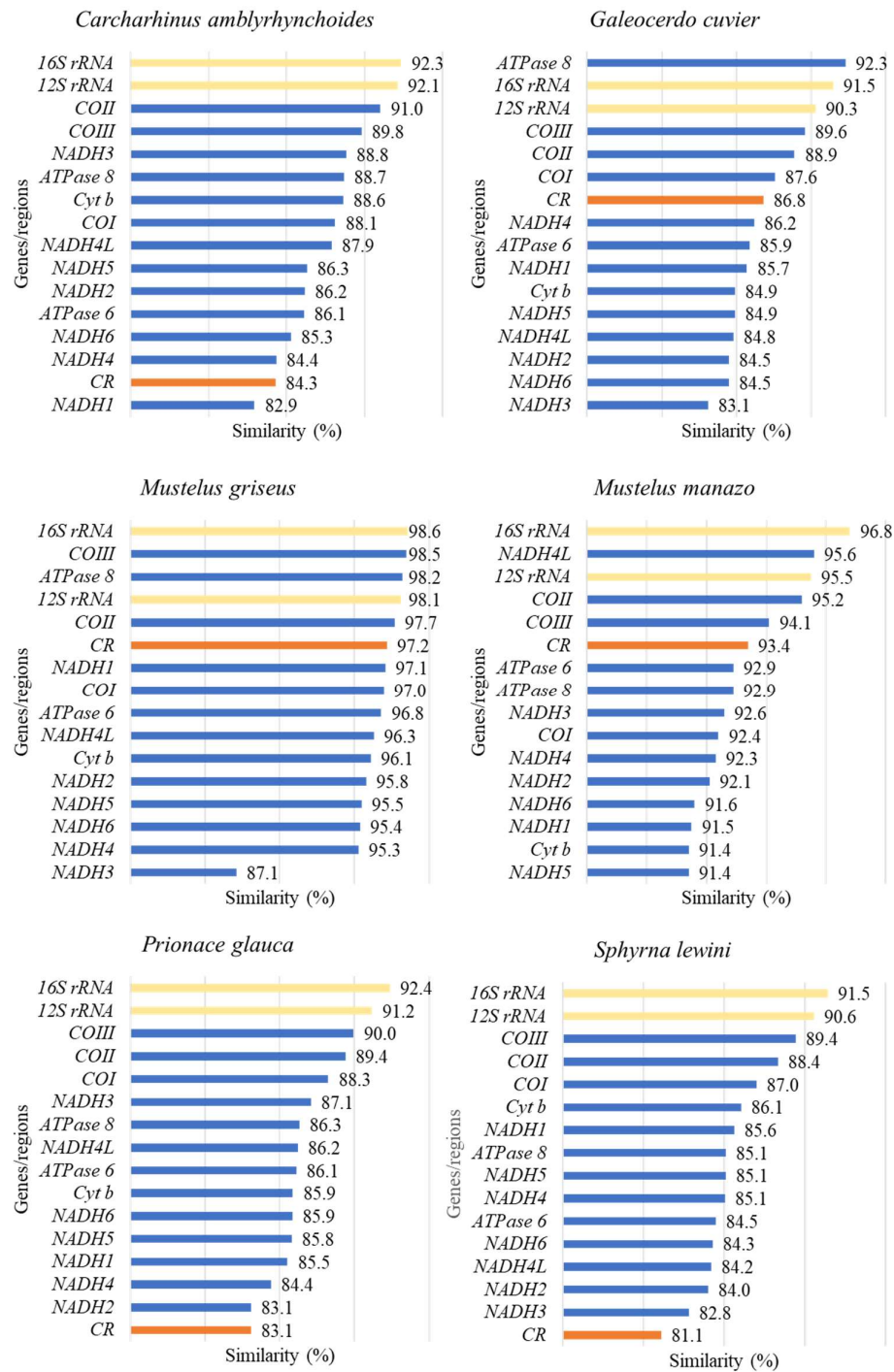


Figure 2.3 Sequence comparison of coding and non-coding regions of the mitochondrial genome of *Mustelus mustelus* to six species of the Carcharhiniformes order, in decreasing order of sequence similarity. Yellow bars – rRNA genes; blue bars – protein-coding genes; orange bar – control region.

2.4 Discussion

The order and content of the mitochondrial genome of *Mustelus mustelus* displays synteny with other sharks, and more broadly, most vertebrates, further illustrating the highly conserved nature of this organelle within the phylum Chordata, of which all animals' forms part of. Furthermore, the phylogenetic analysis of 31 mitogenomes provided clear resolution between the eight orders of sharks, indicating the improved statistical power to differentiate between closely related taxa on a genome-wide level, rather than on a genic level. Within Carcharhiniformes, the *Mustelus* clade comprising *M. griseus*, *M. manazo* and *M. mustelus* is highly supported (**Figure 2.2**), with *M. mustelus* and *M. griseus* being sister taxa. This positioning could be explained by the reproductive mode of the two species, as they are both viviparous placental, in contrast to *M. manazo*, which is aplacental (Teshima and Koga 1973; Smale and Compagno 1997). The phylogenetic placement of the common smoothhound genome supports the paraphyly of the genus (López *et al.* 2006; Boomer *et al.* 2012; Naylor *et al.* 2012), even at the mitogenome level.

Notably, the mitochondrial control region (mtCR) displayed higher levels of variation in the different genera assessed (sequence similarity: 81.1 – 86.8%), but was fairly conserved within the *Mustelus* genus itself (sequence similarity: 93.4 – 97.2%). As it is a non-coding region, the accumulation of adaptative changes may occur at a higher rate relative to other coding regions (Awise 2012), which has led to the increasing popularity of this mitochondrial marker in the assessment of cosmopolitan shark species (Chabot and Allen 2009; Tillett *et al.* 2012; Veríssimo *et al.* 2017). The results of this chapter further illustrate the higher level of variation displayed by the entire mtCR, making it a suitable candidate for assessing micro-evolutionary processes of species within this order of shark.

Additionally, the sequence variation within the Carcharhiniformes order suggests that the *NADH dehydrogenase* genes (*NADH 1* – *NADH 6*) are variable regions across the six species assessed in the current study, generally displaying the lowest sequence similarity (82.8 – 97.1%) of the protein-

coding regions of the mitochondrion (**Figure 2.3, Table S2.1**). These genes serve an important function, in that they encode proteins that form respiratory complex I, an enzyme housed in the membrane of the mitochondrion that functions as a transporter of electrons into the organelle for later use in the production of adenosine triphosphate (ATP) (Weiss *et al.* 1991). Theoretically, these genes should be more conserved, due to their integral function in energy production. Despite this assumption, several studies have utilised at least one of these genes in assessing various genetic aspects of natural populations of shark species (Maduna *et al.* 2016; Bester-van der Merwe *et al.* 2017; Feitosa *et al.* 2018). This level of sequence diversity can be explained by the process through which mutations or variation are propagated in a population. Mutations occur at a specific rate per individual, generation and nucleotide, and these mutations are eventually lost or fixed at a rate dependent on the fitness effect of the mutation, as well as the population size (Ohta 1973; Frankham 2005). If the mutation is neutral, the only process governing the fate of the substitution is genetic drift, unless there is a degree of linkage to sites under selection (Kimura 1968; Frankham 2005). However, if the mutation is advantageous to the population as a whole, the rate of fixation is higher than that of a neutral mutation (Ho *et al.* 2011). As these species occupy a wide variety of habitats across the world's oceans, and are characterised by different life-history traits, the variation within these genes could be a result of selective pressures favouring specific genotypes, and by extension phenotypes (Ho *et al.* 2011).

Conversely, the *rRNA* genes were consistently conserved (sequence similarity: 90.3 – 98.6%) across the genera assessed, most likely due to their role in coding for ribosomal subunits of the mitochondrion, an important component in the processing of transcripts of the coding regions, culminating in protein synthesis (Noller *et al.* 1992). These genes have been shown to be useful phylogenetic markers in vertebrates (Springer *et al.* 2001), and in the phylogenetic assessment of elasmobranch species (Douady *et al.* 2003; Vella and Vella 2017), as well as being suitable markers for species identification (Quraishia *et al.* 2015). The results of this chapter further support the use of these markers in future phylogenetic studies within the Carcharhiniformes order of sharks.

2.5 Conclusion

The complete mitogenome for *M. mustelus* is an important resource for future conservation and evolutionary biology research, such as in-depth phylogenetic placement of species of *Mustelus* or other genera with alternate modes of reproduction, or the investigation of the macro-evolutionary processes at work in this genus and the broader orders of modern sharks, as well as micro-evolutionary processes within species, with the non-coding mtCR displaying the most sequence variation within the mitochondrial genome of this order of sharks. This region should be utilised in future studies on species within the Carcharhiniformes order for a more comprehensive assessment of the species in question.

CHAPTER III

Population structure of the common smoothhound shark, *Mustelus mustelus*, based on mtDNA sequence data

Abstract

The cosmopolitan common smoothhound shark, *Mustelus mustelus*, displays a widespread distribution pattern along continental shelves, with a high degree of regional endemism throughout several ocean basins. When considering this from a managerial perspective, it is necessary to understand the past and present distribution of a species' genetic diversity to develop adequate long- and short-term conservation strategies. Here the focus is on the distribution of genetic diversity of *M. mustelus* from a more historical perspective and is based on mtDNA data of samples ($n = 67$) representative of three oceanic regions. A 571 bp fragment of the non-coding mitochondrial control region revealed 15 polymorphic sites, 18 haplotypes, and two main haplogroups representing the northern and southern hemisphere populations. The level of divergence however was shallow, indicating limited mutational events accumulating over time, and a potentially slow mitochondrial mutation rate within this species of shark. Signals of population divergence were strong overall ($\Phi_{ST} = 0.658$, $P < 0.01$), with significant inter-oceanic divergence ($\Phi_{CT} = 0.427$, $P < 0.01$). Furthermore, pairwise Φ_{ST} estimates indicated significant divergence ($P < 0.01$) between all sampling populations, except within the Mediterranean Sea and the south-east Atlantic/south-west Indian Oceans. In accordance with previous studies, the phylogenetic analysis was suggestive of a northern hemisphere origin of the species before gradual range expansions resulted in the colonisation of the southern African coastline.

3.1 Introduction

Sharks occur in a variety of oceanic regions, including coastal, pelagic and benthic areas (Dudgeon *et al.* 2012). This variation in habitat usage translates to wider distribution ranges for many species, and as such, results in divergent or distinct genetic populations for many species (Mendonça *et al.* 2013). Population genetic structure in sharks and other marine species is most often a result of the interplay between evolutionary forces (genetic drift, gene flow and mutation), life history characteristics, and seascape features (currents, temperature fluctuations and upwellings) of the oceans they inhabit (Ovenden 2013). Sharks that typically exhibit high dispersive or migratory abilities display little genetic differentiation, even across ocean basins, which has been observed for the basking shark, *Cetorhinus maximus* (Hoelzel *et al.* 2006) and the whale shark, *Rhincodon typus* (Schmidt *et al.* 2009). Contrastingly, demersal species with low dispersal potential or fragmented distribution ranges usually exhibit some level of spatial genetic structure, as was found in the Caribbean sharpnose shark, *Rhizoprionodon porosus* (Mendonça *et al.* 2013) and the small-spotted catshark, *Scyliorhinus canicula* (Kousteni *et al.* 2015).

On a more historic timescale, genetic divergence between populations or regions is either attributed to dispersal ability or vicariant events (Mooi and Gill 2002). Dispersal ability of a species explains the allopatric distribution of species by the movement of some members of an ancestral population from a point of origin across an existing barrier to new areas where they subsequently diverge into distinct populations (Mooi and Gill 2002; Musick *et al.* 2004). Vicariant events can be described as the separation of a natural population by the formation of a physical barrier, leading to the divergence of said population from the original population (Musick *et al.* 2004; Adnet and Cappetta 2008). For marine species, these historic drivers of population structure are closely tied to the dispersal ability of the species and the oceanographic features of the areas they inhabit. For instance, the open ocean was found to restrict gene flow in the scalloped hammerhead (*Sphyrna lewini*), the lemon shark (*Negaprion brevirostris*) and the sicklefin lemon shark (*Negaprion*

acutidens) (Duncan *et al.* 2006; Schultz *et al.* 2008) whereas temperature fluctuations appear to act as a restrictive force in temperate species such as the tope shark (*Galeorhinus galeus*) (Chabot and Allen 2009).

Understanding how these biogeographical processes influence the underlying patterns of population structure across the distribution range of a species is critical for the identification of management units (MUs), or distinct populations (in terms of allele frequencies) that ideally should be managed as separate units to ensure the sustainability of the population at large (Mortiz 1994; Funk *et al.* 2012). From an evolutionary perspective, it is crucial to identify biological units to be conserved, such as a group of historically-isolated populations with unique adaptive lineages, or evolutionary significant units (ESUs) (Moritz 1994; Funk *et al.* 2012). This is especially important in instances where populations display restricted distributions and are subject to anthropogenic pressures, which holds for the common smoothhound shark, *M. mustelus*.

The common smoothhound is a small coastal shark species, characterised by a relatively low reproductive capacity and limited dispersal ability (Smale and Compagno 1997; Saidi *et al.* 2008; da Silva *et al.* 2013), with site fidelity observed, for example, in a South African population (da Silva *et al.* 2013). Previous regional studies conducted along the southern African coast indicate genetic structure on a nuclear and mitochondrial level, based on the *NADH dehydrogenase subunit 4 (ND4)* (Bitalo *et al.* 2015; Maduna *et al.* 2016). Thus, this chapter aims to expand the scope of previous population genetic studies, in order to elucidate historic population structure on a global scale, analysing sequence data from the non-coding mitochondrial control region (mtCR). Hypotheses of hydrodynamic barriers to gene flow, and isolation by distance (IBD) (Wright 1943) as possible drivers to population differentiation were tested, in order to identify ESUs along the global distribution range of *M. mustelus*. The results of this chapter are also compared with the more contemporary patterns of population structure elucidated through species-specific microsatellite markers (Chapter IV).

3.2 Materials and methods

3.2.1 Sample collection and DNA extraction

Samples were collected between 2011 to 2017 in an attempt to cover the international distribution of *M. mustelus*. Individuals were sampled onboard commercial fishing vessels and research surveys in the Mediterranean Sea (MED), the southern north-east Atlantic Ocean (SNEAO), the south-east Atlantic Ocean (SEAO), and the south-west Indian Ocean (SWIO). Adriatic Sea individuals were obtained from local fisheries, during surveys or at the fish market of Chioggia, where the landings of the major fishing fleet of the basin occur (Mazzoldi *et al.* 2014). Sicilian samples were collected both from trawl surveys (i.e. MEDITS: International Bottom Trawl Survey in the Mediterranean) and commercial landings of the Mazara del Vallo fishing fleet (Marino *et al.* 2017). Samples from the southern north-east Atlantic were collected during research cruises undertaken between 2011 and 2012 by the Institute of Marine Research (collector: Diana Zaera-Perez). Fishing permits for the southern African samples were originally issued by the Department of Agriculture, Forestry and Fisheries (DAFF, Republic of South Africa). Samples were also collected on the R.S Ellen Khuzway during National Shark surveys, as well as during research fishing trips conducted within the Port of Ngqura between 2014 and 2017. Due to the nature in which these samples were obtained, phenotypic data, such as size, sex and maturity, could not be recorded for all individuals sampled. A total of 67 individuals were selected for mtDNA sequencing and analysis, representing three broad oceanic regions, including the Mediterranean Sea (MED), the southern north-east Atlantic (SNEA), and the south-east Atlantic and south-west Indian Oceans combined (SAI) (**Figure 3.1**).

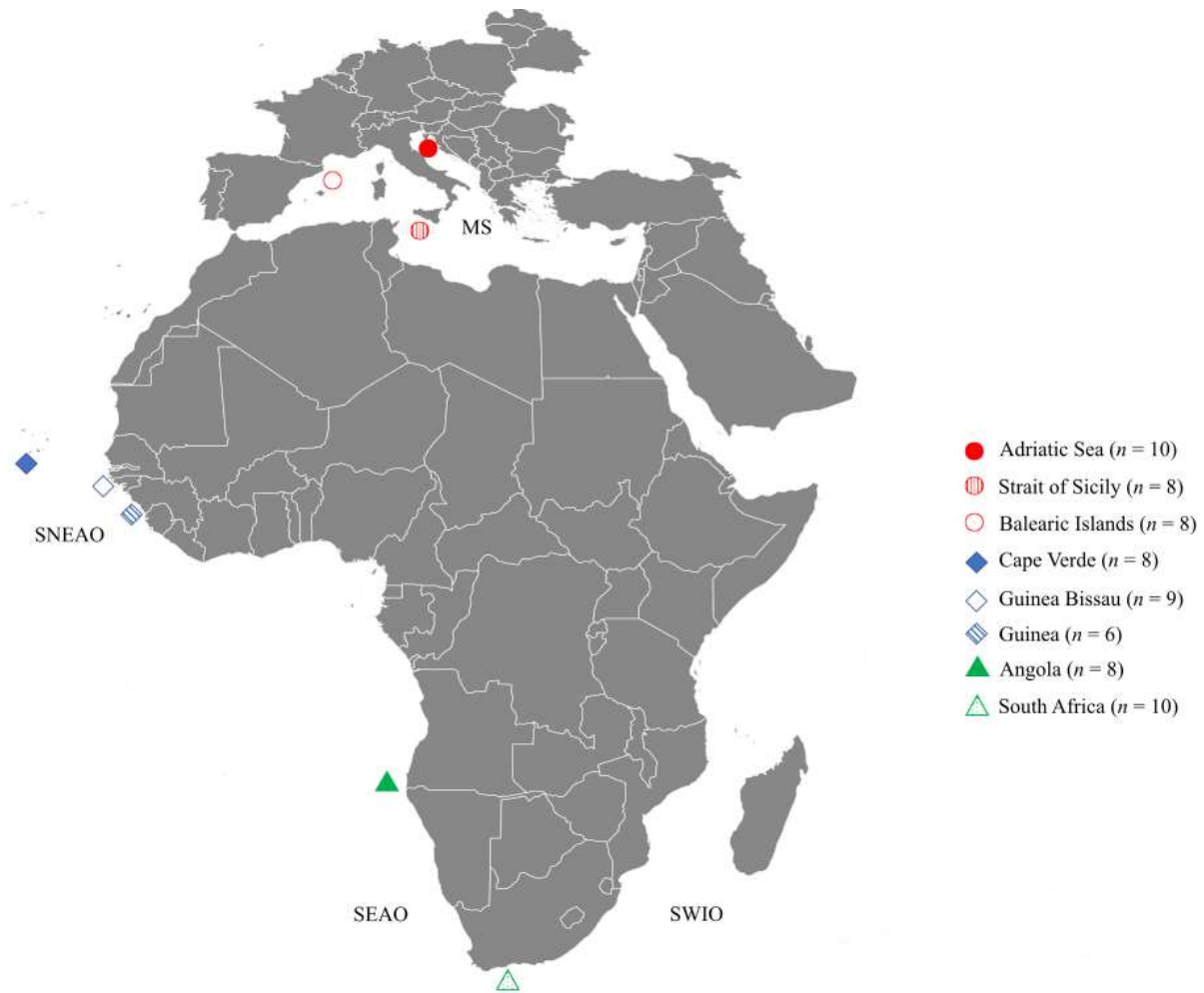


Figure 3.1 Global sampling sites of *Mustelus mustelus* in the Mediterranean (circles), southern north-east Atlantic (diamonds) and south-east Atlantic/south-west Indian Oceans (triangles) populations, with sample size (n) and oceans indicated. MS – Mediterranean Sea; SNEAO – southern north-east Atlantic Ocean; SEAO – south-east Atlantic Ocean; SWIO – south-west Indian Ocean.

Fin clips were stored in 99% ethanol at room temperature until further use. Total genomic DNA was isolated from the tissue samples using a modified cetyl trimethylammonium bromide (CTAB) extraction method (Sambrook and Russell 2001). Extracted DNA was quantified using a Nanodrop 2000 Spectrophotometer (*NanoDrop®*), adjusted to a working concentration of 50 ng/ μ l with distilled deionised water (ddH₂O) and stored at -20°C.

3.2.2 Mitochondrial control region amplification and genetic diversity analyses

A fragment of the mitochondrial control region (mtCR) was amplified in approximately ten samples per geographic sampling population with the primer pair MaCYB 5' -TAA CTT GAA TTG GRG GRC AAC- 3' and MaDLP 5' -GCA TTA ATC AGA TGY CAG RT- 3', as previously described in Boomer *et al.* (2012). Polymerase Chain Reaction (PCR) conditions were optimised and performed in 15 µl reactions, consisting of 1X GoTaq Flexi PCR buffer, 2 mM MgCl₂, 200 µM dNTPs, 0.5 µM of each primer, and 1 unit of GoTaq® DNA polymerase (Promega Corporation). The PCR cycling conditions included an initial heating step of 2 minutes at 94°C, followed by 30 cycles of 30 seconds denaturation at 94°C, 30 seconds for the annealing of the primers at 52°C, 30 seconds of extension at 68°C, and a final extension step of 5 minutes at 68°C. PCR products were separated on a 2% w/v agarose gel for 30 minutes at 100V to confirm successful amplification at the expected fragment size.

Bi-directional sequencing reactions were performed using a BigDye® terminator v3.1 cycle sequencing kit (Life Technologies) in a reaction volume of 10 µl according to the manufacturer's specifications. In short, cycling conditions included an initial denaturation period of 1 minute at 96°C, followed by 25 cycles of 10 seconds at 96°C, 5 seconds at 50°C and 4 minutes at 60°C, as per the manufacturer's instructions. Sequencing reactions were sent to the Central Analytical Facility (CAF), Stellenbosch University, for Sanger sequencing on an ABI 3730XL DNA Analyser. All sequences were manually trimmed and edited resulting in a final sequence length of 571 bp. These sequences were then aligned in MEGA v7.0 (Kumar *et al.* 2016) using a ClustalW alignment algorithm, with default parameters.

Diversity indices were calculated in DNASP v5.0 (Librado and Rozas 2009), including the total number of haplotypes (H), haplotype (h) and nucleotide diversity (π), and average number of nucleotide substitutions (k) for both global and oceanic datasets. Unique haplotypes were subsequently identified in DNASP, and the evolutionary relationships among haplotypes was inferred

and visualized by constructing a 95% Median Joining (Bandelt *et al.* 1999) inference network as implemented in NETWORK v5.0.0.3 (<http://www.fluxus-engineering.com>).

3.2.3 Phylogenetic analysis

The nucleotide substitution model for the alignment was determined in JMODELTEST v2.0 (Darriba *et al.* 2012), resulting in the Hasegawa, Kishino and Yano (Hasegawa *et al.* 1985) with a number of invariable sites (HKY+I) model ranked as the best fit for the dataset according to the Bayesian Information Criterion (BIC, Schwarz 1978). Subsequently, mean genetic distances between sampling populations were calculated, and Maximum Parsimony and Maximum Likelihood analyses (1,000 bootstraps) were implemented in MEGA to infer the phylogenetic position of the determined haplotypes. Additionally, Bayesian inference of the phylogenetic relationships among haplotypes was performed in MRBAYES v3.2.6 (Ronquist *et al.* 2012), assuming the HKY+I model. The runs included 5,000,000 generations, with a standard variation threshold of 0.05, with the inclusion of a molecularly identified *Mustelus mosis* mtCR sequence (Maduna *et al.* in review) as an outgroup. The subsequent consensus tree was visualized in FIGTREE v1.4.3 (<http://tree.bio.ed.ac.uk/software/figtree>).

3.2.4 Spatial patterns of population divergence

Genetic divergence among sampling populations, and between oceanic regions, was determined in ARLEQUIN v3.5.2 (Excoffier and Lischer 2010), by means of pairwise Φ_{ST} tests (10,000 permutations, $P < 0.01$). Additionally, pairwise Jost's D_{est} statistics (Jost 2008) were computed between sampling populations using R scripts, as outlined in Pennings *et al.* (2011), employing the packages *seqinr* v3.4.5 (Charif and Lobry 2007) and *ape* v5.1 (Paradis *et al.* 2004). Statistical significance ($P < 0.01$) was based on 10,000 permutations of the sequence data. Furthermore, a hierarchical analysis of molecular variance (AMOVA) was performed in ARLEQUIN, with 10,000 permutations to determine statistical significance ($P < 0.05$). The hypothesis of genetic homogeneity among groups was evaluated, using both global (all sampling populations treated separately) and

oceanic (populations grouped according to broad oceanic basins) datasets. A Benjamini-Hochberg (B-H) test was performed to correct for multiple comparisons.

The hypothesis of geographic distance limiting gene flow between sampling populations was assessed by performing a Mantel test (Mantel 1967) implemented in GENALEX v6.501 (Peakall and Smouse 2006), using Φ_{ST} estimates determined in ARLEQUIN as a measure of genetic distance, and geographic distance between sampling populations (in 1,000 km) measured in Google Earth Pro (<https://www.google.com/earth>) along the coast of the landmasses, as this was the most likely path of migration for this species.

3.2.5 Historical demographic analysis

The alignment of the mtCR were used to determine fluctuations in population sizes in the past in both the global and oceanic datasets by means of Fu's F_S (Fu 1997) and Tajima's D (Tajima 1989) neutrality tests, using 10,000 simulations of random data and $\alpha = 0.02$ and $\alpha = 0.05$, respectively, based on an infinite-site model without recombination as implemented in ARLEQUIN. These analyses assume no selective advantage between haplotypes and that significant mutational unbalance is associated with a recent population expansion event. Additionally, nucleotide mismatch distributions of the pairwise differences between pairs of haplotypes were determined for each sampling population and the oceanic regions based on 10,000 permutations in DNASP. Corresponding Harpending's raggedness (H_R) and sum of squared deviations (SSD) indices were calculated in ARLEQUIN to determine whether the observed mismatch distributions were drawn from an expanded population (small value) or a stationary one (large value) (Harpending 1994).

3.3 Results

3.3.1 Global genetic diversity

A total of 67 individuals sampled across the global distribution of the species were sequenced successfully for a fragment of the mtCR, and then trimmed to a final length of 571 bp. Analysis resulted in 15 polymorphic sites (seven of which were singletons and eight were parsimony

informative sites), which consisted of three transversions and twelve transitions, (**Table 3.1**). Eighteen haplotypes were recovered (**Table 3.2**), with an overall mean haplotype and nucleotide diversity of 0.867 and 0.00437, respectively. The genetic diversity displayed by the mtCR varied considerably between sampling regions (**Table 3.3**), with the lowest haplotype and nucleotide diversity in the MED ($h = 0.443$; $\pi = 0.00083$), and the highest in the SNEA ($h = 0.874$; $\pi = 0.00500$). The haplotype network representing the eight individual populations showed two main groups of haplotypes (haplogroups), with a single high frequency haplotype per group (H1, 19.40%; and H3, 28.36 %) separated by only two mutations and connected by a single low frequency haplotype (H11) (**Figure 3.2**). The first haplogroup consisted of all MED sampling populations, whereas the second consisted of all SAI sampling populations. However, individuals from the SNEA were represented in both haplogroups, with individuals from Guinea Bissau (GB) and Guinea (GC) being shared between haplogroups (H8 – H13), while Cape Verde (CV) was characterized by three private haplotypes (H5 – H7) nested within the southern hemisphere clade.

Table 3.1 Polymorphic nucleotide positions in *Mustelus mustelus* mtCR haplotypes. A dot indicates that the base at that position is the same as the base in haplotype 1.

Haplotypes	Nucleotide position														
H1	G	G	C	G	C	C	G	A	T	T	A	C	C	T	A
H2	.	.	.	A	T	T	.	.
H3	T	T	.	.
H4	.	.	T	T	T	.	.
H5	T	.	A	.	C
H6	.	C	.	.	T	.	A	.	C
H7	T	.	.	.	T	.	A	.	C
H8	C	.	T	T	T	.	.
H9	T	.	T	.	.
H10	C
H11	T	.	.
H12	G	C	.	T	T	T	.	.
H13	C	.	.	T	T	.	.
H14	T
H15	C
H16	T	C
H17	T	A	.
H18	T	T	T	.	.

Table 3.2 Geographic distributions of *Mustelus mustelus* haplotypes and the number of individuals from each sampling location.

Sampling population	<i>n</i>	<i>Mustelus mustelus</i> haplotype number																	
		1	2	3	4	5	6	7	8	9	10	11	12	13	14	15	16	17	18
Adriatic Sea	10	0	3	6	1	0	0	0	0	0	0	0	0	0	0	0	0	0	0
Strait of Sicily	8	0	2	5	0	0	0	0	0	0	0	0	0	0	0	0	0	0	1
Balearic Islands	8	0	0	8	0	0	0	0	0	0	0	0	0	0	0	0	0	0	0
Cape Verde	8	0	0	0	0	6	1	1	0	0	0	0	0	0	0	0	0	0	0
Guinea Bissau	9	1	0	0	0	0	0	0	4	2	1	1	0	0	0	0	0	0	0
Guinea	6	0	0	0	0	0	0	0	0	0	4	0	1	1	0	0	0	0	0
Angola	8	8	0	0	0	0	0	0	0	0	0	0	0	0	0	0	0	0	0
South Africa	10	4	0	0	0	0	0	0	0	0	0	1	0	0	2	1	1	1	0

Chapter III

Historic population structure

Table 3.3 Genetic diversity indices for *Mustelus mustelus* based on a 571 bp fragment of the mitochondrial control region. n – sample size; H – number of haplotypes; h – haplotype diversity; π - nucleotide diversity, k – average number of nucleotide changes.

Sampling location	n	H	h	π	k
<i>Mediterranean Sea (MED)</i>	26	4	0.443	0.00083	0.477
Adriatic Sea (AS)	10	3	0.6	0.00115	0.667
Strait of Sicily (SS)	8	4	0.607	0.00117	0.679
Balearic Islands (BI)	8	1	0	0	0
<i>Southern north-east Atlantic (SNEA)</i>	23	9	0.884	0.00508	2.946
Cape Verde (CV)	8	4	0.643	0.00127	0.75
Guinea Bissau (GB)	9	6	0.844	0.00379	2.2
Guinea (GC)	6	3	0.6	0.00296	1.733
<i>South-east Atlantic/south-west Indian (SAI)</i>	18	6	0.562	0.00164	0.948
Angola (AN)	8	1	0	0	0
South Africa (SA)	10	6	0.844	0.00275	1.622
Global	67	18	0.867	0.00437	2.498

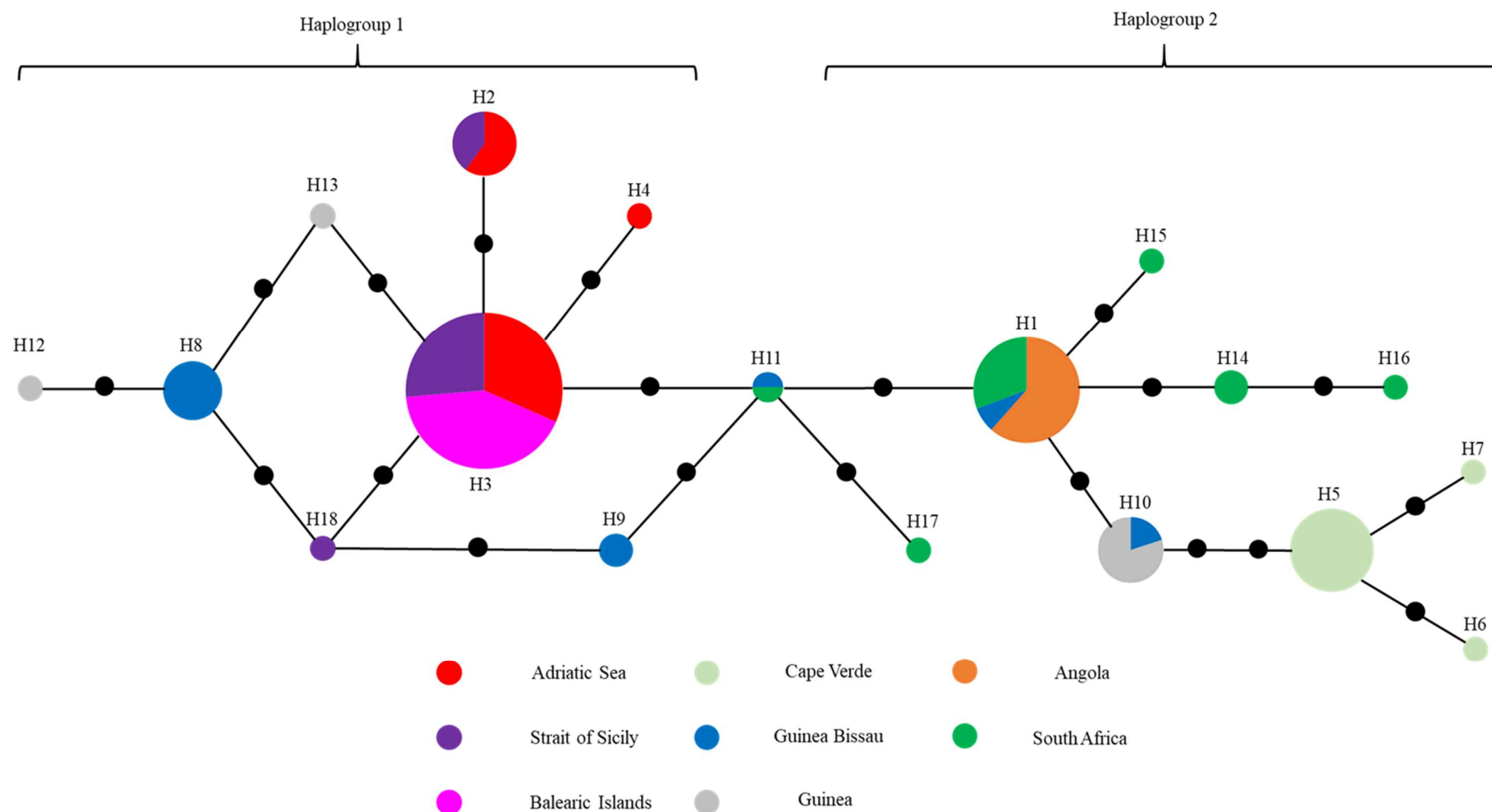


Figure 3.2 Median Joining haplotype network based on mitochondrial control region sequence data for global sampling populations of *Mustelus mustelus*, with mutations separating haplotypes indicated as slashes.

3.3.2 *Phylogenetic placement of Mustelus mustelus haplotypes*

Genetic distance between sampling populations was low (0.001 – 0.01, **Table S3.1**), indicating limited mutational events between populations. However, the reconstruction of phylogenetic relationships between sampling populations revealed clear distinctions between oceanic regions as well as sampling populations. Bayesian inference of phylogenetic relationships among *M. mustelus* haplotypes supported the existence of two main haplogroups, separated into northern and southern hemisphere groups, with moderate to high bootstrap support (**Figure 3.3**). Additionally, Maximum Likelihood (**Figure 3.4a**) and Maximum Parsimony (**Figure 3.4b**) trees coincided with the existence of two groups/clades, albeit with lower posterior probability support of the inferred haplotypes and haplogroups in relation to the BI tree.

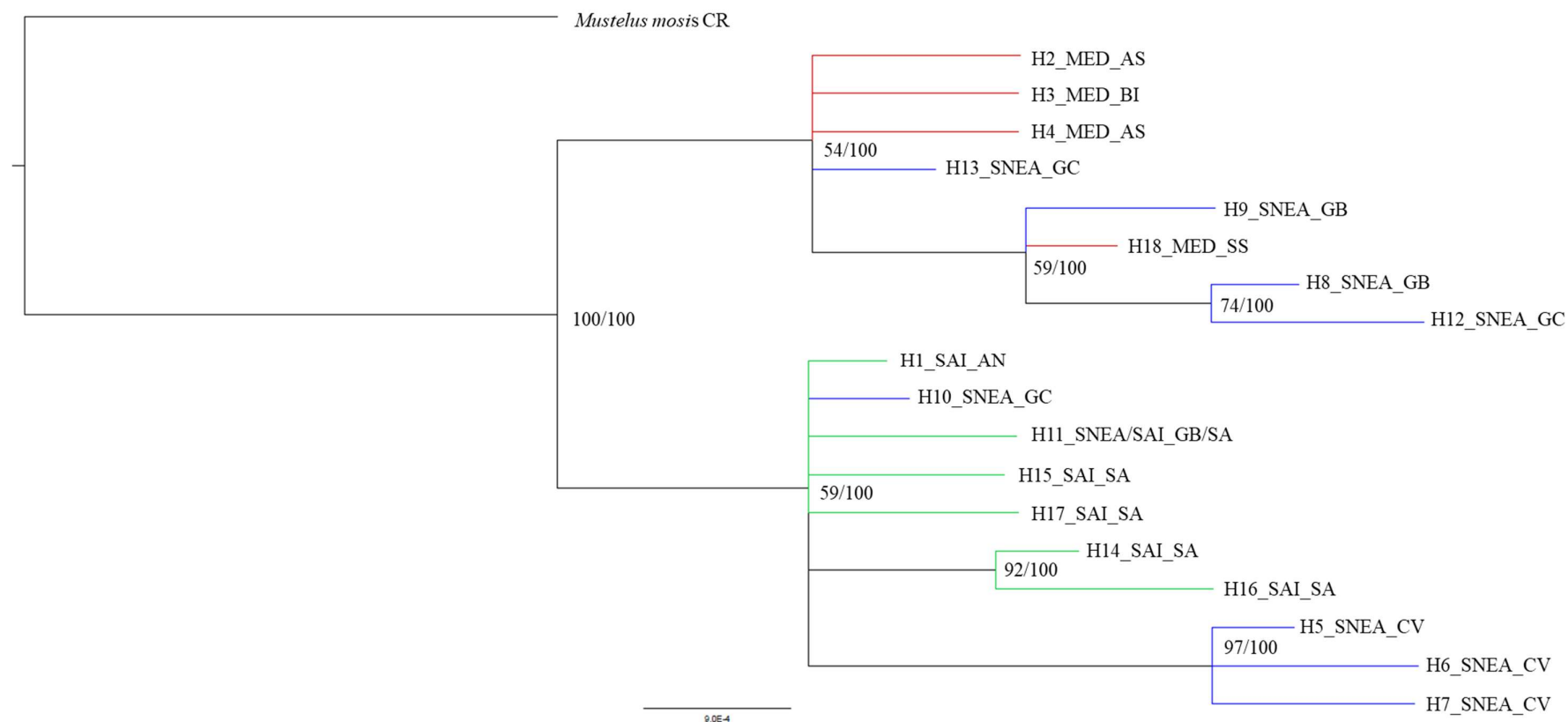


Figure 3.3 Bayesian Inference tree based on global sampling populations of *Mustelus mustelus*, with numbers on the tree indicating posterior probability. Red branches indicate haplotypes from the Mediterranean (MED), blue branches indicate haplotypes from southern north-east Atlantic (SNEA), and green branches indicate haplotypes from south-east Atlantic/south-west Indian (SAI) populations.

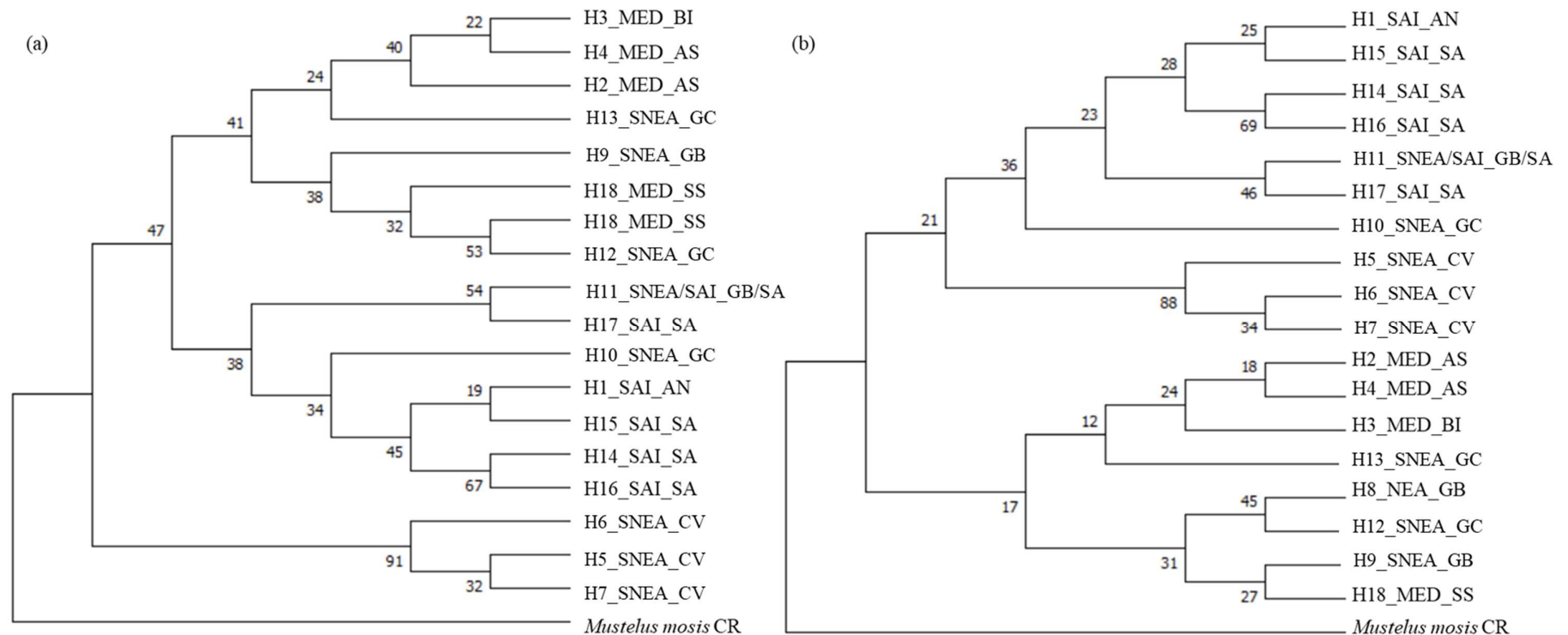


Figure 3.4 Maximum Likelihood (a) and Maximum Parsimony (b) phylogenies of global sampling populations of *Mustelus mustelus* based on a 571 bp fragment of the mitochondrial DNA control region. Both methods employed the Hasegawa, Kishino and Yano model of nucleotide substitution model with a number of invariable sites (HKY+I) to allow for non-uniformity of rates among sites. The reliability of the trees was tested using bootstrap analysis with 1,000 replicates (bootstrap values given at branching points).

3.3.3 Population divergence

The global dataset displayed high and statistically significant pairwise Φ_{ST} values (**Table 3.4**) ranging from 0.303 to 1.000 ($P < 0.01$), with the exception of populations within the MED and SAI. Pairwise D_{est} values (**Table S3.2**) indicated similar structuring patterns as the pairwise Φ_{ST} comparisons (**Table 3.4**), with significantly ($P < 0.01$) high levels of differentiation observed between the majority of sampling populations. A pattern of increasing geographic distance resulting in greater levels of genetic differentiation was observed between the oceanic regions (**Table S3.3**). However, no correlation was found between genetic and geographic distance, even when island populations (BI and CV) were excluded from the dataset (**Figure 3.5a, b**). The hierarchical AMOVA (**Table 3.5**) supports genetic discontinuity between the ocean basins, with significant divergence among oceans ($\Phi_{CT} = 0.427$, $P < 0.01$), within oceans ($\Phi_{SC} = 0.466$, $P < 0.01$), and within populations ($\Phi_{ST} = 0.694$, $P < 0.01$), and thus gene flow was either restricted by oceanic currents or physical distance between sampling populations.

Table 3.4 Genetic differentiation between eight sampling populations of *Mustelus mustelus* based on the mitochondrial control region. Φ_{ST} estimates below the diagonal.

	AS	SS	BI	CV	GB	GC	AN	SA
AS								
SS	-0.076							
BI	0.134	0.095						
CV	0.895*	0.895*	0.952*					
GB	0.377*	0.303*	0.384*	0.692*				
GC	0.645*	0.619*	0.718*	0.681*	0.181			
AN	0.846*	0.857*	1.000*	0.923*	0.526*	0.619*		
SA	0.627*	0.610*	0.676*	0.751*	0.392*	0.418*	0.080	

* indicates statistical significance at a 0.01 level; **bold values indicate statistical significance after B-H correction**

Table 3.5 Hierarchical analysis of molecular variance (AMOVA) for different grouping hypotheses of *Mustelus mustelus* based on separate sampling populations and broad oceanic regions

<i>Hypothesis tested</i>	<i>Source of variation</i>	<i>Variation (%)</i>	<i>Fixation index</i>
Panmixia	Among populations	65.85	$\Phi_{ST} = \mathbf{0.658^*}$
	Within populations	34.15	
Inter-oceanic	Among oceans	42.7	$\Phi_{CT} = \mathbf{0.427^*}$
	Within oceans	26.71	$\Phi_{SC} = \mathbf{0.466^*}$
	Within populations	30.6	$\Phi_{ST} = \mathbf{0.694^*}$

*indicates statistical significance at a 0.01 level; **bold values indicate statistical significance after B-H correction**

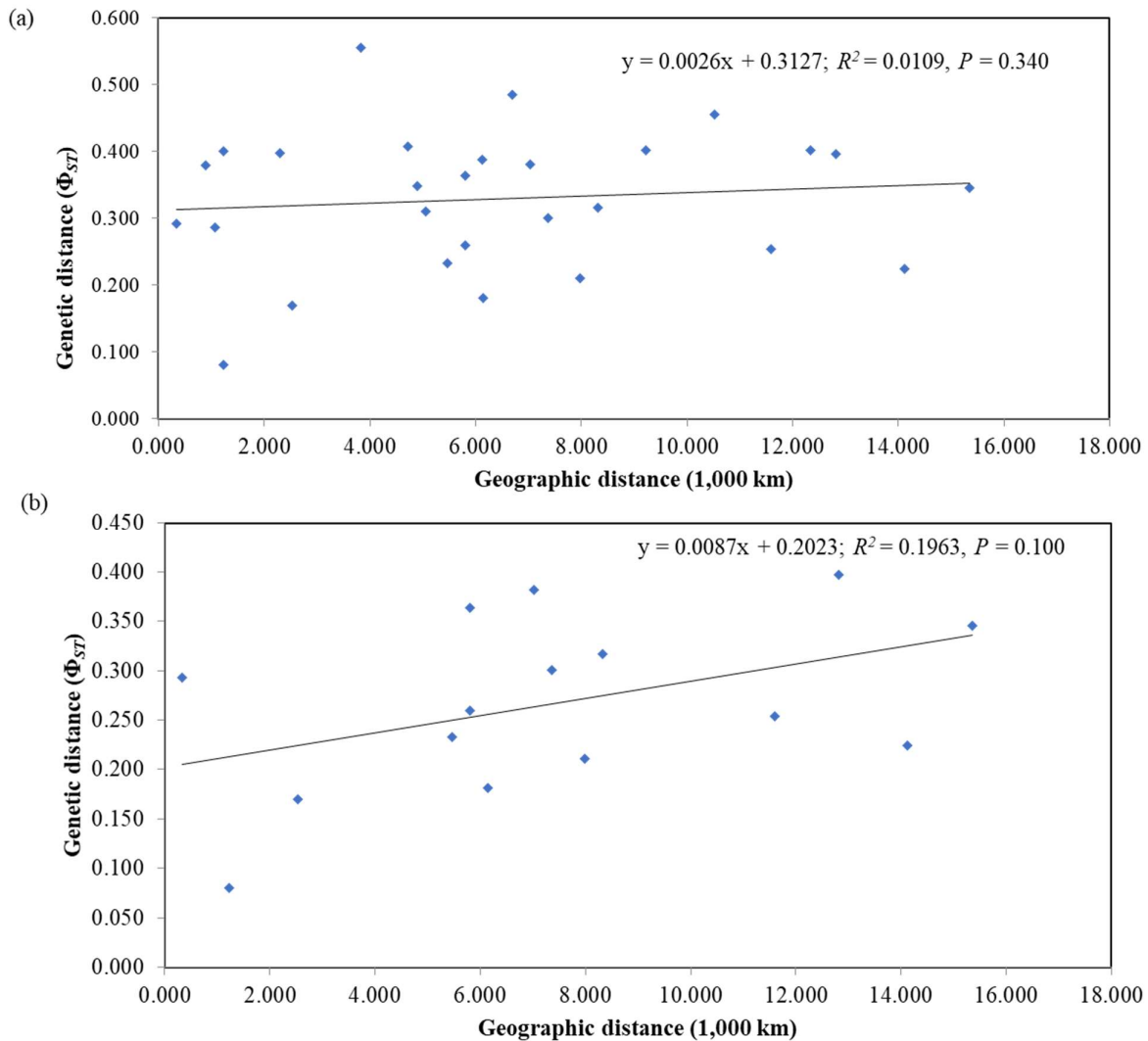


Figure 3.5 Isolation by distance assessment of global *Mustelus mustelus* sampling populations, (a) including all sampling populations, and (b) excluding island locations.

3.3.4 Demographic analyses of global *Mustelus mustelus* sampling population

Neutrality parameters (**Table 3.6**) were indicative of historical population expansions in the SA population (Fu's $F_s = -2.781$, $P = 0.006$), and the greater SAI oceanic region (Fu's $F_s = -3.016$, $P = 0.004$). This was further supported by the small, non-significant H_R and SSD values for both populations, indicating that the mismatch distributions for these groups were drawn from an expanding population. However, this model of expansion was rejected for the MED and SNEA populations, as estimates were not statistically significant for either Fu's F_s and/or Tajima's D statistic.

Chapter III

Historic population structure

Table 3.6 Demographic analysis parameters for mtCR sequences for global sampling populations and oceanic regions of *Mustelus mustelus*

<i>Populations</i>	<i>Fu's Fs</i>	<i>Tajima's D</i>	<i>H_R</i>	<i>SSD</i>
MED	-1.436 ($P = 0.074$)	-0.965 ($P = 0.190$)	0.164 ($P = 0.997$)	0.0107 ($P = 0.904$)
Adriatic Sea	-0.271 ($P = 0.304$)	-0.184 ($P = 0.348$)	0.240 ($P = 0.242$)	0.0373 ($P = 0.129$)
Strait of Sicily	-0.478 ($P = 0.134$)	-0.448 ($P = 0.356$)	0.241 ($P = 0.038$)	0.0377 ($P = 0.050$)
Balearic Islands	No polymorphism	No polymorphism	n.d	n.d
SNEA	-3.161 ($P = 0.058$)	0.728 ($P = 0.786$)	0.042 ($P = 0.399$)	0.0105 ($P = 0.401$)
Cape Verde	-0.999 ($P = 0.063$)	-1.310 ($P = 0.092$)	0.167 ($P = 1.000$)	0.0136 ($P = 0.000$)
Guinea Bissau	-0.848 ($P = 0.242$)	1.459 ($P = 0.957$)	0.086 ($P = 0.526$)	0.0249 ($P = 0.336$)
Guinea	0.758 ($P = 0.617$)	-0.057 ($P = 0.505$)	0.524 ($P = 0.227$)	0.134 ($P = 0.157$)
SAI	-3.016 ($P = 0.004$)	-1.343 ($P = 0.094$)	0.0569 ($P = 0.792$)	0.001 ($P = 0.667$)
Angola	No polymorphism	No polymorphism	n.d	n.d
South Africa	-2.781 ($P = 0.006$)	-0.783 ($P = 0.281$)	0.040 ($P = 0.198$)	0.129 ($P = 0.477$)

n.d - determined due to no sequence polymorphism for the population

3.4 Discussion

3.4.1 Genetic diversity

The mitochondrial control region (mtCR) has been suggested as a suitable marker to evaluate genetic diversity and population structure in animals, due to the uniparental mode of inheritance of the mitochondrion and high mutation rate within the region itself (Avice 2012). Furthermore, the high variability observed in this region within the Carcharhiniformes order (Chapter II) provides compelling evidence for its usage in the assessment of micro-evolutionary processes at work within this order of shark. Based on the results of this chapter, a high degree of haplotype diversity was observed across the global distribution of the species ($h = 0.867$). This level of diversity was comparable to that found for the mtCR for both coastal species, such as the scalloped hammerhead, *Sphyrna lewini* (Duncan *et al.* 2006), the lemon shark, *Negaprion brevirostris*, and the sicklefin lemon shark, *N. acutidens* (Schultz *et al.* 2008) and pelagic species, including the bull shark, *Carcharhinus leucas*, (Karl *et al.* 2011), the copper shark, *Carcharhinus brachyurus* (Benavides *et al.* 2011) and the tiger shark, *Galeocerdo cuvier*, (Bernard *et al.* 2016). Furthermore, the level of diversity found for *M. mustelus* in the current study is considerably higher than other *Mustelus* species: *M. antarcticus* ($h = 0.456$, $\pi = 0.0008$) and *M. lenticulatus* ($h = 0.531$, $\pi = 0.0009$) (Boomer *et al.* 2012). Given the movement patterns of *M. mustelus*, in that they are limited to continental shelves and thus lack pelagic movement potential (Smale and Compagno 1997), it was hypothesised that this species would be genetically heterogeneous, given the fragmented distribution of this shark on a global scale, in contrast to species characterised by a continuous distribution pattern (Grave 1998; Chabot and Allen 2009). A lack of connectivity between geographically distant populations would eventually result in the accumulation of unique alleles through the process of genetic drift. This was evident in the variation displayed between individual populations and oceanic regions, as the haplotype and nucleotide diversity deviated greatly from the overall diversity, particularly in the Mediterranean Sea (**Table 3.3**). Sampling populations in this oceanic region displayed the lowest estimates of genetic diversity

relative to other regions (Table 3.3), despite being the most represented region in terms of sample size in the present study.

The overall nucleotide diversity found for *M. mustelus* ($\pi = 0.00437$) was comparable to several coastal elasmobranch species assessed using the same marker. For instance, Duncan *et al.* (2006) observed a nucleotide diversity of $\pi = 0.0130$ in the global population of the scalloped hammerhead (*Sphyrna lewini*), while Keeney *et al.* (2005) reported π values at a maximum of 0.00214 for blacktip sharks (*Carcharhinus limbatus*) in the north-west Atlantic, Gulf of Mexico and Caribbean Sea. Additionally, two lemon shark species of the genus *Negaprion* were evaluated on a global scale, with π values of 0.00585 and 0.00056 for *N. brevirostris* and *N. acutidens*, respectively (Schultz *et al.* 2008). While these species are generally limited to coastal distribution patterns, *S. lewini* are known to be capable of oceanic dispersal (albeit rarely), which is suggestive of a higher dispersive ability than *M. mustelus*. Furthermore, *S. lewini* displayed genetic connectivity across larger distances (Duncan *et al.* 2006), which explains the higher nucleotide diversity of *S. lewini* relative to the above-mentioned species. In that sense, the moderate level of nucleotide diversity exhibited by *M. mustelus*, while not necessarily direct evidence of population size, still warrants careful management to conserve the genetic diversity of the species as a whole.

3.4.2 Patterns of genetic divergence

Recently, the historical biogeography of the genus *Mustelus* was assessed to infer the origin of this genus and the most probable mode of expansion from its point of origin (Maduna *et al.* in review). The study found that the genus most likely originated in the northern hemisphere, colonising in a southward direction through gradual range expansions, before two separate colonisation events of southern African waters resulted in the speciation events that gave rise to the current *Mustelus* species in this region (Maduna *et al.* in review). Furthermore, the study suggests that the west African coast was colonised independently from the Mediterranean Sea and southern Africa oceans (Maduna *et al.*

in review), which may explain the high diversity of the SNEA relative to the other ocean basins assessed in the present study.

The results of this chapter are largely in accordance with this hypothesis, with the existence of two main haplogroups coinciding with *M. mustelus* on opposite sides of the equator (**Figure 3.2**). Generally, it appears that the haplotypes are correlated to the sampling location of the individuals utilised in the study. Furthermore, the MED and SNEA populations form the more basal clade of the phylogeographic analysis (**Figure 3.3** and **Figure 3.4b**), which is in accordance with a northern hemisphere origin of the species, before expanding along the African coast, most likely after the opening of the Strait of Gibraltar *c.* 5.33 million years ago (MYA) (Loget and Van Den Driessche 2006), with the southern African populations being recently diverged from their northern hemisphere counterparts (approximately 2.45 MYA; Maduna *et al.* in review). This vicariant fragmentation is apparent based on the lack of shared haplotypes between the MED and SAI populations, even though these haplogroups are only separated by two mutation events and a single low frequency haplotype (H11), thus suggesting that these regions diverged due to geographical distance. Furthermore, the low mean genetic distance between sampling populations further supports the limited mutational events that separate sampling populations and oceanic regions, and therefore shallow divergence of the mtCR in the global sampling population of *M. mustelus* (**Table S3.3**). However, the Mantel tests did not reveal a significant correlation between genetic and geographic distance, even when island populations were excluded from the analysis (**Figure 3.5**). This may be attributed to the applicability of the marker type utilised for this analysis. A recent study by Teske *et al.* (2018) suggested that mtDNA is not as effective as nuclear loci, such as microsatellite markers or single nucleotide polymorphisms (SNPs), at detecting IBD. The authors attribute the failure of mtDNA in detecting IBD to a selection-driven reduction in genetic diversity obscuring spatial genetic differentiation, as well as only a single locus or marker being used to infer IBD, which would explain the rejection of the IBD model in the present study. Therefore, the hypothesis of IBD will be evaluated using

microsatellite markers (Chapter IV), in order to determine if mtDNA is unsuitable for detecting IBD, or if indeed there are no signatures of IBD in the global sampling population of *M. mustelus*.

The high level of inter-oceanic divergence between sampling populations indicated significant divergence between said populations and oceanic regions, with the results of the hierarchical AMOVA being suggestive of restricted connectivity within and between oceans ($\Phi_{SC} = 0.466$, $P < 0.01$; $\Phi_{CT} = 0.427$, $P < 0.01$). While this could be interpreted as evidence of IBD, as the physical distance between sampling populations is greater than 1,000 km in many cases, the non-significant correlation between genetic and geographic distance points to an alternative explanation, most likely the interplay between oceanographic features (currents and temperature gradients) and dispersal ability of this species. However, finer-scale analyses within the Mediterranean Sea and south-east Atlantic/south-west Indian regions revealed no structure using the mtCR (Table 3.4, Table S3.2).

There are three potential explanations for the lack of structure observed in the MED populations specifically. Firstly, the lack of divergence between populations could be indicative of gene flow between populations, in this case propagated by females exclusively, given the mode of inheritance of mitochondria (Avisé 2012). However, this would require these sharks to migrate across the open ocean in the case of the Balearic Islands (BI), which contradicts the movement patterns exhibited by this species. Secondly, the observed connectivity may be a result of the retention of ancestral polymorphisms, termed incomplete lineage sorting, similarly to what has suggested for the tope shark, *Galeorhinus galeus* (Bester-van der Merwe *et al.* 2017). Finally, and perhaps most worryingly, the lack of structure and lower levels of diversity based on the mtCR could be indicative of large declines in population size within the oceanic region. A study by Avisé *et al.* (1984) demonstrated that, in a stable population, there is an increased probability that all haplotypes in the population can be traced back to a single female after $4N_{ef}$ generations, where N_{ef} in this case refers to the effective population size of females. Therefore, reductions in population size or fluctuations in species abundance would accelerate the loss of unique female lineages, resulting in fewer female lineages in the present

population and subsequent shallow or no genetic architecture of the population on a mitochondrial level (Awise *et al.* 1984). To this point, a recent study conducted in the Mediterranean Sea documented broad-scale declines in abundance of smoothhounds (including *M. mustelus*) across their original distribution over the last century, due to unregulated fishing practices in the region (Colloca *et al.* 2017). Given the timescale investigated in the study by Colloca *et al.* (2017), the overexploitation of *M. mustelus* in the MED may have had significant effects on the genetic constitution of the species in this oceanic region.

Similar to the MED, the SAI population displayed no structure, although this can be explained by a recent colonisation of the southern African coast (Maduna *et al.* in review) rather than overexploitation, as recent assessments of the status of chondrichthyan fisheries in southern Africa revealed that these fisheries are relatively well managed and controlled in comparison to developed countries (da Silva *et al.* 2015). However, the assignment of all Angolan (AN) individuals to a single, shared haplotype (H1) with several South African (SA) individuals contradicts the findings of a previous study conducted in the region, which found three haplotypes within the AN population, of which two were unique, using the *NADH dehydrogenase subunit 4 (ND4)* gene (Maduna *et al.* 2016). Additionally, significant Φ_{ST} values were observed between three SA populations and the AN population (Maduna *et al.* 2016), illustrating a degree of divergence on a mitochondrial level, which was absent in the present study. While the results of the present study suggests female gene flow is occurring between these populations, when compared to the observations of the previous regional study (Maduna *et al.* 2016), a more likely explanation for the lack of mtDNA differentiation can be attributed to a lower rate of mutation in the mtCR relative to the *ND4*, which would lead to signatures

of shared ancestral lineages, or incomplete lineage sorting, as has been seen for several marine species (Grant and Bowen 1998; Cunha *et al.* 2012; DeBiasse *et al.* 2014).

3.4.3 Historical demography

The SA population, and the broader SAI oceanic region, were the only populations to display signatures of population expansion within the study, based on a statistically significant Fu's F_s value, and non-significant, small Harpending's raggedness (H_R) and sum of squared deviations (SSD) values, which indicates an expanding natural population and is in accordance with previous conclusions of population expansion in the same region (Maduna *et al.* 2016). This is further supported by the star-like pattern of the haplotype network, specifically within the southern hemisphere group (**Figure 3.2**). In the northern hemisphere, while the estimates were negative for MED and SNEA, they were not statistically significant, and thus population expansion or contraction cannot be confirmed in the current study for these areas, but were still indicative of the MED population being the “founder population”.

Future studies should aim to assess the locus-specific mutation rate for the mtCR in *M. mustelus* to accurately calibrate the molecular clock for the species in order to infer the evolutionary timescale at which the gene region diverged throughout its global distribution. Previous studies within the *Mustelus* genus (Boomer *et al.* 2012; Maduna *et al.* 2016; Maduna *et al.* in review) utilised the mutation rate of the mtCR in the scalloped hammerhead, *Sphyrna lewini* (Duncan *et al.* 2006) and the lemon shark, *Negaprion brevirostris* (Schultz *et al.* 2008) to calibrate a different mtDNA region (specifically, the *ND4* gene). However, this calls into question the accuracy of this approach (Ho *et al.* 2011), with several studies being hesitant to rely on the mutation rates themselves (Duncan *et al.* 2006; Keeney and Heist 2006).

3.5 Conclusions

To summarise, the findings reported in this chapter are in accordance with molecular evidence of a northern hemisphere origin and range expansion of the species. Significant mitochondrial genetic

differentiation between oceanic regions point to the limited dispersal ability of this shark and suggest that these oceanic populations diverged from one another over time. The data presented in this chapter also confirms concerning trends of population declines in the Mediterranean Sea, and that reassessments of *M. mustelus* within the region are warranted. Combining these results with an assessment of contemporary population dynamics (i.e. on a nuclear level) will allow for conclusions to be drawn regarding the overall genetic composition of these exploited shark populations in terms of short and long-term management and conservation.

CHAPTER IV

Contemporary population structure and demographics of *Mustelus mustelus* inferred from nuclear markers

Abstract

In marine animals, the genetic connectivity between spatially separated populations is correlated to dispersal ability of the species, which is influenced by the oceanographic features of areas inhabited by said species. Species characterised by limited dispersal ability are unable to migrate long distances, leading to the genetic differentiation of populations across large distances. It is thus important to identify genetic stocks, particularly in commercially important species with a cosmopolitan distribution. The common smoothhound shark, *Mustelus mustelus*, is an overexploited, commercially important marine resource fished heavily across its global distribution. Considering its wide-spread distribution and lack of genetic data in many regions of said distribution, this study aimed to assess the genetic variability and population connectivity of the species across nine species-specific microsatellite markers. Low to moderate levels of diversity (A_N : 2.3 – 4.4; H_E : 0.214 – 0.565) were observed between ocean basins, with high levels of inter-oceanic genetic differentiation inferred from pairwise F_{ST} (0.070 – 0.556, $P < 0.01$), hierarchical AMOVA, multivariate and Bayesian clustering analyses, with finer-scale clustering analyses alluding to the existence of six genetic stocks. For future sustainable harvesting of the common smoothhound, a cautious approach to the management of the species should be taken, as some regions appear to have a degree of connectivity despite being significantly differentiated. Ultimately, this chapter provides a baseline assessment for the global management of this threatened coastal shark.

4.1 Introduction

The sustainability of any fisheries is dependent on proper resource management that requires fisheries data captured both over time and space (Clarke *et al.* 2006). This could be problematic for species that share overlapping morphological characteristics or distribution ranges, and in some cases the distribution of these species' crosses country borders, entering different management or jurisdictions areas. Furthermore, different countries have different customs or cultures based around the fishing of marine species, ranging from the only source of income for a household in many developing countries (Diop and Dossa 2011), to broad-scale industrial harvesting to satisfy local or international fishing demands (Cavanagh and Gibson 2007). These diverse fishing practices complicates the acquisition of accurate catch data, resulting in incomplete stock assessments of species. While some species are capable of being fished sustainably, or can recover from this pressure over subsequent generations, elasmobranchs (sharks, rays and skates, henceforth referred to as sharks) are generally less fortunate. Sharks are characterised by *K*-selected life history traits, meaning that they grow and reach sexual maturity slowly, and only produce a few offspring per mating season after a long gestation period (Compagno 1984; Ebert *et al.* 2013), making them particularly vulnerable to anthropogenic effects (Stevens *et al.* 2000; Barker and Schluessel 2005). These life history traits, in conjunction with an expanding market for fins and other shark related products, driven largely by the Asian market, have resulted in increased fishing pressure on many species on a global scale (Clarke *et al.* 2006).

This fishing pressure, coupled with changes in the environment, could be detrimental to many species of shark, in particular to those that exhibit residency to unique and specific areas. A growing body of evidence suggests that species that remain genetically connected across entire ocean bodies generally display greater levels of diversity, and thus a greater resilience to fishing pressure and environmental changes (Frankham 2005). Therefore, populations of shark species with higher dispersal ability, such as the whale shark, *Rhincodon typus* (Schmidt *et al.* 2009) and the blue shark,

Prionace glauca (Veríssimo *et al.* 2017) will likely respond better to anthropogenic pressures imposed on them. Conversely, smaller-bodied sharks are generally unable to cross open-ocean waters, either due to their inability to overcome oceanic currents (Ovenden 2013), or their inability to withstand temperature changes (Simpfendorfer and Heupel 2004). This results in fragmented populations, over large and small geographic ranges, with lower overall diversity.

The integration of genetic information with conservation management of shark populations could allow for the identification of distinct populations that should be managed separately, termed Management Units (MUs) (Funk *et al.* 2012). Especially in the context of globally distributed species, the identification of MUs is of paramount importance, as the conservation of the species as a whole is affected by the way different countries manage a marine resource. Particularly, in small to medium sized species with a wider distribution, significant population structure has been observed across their ranges, such as for the blacktip shark, *Carcharhinus limbatus* (Keeney *et al.* 2005), the tope shark *Galeorhinus galeus* (Bester-van der Merwe *et al.* 2017) and the small-spotted catshark, *Scyliorhinus canicula* (Kousteni *et al.* 2015), which is suggestive of limited movement potential in these less vagile sharks.

Therefore, the aim of this chapter was to investigate the genetic diversity and population structure of the common smoothhound shark on a global scale, in order to assess the contemporary genetic health and connectivity of this species as a whole. Considering the vast geographic range and movement patterns of this shark, the hypothesis of geographic distance between sampling sites being the limiting factor of gene flow was investigated. Furthermore, it was expected that populations sampled at geographically isolated locations, such as islands far from the continental shore, would display a degree of genetic differentiation from other local populations, as these sharks are less likely to migrate across open oceans. Additionally, oceanographic features, such as currents and temperature fluctuations, have been found to have an effect on genetic connectivity in *M. mustelus* and other houndshark species (Maduna *et al.* 2016, 2017). Therefore, the hypothesis of oceanographic features,

particularly currents, influencing structuring patterns was investigated; firstly, considering all sampling sites as geographically separated collections, and secondly, separating sampling sites into three main basins, namely the Mediterranean Sea, southern north-east Atlantic, and south-east Atlantic/south-west Indian regions. Ultimately, this chapter broadens the understanding of the global contemporary dynamics of this threatened marine resource that can be used to facilitate reforms to fisheries management in areas in which this species is currently exploited.

4.2 Materials and methods

4.2.1 Sample collection and DNA extraction

Samples were collected from 2011 to 2017, covering the global distribution of *M. mustelus*. A total of 105 common smoothhound individuals were sampled onboard commercial fishing vessels and research surveys in the Mediterranean Sea (MED) the southern north-east Atlantic Ocean (SNEAO), the south-east Atlantic Ocean (SEAO), and the south-west Indian Ocean (SWIO) (**Figure 4.1**). Adriatic individuals were obtained from local fisheries, during surveys or at the fish market of Chioggia, where the landings of the major fishing fleet of the basin occur (Mazzoldi *et al.* 2014). Sicilian samples were collected both from trawl surveys (i.e. MEDITS: International Bottom Trawl Survey in the Mediterranean) and commercial landings of the Mazara del Vallo fishing fleet (Marino *et al.* 2017). Samples from the southern north east Atlantic were collected during research cruises undertaken between 2011 and 2012 by the Institute of Marine Research (collector: Diana Zaera-Perez). Fishing permits for the southern African samples were originally issued by the Department of Agriculture, Forestry and Fisheries (DAFF, Republic of South Africa). Samples were also collected on the R.S Ellen Khuzway during National Shark surveys, as well as during research fishing trips conducted within the Port of Ngqura between 2014 and 2017. However, to avoid the introduction of sampling bias through the over-representation of a single geographic location, individuals from South Africa were subsampled across both ocean basins. Due to the nature in which these samples were

obtained, phenotypic data, such as size, sex and maturity, were not available for all individuals sampled.

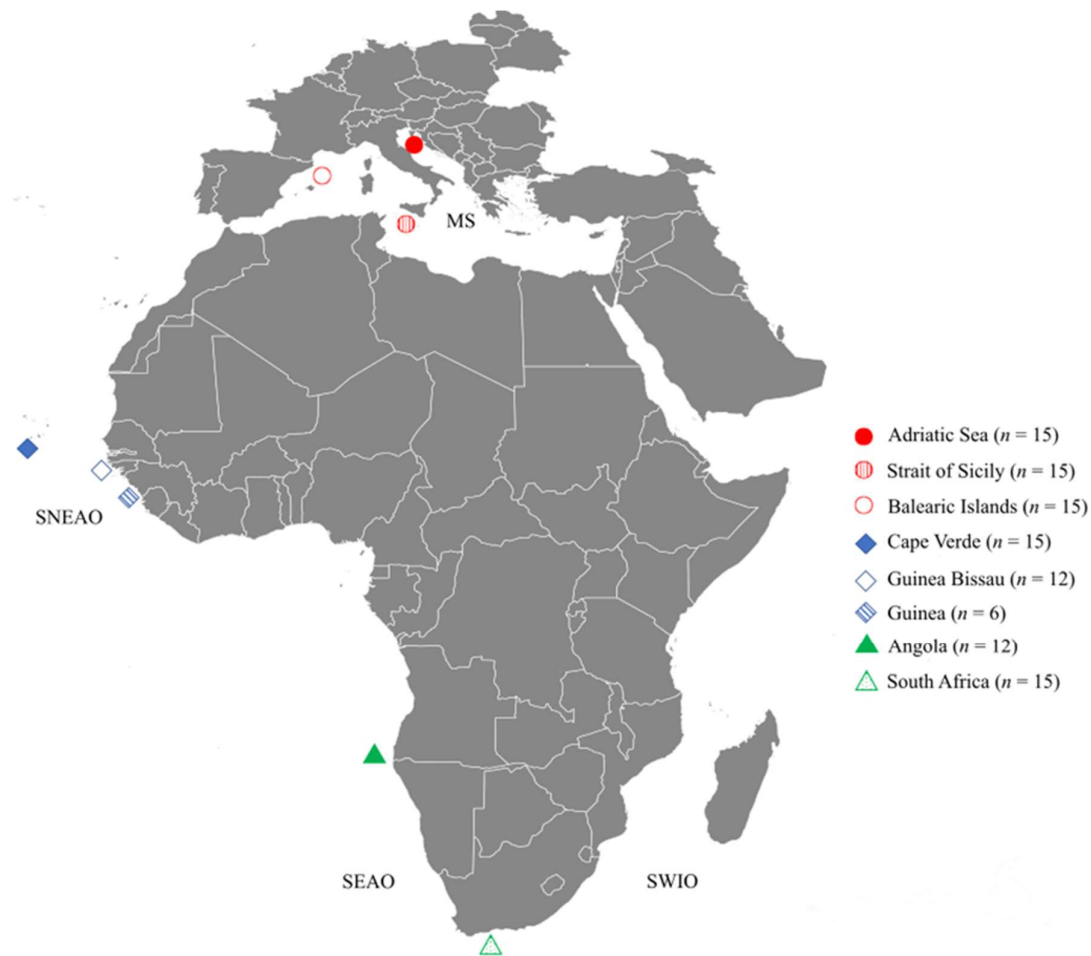


Figure 4.1 Global sampling sites of the common smoothhound in the Mediterranean (circles), southern north-east Atlantic (diamonds) and south-east Atlantic/south-west Indian Oceans (triangles) populations, with sample size and oceans indicated. MS – Mediterranean Sea; SNEAO – southern north-east Atlantic Ocean; SEAO – south-east Atlantic Ocean; SWIO – south-west Indian Ocean.

Fin clips were stored in 95% ethanol and were kept at room temperature until further use. Genomic DNA was isolated from the tissue samples using a modified cetyl trimethylammonium bromide (CTAB) extraction method (Sambrook and Russell 2001). Extracted DNA was quantified using a Nanodrop 2000 Spectrophotometer, adjusted to a working concentration of 50 ng/μl with distilled deionised water (ddH₂O) and stored at -20°C.

4.2.2 *Microsatellite amplification*

Nine species-specific microsatellite markers previously optimized into multiplex panels (Maduna *et al.* 2017) were amplified in a total of 105 individuals. Each multiplex reaction consisted of 50 ng of template DNA, 5 µl QIAGEN Multiplex Kit, and 1 µl 10X primer mix (2 µM per primer) in a total volume of 10 µl. Polymerase Chain Reaction (PCR) cycling conditions included an initial denaturation phase at 95°C for 15 minutes, followed by 35 cycles including denaturation at 94°C for 30 seconds, annealing at the respective annealing temperatures (T_A) of the primers for 90 seconds (**Table S4.1**), extension at 72°C for 60 seconds, and the PCR was concluded with a final extension phase at 60°C for 30 minutes. Amplification products were separated on a 2% w/v agarose gel for 30 minutes at 100V to confirm successful amplification at the expected fragment size. Amplicons were then diluted in a 1:1 ratio with ddH₂O and sent to the Central Analytical Facility (CAF) at Stellenbosch University for automated capillary electrophoresis. GENEMAPPER v5.0 (Applied Biosystems) was used for binning and scoring of microsatellite alleles.

4.2.3 *Genetic diversity analyses*

Microsatellite genotypes were evaluated for stuttering, allelic dropout and the presence of null alleles while the frequency of null alleles per locus per population were calculated using MICROCHECKER v2.2.3 (Van Oosterhout *et al.* 2004). GENEPOP ON THE WEB v4.2 (Rousset 2008) was used to test for between-loci linkage disequilibrium (LD) within and across sampling populations and for loci deviating from Hardy-Weinberg Equilibrium (HWE) expectations (10,000 dememorisations, 100 batches, and 10,000 iterations per batch). The inbreeding coefficient (F_{IS}) for each sampling population and oceanic region were also estimated in GENEPOP. Markers were also tested for selection in ARLEQUIN v3.5.2 ($P < 0.01$) (Excoffier and Lischer 2010). Genetic diversity indices were calculated for two datasets: 1) sampling populations treated separately (global dataset) and 2) sampling populations grouped into broad geographic regions (oceanic dataset). This included the average number of alleles per locus (A_N), the effective number of alleles per locus (A_E), the number

of private alleles per locus (A_P), observed and expected heterozygosity (H_O and H_E), Shannon's index (I), and fixation index (F) calculated in GENALEX v6.501 (Peakall and Smouse 2006). Polymorphism information content (PIC) of each marker was determined in MSATTOOLS v3.1.1 (Park 2001). The rarefied allelic richness per locus (A_R) was calculated for both datasets in HP-RARE (Kalinowski 2005). A Kruskal-Wallis test was performed in XL STATISTICS v2016.5 (Carr 2010) to evaluate the significance ($P < 0.05$) of the variation in genetic diversity estimates between any of the sampling sites.

4.2.4 Genetic structuring analyses

Pairwise F_{ST} and significance (9,999 permutations, $P < 0.01$) were calculated for both the global and oceanic datasets, and were based on observed allelic frequencies, as calculated in GENALEX. A Benjamini-Hochberg (B-H) test was performed to correct for multiple comparisons. The genetic clustering patterns among sampling populations were evaluated using two clustering methods; firstly, a multivariate discriminant analysis of principal components (DAPC) was performed, utilizing the K -means method (Jombart *et al.* 2010), available in the R package *adegenet* (Jombart 2008). Prior to running the DAPC, the alpha score was estimated to determine the optimal number of principal components (PCs) to retain. The K -means method was run for $K = 1 - 15$, and the best K value was determined based on where the Bayesian Information Criterion (BIC, Schwarz 1978) graph begins to plateau (Jombart *et al.* 2010). The DAPC was performed using the most likely K value and first six PCs explaining approximately 80% of the variance, as well as using location information as a prior. Secondly, a Bayesian clustering analysis was implemented in the program STRUCTURE v2.3.4 (Pritchard *et al.* 2000), assuming an admixture ancestry model with independent allelic frequencies. Ten replicates were run for each K tested ($K = 1 - 15$), using a 50,000 burn-in followed by 500,000 steps where data points were retained. The best K -value was chosen based on six statistical tests employed by the program STRUCTURESELECTOR (Li and Liu 2018), namely Delta K , the corrected Evanno statistic ($\text{Ln Pr}(X|K)$) (Evanno *et al.* 2005), and the four tests of Puechmaille (2016),

namely *MedMedK*, *MedMeaK*, *MaxMedK* and *MaxMeaK*. Assignment plots were generated and visualized using the web service software CLUMPAK (Kopelman *et al.* 2015). To test whether genetic differentiation between sampling populations is correlated to the geographical distance, a Mantel test (Mantel 1967) was conducted in GENALEX v6.501, with linearised pairwise F_{ST} estimates representing genetic distance between sampling populations, and geographical distance (in 1,000 km) measured in Google Earth Pro (<https://www.google.com/earth>) along the coast of the landmasses. This analysis was performed twice, first including all sampling populations, and second excluding island locations.

Finally, a hierarchical analysis of molecular variance (AMOVA) was performed in ARLEQUIN v3.5.2, with 10,000 permutations to determine statistical significance, to test the hypothesis of genetic homogeneity among groups, using both global (all sampling populations treated separately) and oceanic (populations grouped according to broad ocean basins) datasets.

4.2.5 Demographic analyses

The program BOTTLENECK v1.2.02 (Cornuet and Luikart 1996) was used to determine if any of the sampling populations have experienced recent reductions in N_E . This was performed by calculating the expected heterozygosity from allele frequencies for each sampling population, and comparing these estimates to the expected equilibrium heterozygosity (1,000 permutations). To evaluate mutation drift equilibrium, three mutational models were applied: the infinite allele model (IAM), stepwise mutational model (SMM), and two-phase model (TPM) with 95% single-step mutations and 5% multiple-step mutations (multiple-step mutation variance of 12; significance testing: Wilcoxon signed-rank test).

To better understand the impact of oceanographic features on dispersal ability of *M. mustelus*, several migration models were evaluated, using the program MIGRATE-N (Beerli and Palczewski 2010). Sampling populations were separated into three oceanic regions (MED, SNEA, and SAI) to determine the degree of gene flow between the populations in these basins. In general, two models

were tested for all oceanic regions: 1) a full model with distinct populations, with migration to and from each population; 2) a model assuming complete panmixia between all populations. For the MED and SNEA regions, two additional models were tested: 3) a model assuming migration from island locations (BI or CV) to the other populations along the continental shelves; and 4) a model assuming migration to island locations from continental shelves. For the SAI region, asymmetric gene flow between AN and SA was assessed, assuming 3) migration from AN to SA; and conversely 4) migration from SA to AN. The mutation scaled effective population size $\Theta = 4N_E\mu$, where N_E is the effective population size and μ is the mutation rate per generation per locus, and mutation- scaled migration rates $M = m/\mu$, where m is the immigration rate per generation, among regions was also calculated in MIGRATE-N. A Brownian process was used to model microsatellite mutations and run using random genealogy and values of the parameters Θ and M produced by F_{ST} calculation as a starting condition. Bayesian search strategy was conducted using the following parameters: an MCMC search of 5×10^5 burn-in steps followed by 5×10^6 steps with parameters recorded every 1,000 steps. A static heating scheme with four different temperatures (1.0, 1.5, 3.0 and 1×10^6) was employed, where acceptance–rejection swaps were proposed at every step.

4.3 Results

4.3.1 Global genetic diversity

In total, 105 individuals were successfully genotyped for nine species-specific markers, with the average number of alleles ranging from 1 to 10 per marker (**Table S4.2**). Genotypic patterns associated with null alleles, as well as high fixation indices were detected at several loci, with null allele frequencies reaching a maximum of 0.30 for locus *Mmu3* (**Table S4.2**). Across all sampling populations, several loci deviated from HWE, although no significant deviations from neutrality or linkage disequilibrium were observed for these markers, and this deviation was attributed to fixation of alleles at these loci. However, locus *Mmu7* showed evidence for null alleles, deviations from the HWE, and linkage disequilibrium ($P < 0.01$) only in the Guinea Bissau population. However, no

difference in results were obtained when this locus was excluded, thus all nine loci were retained for downstream analyses.

Genetic diversity estimates were low to moderate for the global sampling populations of *M. mustelus* (**Table 4.1, Figure 4.2**), with the south-east Atlantic/south-west Indian (SAI) generally displaying the greatest genetic diversity ($N_A = 3.9$; $A_R = 3.2$; $H_E = 0.454$), whereas the southern north-east Atlantic (SNEA) populations were characterised by the lowest diversity ($N_A = 2.9$; $A_R = 2.6$; $H_E = 0.325$). Inbreeding coefficients indicated increased levels of homozygosity in both Mediterranean (MED) and SNEA (F_{IS} : 0.428 and 0.209, respectively; $P < 0.05$), whereas populations in SAI displayed lower levels of homozygosity than their northern counterparts (F_{IS} : 0.029, $P < 0.05$).

Chapter IV

Contemporary population structure

Table 4.1 Genetic diversity indices for global sampling populations of *Mustelus mustelus* based on nine microsatellite loci. n – sample size; A_N – mean number of alleles per locus; A_R – allelic richness; H_E – expected heterozygosity; F_{IS} – inbreeding coefficient.

Sampling location	n	A_N	A_R	H_E	F_{IS}
<i>Mediterranean</i>	45	3.5	2.84	0.374	0.428
Adriatic Sea	15	2.9	2.16	0.306	0.464
Strait of Sicily	15	4.4	3.00	0.488	0.245
Balearic Islands	15	3.2	2.28	0.326	0.240
<i>Southern north-east Atlantic</i>	33	2.9	2.63	0.325	0.209
Cape Verde	15	2.3	1.71	0.214	-0.229
Guinea Bissau	12	3.3	2.54	0.419	-0.067
Guinea	6	2.9	2.54	0.341	-0.099
<i>South-east Atlantic/south-west Indian</i>	27	3.9	3.18	0.454	0.029
Angola	12	3.6	2.45	0.342	-0.218
South Africa	15	4.2	3.20	0.565	-0.066
Global	105	3.4	2.50	0.375	0.028

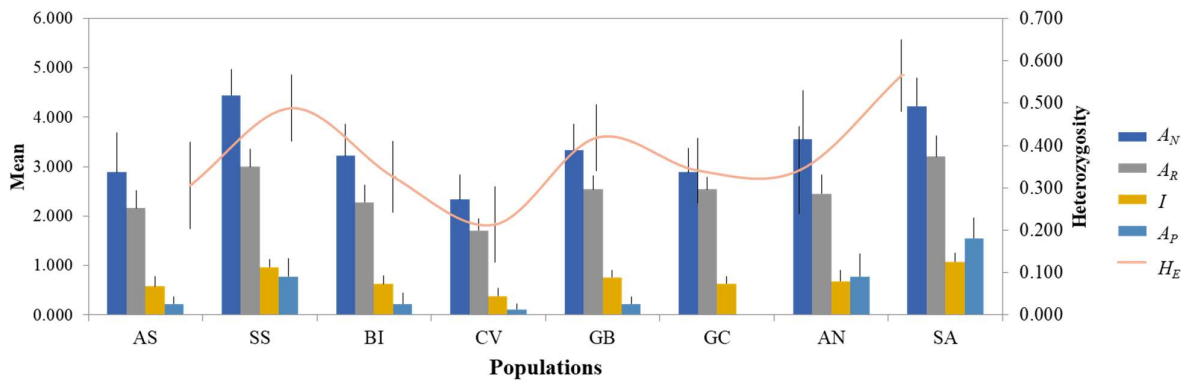


Figure 4.2 Graphical representation of mean genetic diversity estimates for each sampling population using nine microsatellite loci. A_N = number of alleles; A_R = allelic richness (rarefied); I = Shannon's Index; A_P = private alleles; H_E = expected heterozygosity

4.3.2 Spatial patterns of genetic differentiation

Pairwise F_{ST} estimates ranged from 0.070 to 0.556 ($P < 0.01$), indicating a large degree of genetic differentiation between all populations and geographical regions (**Table 4.2**), with differentiation increasing as geographic distance between sampling locations (**Table 4.2**) or oceanic regions increased (**Table S4.3**). However, no correlation was found between genetic and geographic distance, including all populations ($R^2 = 0.0034$, $P = 0.415$) and when excluding island locations ($R^2 = 0.1860$, $P = 0.070$), although a positive correlation was observed for both comparisons (**Figure 4.3**). Furthermore, the hierarchical AMOVA (**Table 4.3**) supported genetic differentiation across all levels, with significant differentiation amongst oceans ($F_{CT} = 0.125$, $P < 0.01$), within oceans ($F_{SC} = 0.270$, $P < 0.01$), and within populations ($F_{ST} = 0.362$, $P < 0.01$).

The large degree of genetic differentiation between individual sampling populations was also supported by the clustering analyses. The multivariate DAPC resulted in an optimal number of clusters being identified as six using the K -means method (**Figure 4.4**), which illustrated three broad clusters corresponding to the three ocean basins with further subdivision within each basin. Additionally, the Bayesian clustering analysis revealed a variety of clustering patterns, including $K = 3$ (Delta K), $K = 5$ (MedMed/MedMean K), $K = 6$ (MaxMed/MaxMean K), and $K = 7$ (Ln Pr($X|K$))

(**Figure 4.5**). The pattern of structuring based on the Delta K method provided clear distinctions between the MED, SNEA and SAI basins, which supports the hierarchical AMOVA results of inter-oceanic differentiation ($F_{CT} = 0.125$, $P < 0.01$). However, finer-scale structuring was observed within the three oceans ($K = 5$ and $K = 6$), revealing genetically distinct island locations (Cape Verde, CV; Balearic Islands, BI) from the coastal populations of *M. mustelus*, which coincides with the statistically significant, high pairwise F_{ST} estimates (**Table 4.2**). At $K = 7$, an additional cluster was observed within the South African (SA) population, further differentiating SA from Angola (AN). Additionally, the low level of differentiation ($F_{ST} = 0.070$, $P = 0.001$) between the Adriatic Sea (AS) and Strait of Sicily (SS) populations was supported by the assignment of these populations to a single genetic cluster, both in the multivariate DAPC and Bayesian STRUCTURE analyses (**Figure 4.4** and **Figure 4.5**).

Table 4.2 Genetic differentiation estimates for global sampling locations of *Mustelus mustelus*. F_{ST} estimates below the diagonal.

	AS	SS	BI	CV	GB	GC	AN	SA
AS								
SS	0.070*							
BI	0.392*	0.281*						
CV	0.384*	0.347*	0.556*					
GB	0.372*	0.253*	0.402*	0.378*				
GC	0.288*	0.172*	0.308*	0.408*	0.289*			
AN	0.393*	0.252*	0.456*	0.489*	0.362*	0.240*		
SA	0.343*	0.223*	0.403*	0.406*	0.316*	0.216*	0.175*	

* statistical significance at a 0.01 level; **bold values indicate statistical significance after B-H correction**

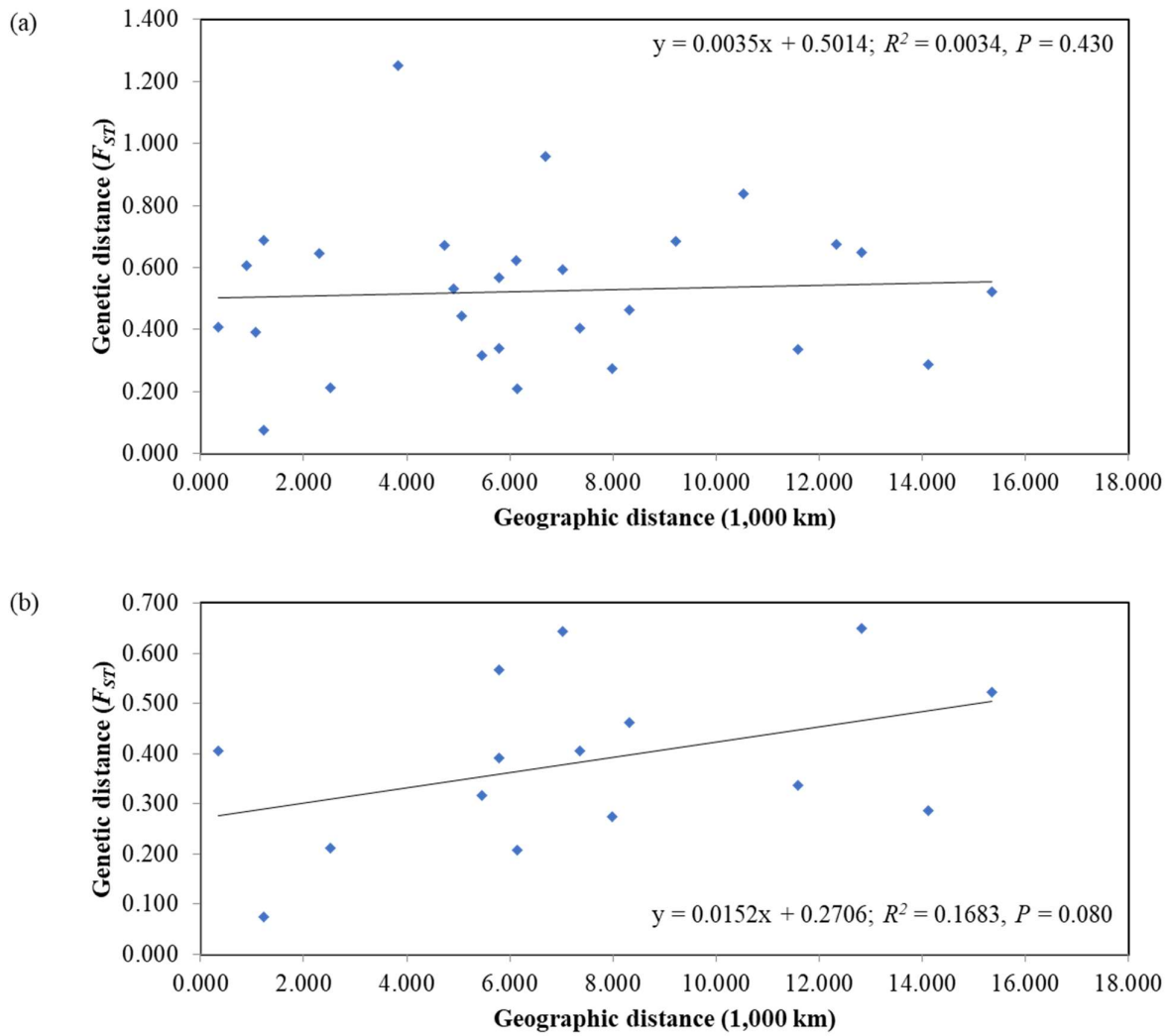


Figure 4.3 Isolation by distance (IBD) scatter plots using geographic distance in 1,000 km and genetic distance measured by linearised pairwise F_{ST} estimates, with (a) all sampling populations and (b) excluding island populations.

Table 4.3 Hierarchical analysis of molecular variance (AMOVA) results for different structuring hypotheses of *Mustelus mustelus* based on separate sampling populations and different ocean basins.

<i>Hypothesis tested</i>	<i>Source of variation</i>	<i>Variation (%)</i>	<i>Fixation index</i>
Panmixia	Among populations	34.09	$F_{ST} = \mathbf{0.341}^*$
	Within populations	65.91	
Inter-oceanic	Among oceans	12.52	$F_{CT} = \mathbf{0.125}^*$
	Among populations within oceans	23.64	$F_{SC} = \mathbf{0.270}^*$
	Within populations	63.85	$F_{ST} = \mathbf{0.362}^*$

* statistical significance at 0.01 level; **bold values indicate statistical significance after B-H correction**

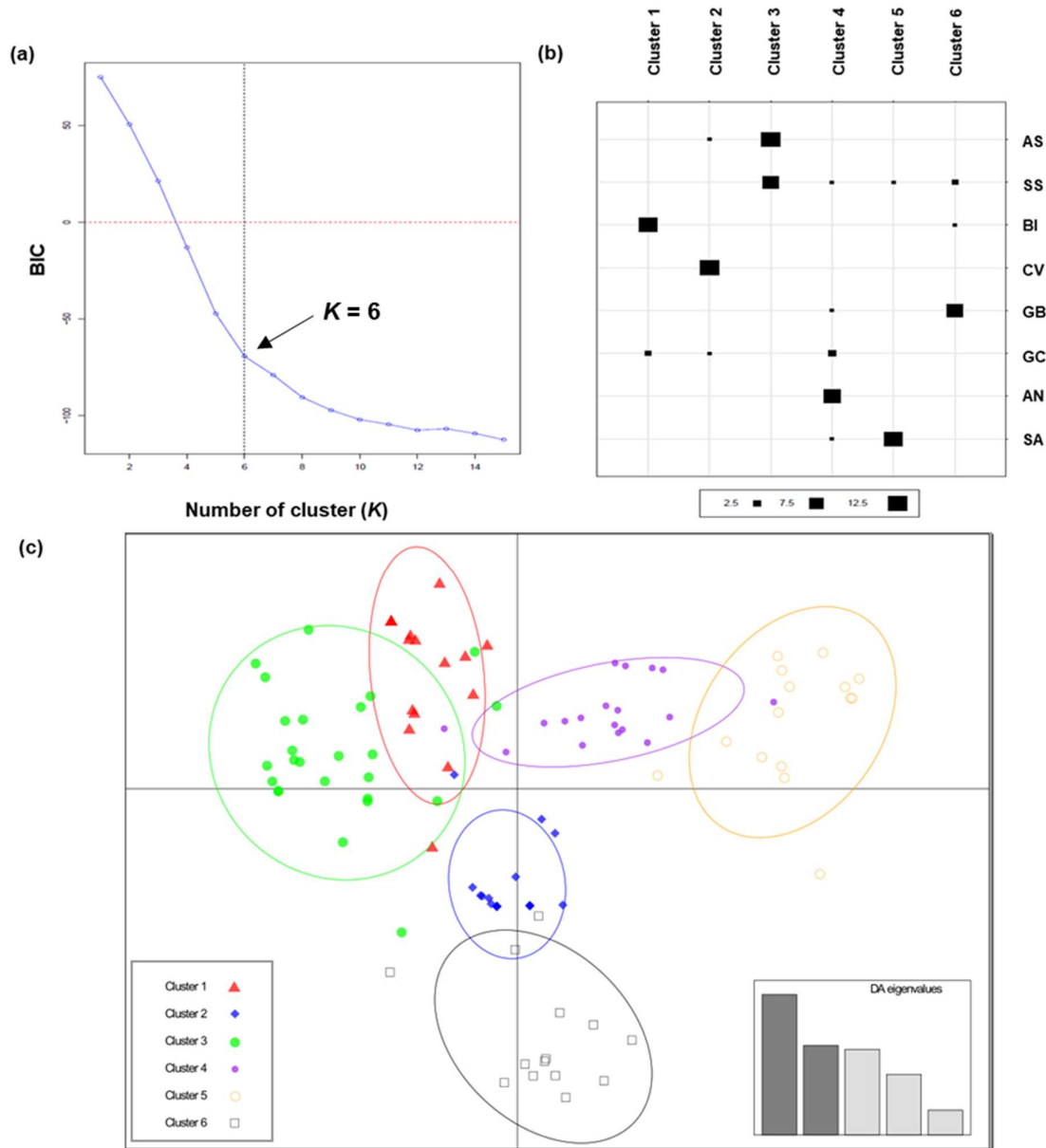


Figure 4.4 Discriminant Analysis of Principal Components (DAPC) analysis of global *Mustelus mustelus* populations. (a) Inference of the number of genetic clusters based on BIC statistic. (b) Assignment of individuals from their respective populations to genetic clusters, with the size of the square correlated to number of individuals assigned to a cluster. (c) Scatterplot illustrating clustering patterns on a global scale, with the colour and shape of each data point representing a genetic cluster as defined in (b).

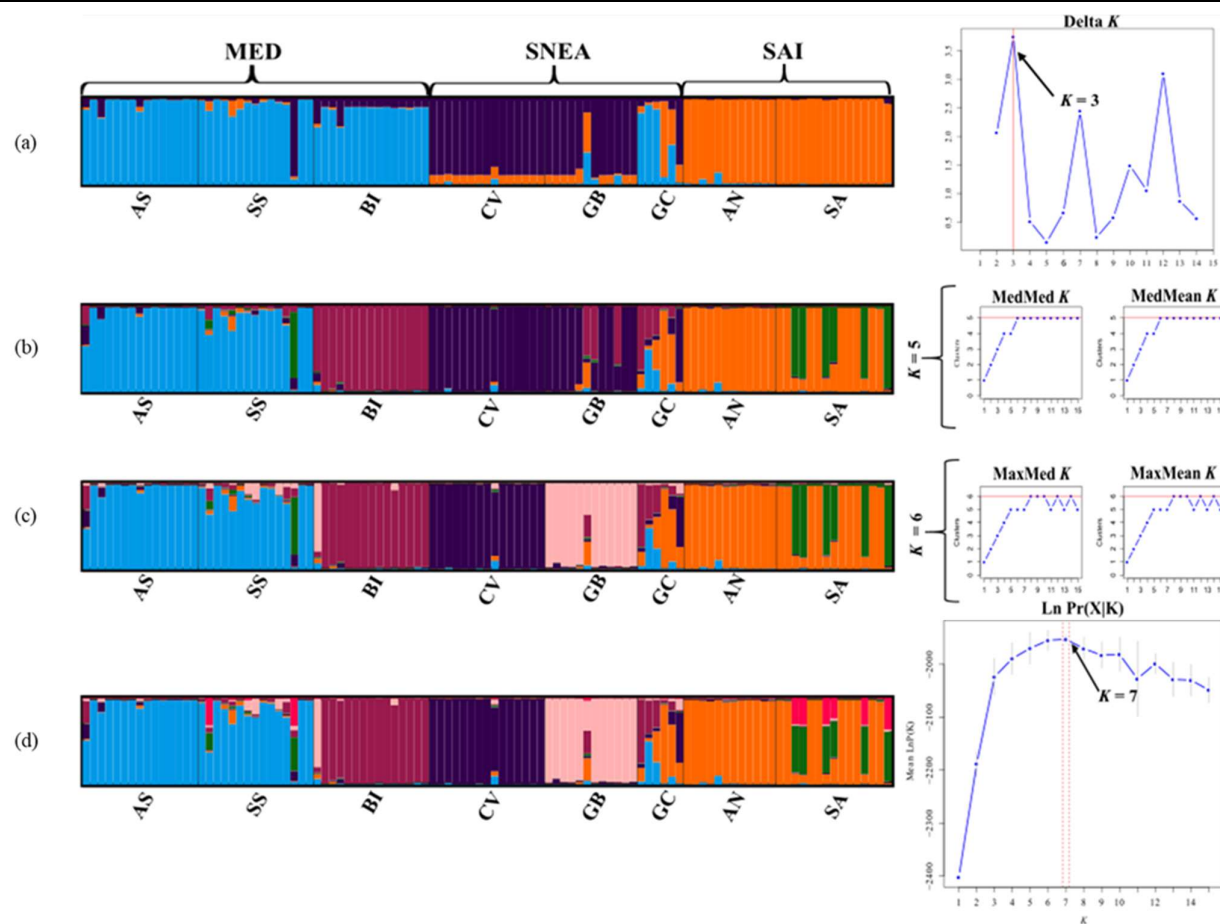


Figure 4.5 Genetic structure of *Mustelus mustelus* based on Bayesian clustering analyses for $K = 3$ to $K = 7$, using six analytical methods [(a) $K = 3$ –Delta K (Evanno *et al.* 2005); (b) $K = 5$ – MedMed K , MedMea K ; (c) $K = 6$ – MaxMed K , MaxMea K (Puechmaille 2016); (d) $K = 7$ – Ln $\Pr(X|K)$ (Evanno *et al.* 2005)].

4.3.3 *Demographic assessment of *Mustelus mustelus**

The majority of sampling populations displayed signatures of past bottleneck events under several mutational models (**Table 4.4**), which is suggestive of broad-scale declines in population size of the meta-population as a whole. Furthermore, four migration models were assessed for each ocean basin. For the MED populations, the full migration model ranked highest and was most likely, with asymmetric gene flow between all pairs of the three sampling populations (**Table 4.5**). In the SNEA basin, the most likely model of migration indicated gene flow from the island of Cape Verde to the coastal sampling populations (**Table 4.6**) while the most likely migration model for the SAI basin was a full migration model, with a net gene flow from South Africa to Angola (**Table 4.7**).

Table 4.4 Bottleneck test (Wilcoxon) of global *Mustelus mustelus* sampling populations under three mutational models; infinite allele model (IAM), two-phase model (TPM), and stepwise mutational model (SMM).

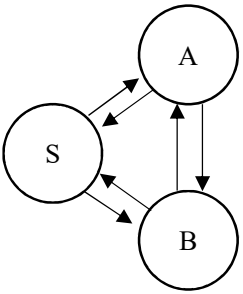
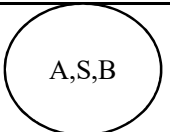
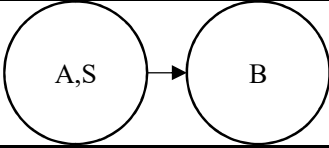
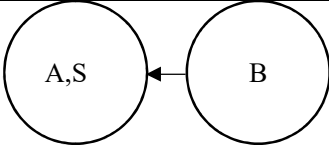
<i>Parameter</i>	<i>AS</i>	<i>SS</i>	<i>BI</i>	<i>CV</i>	<i>GB</i>	<i>GC</i>	<i>AN</i>	<i>SA</i>
<i>Sample size</i>	15	15	15	15	12	6	12	15
<i>Wilcoxon test</i>								
<i>IAM</i>	n.s.	n.s.	n.s.	n.s.	n.s.	< 0.05	n.s.	< 0.05
<i>TPM</i>	n.s.	< 0.05	< 0.05	< 0.05	n.s.	< 0.05	< 0.05	n.s.
<i>SMM</i>	n.s.	< 0.05	< 0.05	< 0.05	n.s.	< 0.05	< 0.05	n.s.

n.s. = not significant

Chapter IV

Contemporary population structure

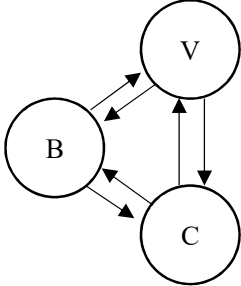
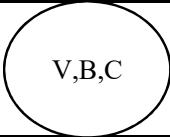
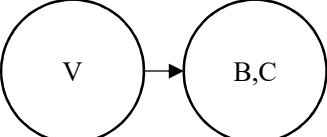
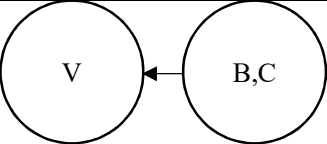
Table 4.5 Log Bayes Factor (LBF) using thermodynamic integration of different gene flow models M_i compared with Model 1 for three sampling regions of *Mustelus mustelus* within the Mediterranean Sea (A: Adriatic Sea; S: Strait of Sicily; B: Balearic Islands); p_{M_i} - model choice probability; lmL - log marginal likelihood.

Model	Parameters (97.5% CI)	Bézier lmL	LBF for model	Model rank	p_{M_i}
1 	$\Theta_A = 0.484$ (0.413 – 0.500) $\Theta_S = 0.492$ (0.439 – 0.500) $\Theta_B = 0.490$ (0.407 – 0.500) $M_{A \rightarrow S} = 15.104$ (0.000 – 30.000) $M_{A \leftarrow S} = 12.498$ (0.000 – 31.333) $M_{S \rightarrow B} = 6.121$ (0.000 – 22.000) $M_{S \leftarrow B} = 11.385$ (0.000 – 28.000) $M_{A \rightarrow B} = 10.992$ (0.000 – 28.000) $M_{A \leftarrow B} = 56.205$ (0.000 – 27.333)	-124,797.11	0	1	1
2 	$\Theta_{A,S,B} = 0.48936$ (0.480 – 0.500)	-185,676.92	-60,879.81	4	0
3 	$\Theta_{A,S} = 0.488$ (0.478 – 0.500) $\Theta_B = 0.328$ (0.332 – 0.500) $M_{A,S \rightarrow B} = 8.55$ (0.000 – 25.333)	-135,014.24	-10,217.13	2	0
4 	$\Theta_{A,S} = 0.480$ (0.458 – 0.500) $\Theta_B = 0.476$ (0.452 – 0.500) $M_{A,S \leftarrow B} = 7.22$ (0.000 – 24.000)	-135,807.69	-11,010.58	3	0

Chapter IV

Contemporary population structure

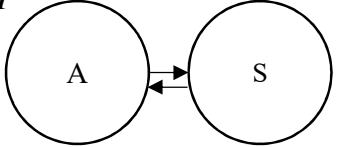
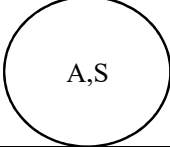
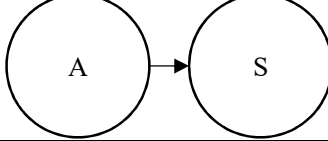
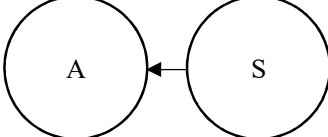
Table 4.6 Log Bayes Factor (LBF) using thermodynamic integration of different gene flow models M_i compared with Model 3 for three sampling populations of *Mustelus mustelus* within the southern north-east Atlantic Ocean (V: Cape Verde; B: Guinea Bissau; C: Guinea); p_{M_i} – model choice probability; $\ln L$ – log marginal likelihood.

Model	Parameters (97.5% CI)	Bézier $\ln L$	LBF for model	Model rank	p_{M_i}
1	 $\Theta_V = 0.096$ (0.092 – 0.100) $\Theta_B = 0.095$ (0.089 – 0.100) $\Theta_C = 0.096$ (0.091 – 0.100) $M_{V \rightarrow B} = 210.907$ (0.000 – 56.667) $M_{V \leftarrow B} = 22.81$ (2.667 – 42.000) $M_{B \rightarrow C} = 101.227$ (0.000 – 152.000) $M_{B \leftarrow C} = 28.097$ (6.000 – 48.667) $M_{V \rightarrow C} = 389.311$ (1.333 – 85.333) $M_{V \leftarrow C} = 63.844$ (0.000 – 81.333)	-183,341.26	-89,792.53	4	0
2	 $\Theta_{V,B,C} = 0.489$ (0.478 – 0.500)	-120,830.19	-27,281.46	3	0
3	 $\Theta_V = 0.476$ (0.446 – 0.500) $\Theta_{B,C} = 0.474$ (0.40 – 0.500) $M_{V \rightarrow B,C} = 5.42$ (0.000 – 22.000)	-93,548.73	0	1	1
4	 $\Theta_V = 0.198$ (0.052 – 0.106) $\Theta_{B,C} = 0.488$ (0.476 – 0.500) $M_{V \leftarrow B,C} = 11.853$ (0.000 – 28.667)	-95,428.89	-1,880.16	2	0

Chapter IV

Contemporary population structure

Table 4.7 Log Bayes Factor (LBF) using thermodynamic integration of different gene flow models M_i compared with Model 1 for two sampling populations of *Mustelus mustelus* within the south-east Atlantic/south-west Indian oceans (A: Angola; S: South Africa); p_{Mi} – model choice probability; lmL – log marginal likelihood.

Model	Parameters (97.5% CI)	Bézier lmL	LBF for model	Model rank	p_{Mi}
1 	$\Theta_A = 0.484$ (0.468 – 0.500) $\Theta_S = 0.487$ (0.475 – 0.500) $M_{A \rightarrow S} = 1.686$ (0.000 – 18.000) $M_{A \leftarrow S} = 10.112$ (0.000 – 30.000)	-94,008.26	0	1	1
2 	$\Theta_{A,S} = 0.490$ (0.481 – 0.500)	-124,726.71	-30,718.45	2	0
3 	$\Theta_A = 0.098$ (0.096 – 0.100) $\Theta_S = 0.474$ (0.094 – 0.100) $M_{A \rightarrow S} = 2.74$ (0.000 – 19.333)	-226,430.19	-132,421.93	3	0
4 	$\Theta_A = 0.488$ (0.477 – 0.500) $\Theta_S = 0.482$ (0.461 – 0.500) $M_{A \leftarrow S} = 2.51$ (0.000 – 18.667)	-226,791.58	-132.783.32	4	0

4.4 Discussion

4.4.1 Genetic composition of *Mustelus mustelus*: cause for concern?

In general, the level of genetic variability in sharks has previously been reported to be low compared to other fish species (Karl *et al.* 2011; Dudgeon *et al.* 2012). However, this does not hold for all shark species, with several studies reporting moderate to high levels of diversity, for example, in the whale shark, *Rhincodon typus* (mean $A_N = 9.0$; $H_E = 0.69$) (Schmidt *et al.* 2009), the bull shark, *Carcharhinus leucas* ($H_E = 0.84$) (Karl *et al.* 2011) and the tiger shark, *Galeocerdo cuvier* ($H_E: 0.59 - 0.71$) (Bernard *et al.* 2016). However, these species are pelagic in nature, capable of migrating across large distances, which would explain the high levels of diversity as populations located across entire ocean basins could remain connected. Coastal sharks, however, mostly lack this high migratory ability, and are generally characterised by lower levels of diversity (Ovenden 2013). The overall diversity observed in the global dataset for *M. mustelus* ($A_N: 2.3 - 4.2$, $H_E: 0.21 - 0.57$; **Table 4.1**) was also low in comparison to global studies on other more vagile coastal shark species, such as the blacktip shark, *Carcharhinus limbatus* ($H_E: 0.48 - 0.56$) (Keeney *et al.* 2005) the lemon shark, *Negaprion brevirostris* ($A_N: 6.8 - 14.0$; $H_E: 0.53 - 0.77$), and the sicklefin lemon shark, *N. acutidens* ($A_N: 1.7 - 8.7$; $H_E: 0.39 - 0.69$) (Schultz *et al.* 2008).

However, this low level of nuclear diversity was not mirrored in the mitochondrial DNA (mtDNA), with a high level of global mtDNA diversity observed for the species ($h = 0.867$, $\pi = 0.00437$; Chapter III). Thus, it seems that the genetic variation at the nuclear and mitochondrial loci included in the current study could be shaped by different evolutionary processes. Most shark species display intermediate levels of diversity across both marker types, with a few species, namely the blacktip shark, *Carcharhinus limbatus* (Keeney *et al.* 2005), the blue shark, *Prionace glauca* (Ovenden *et al.* 2009), and the whale shark, *Rhincodon typus* (Schmidt *et al.* 2009), displaying low nuclear and high mitochondrial diversity. Additionally, a study in South Africa on *M. mustelus* observed similar patterns of discordance across nuclear and mitochondrial loci as the current study

(Maduna *et al.* 2016). Therefore, this varying level of diversity across both marker types warrants further investigation on finer-scale population dynamics of this species in the ocean basins investigated in this study.

4.4.2 Inter-oceanic population stratification of *Mustelus mustelus*

Common smoothhounds are demersal sharks, with evidence suggesting that they migrate predominantly along the coast and are limited to continental shelves (Smale and Compagno 1997). As stated previously, the hypothesis of geographic distance driving genetic differentiation in species with limited dispersal ability (Barker *et al.* 2015; Chabot *et al.* 2015) was a working hypothesis in the investigation of population structure of *M. mustelus*. However, no significant correlation was found between genetic differentiation and geographic distance between sampling populations in the current study (**Figure 4.3**), although the positive correlation between these factors is suggestive of geographic distance influencing divergence. While considerable movement of up to 1,404 km has been reported for this species, conventional tagging studies in South Africa have shown that most *M. mustelus* are recaptured close to their release site, regardless of time at liberty (Mann and Bullen 2009). Furthermore, results from conventional tagging and acoustic telemetry (da Silva *et al.* 2013) suggests that it is not likely that this species migrates long distances. It is much more likely that the differentiation or connectivity observed in this study could be attributed to the combined effect of oceanic currents and other biogeographic barriers on the movement potential of the species, connecting populations in a stepping-stone fashion despite large geographic distance.

For instance, the lowest level of genetic differentiation ($F_{ST} = 0.070$, $P = 0.001$) was observed between the Adriatic Sea (AS) and Strait of Sicily (SS) sampling populations (**Table 4.2**), and these populations were assigned to the same genetic cluster in both the multivariate (**Figure 4.4**) and Bayesian (**Figure 4.5**) clustering analyses. This directly supports a preliminary study conducted in the Mediterranean Sea, which found a similarly low level of differentiation ($F_{ST} = 0.07$, $P = 0.009$) between these areas (Ferrer *et al.* 2017). These sampling populations are geographically distant from

one another, but the outflow from the Adriatic Sea into the Ionian Sea may be the facilitator of gene flow between these two populations (Orlic *et al.* 1992), although limited research has been conducted on the effect of the currents and circulation patterns of the Adriatic Sea, and its impact on gene flow in marine species. In contrast, the Balearic Islands (BI) population displayed high pairwise F_{ST} estimates (**Table 4.2**) between populations in the Mediterranean Sea, indicating restricted gene flow between western and eastern parts of the Mediterranean Sea. This is congruent with previous findings regarding population connectivity of smaller shark species, as a recent study investigated the population structure of the small-spotted catshark, *Scyliorhinus canicula*, in the Mediterranean Sea, and found statistically significant F_{ST} estimates ranging from 0.03 to 0.1 ($P < 0.001$) and thus inferred genetic differentiation between *S. canicula* populations of the western and eastern basins of the Mediterranean Sea (Kousteni *et al.* 2015). However, the location of the BI population at an island explains this high level of differentiation, as *M. mustelus* lacks pelagic movement (Smale and Compagno 1997), and thus the differentiation can be attributed to this characteristic. Furthermore, the recent study by Colloca *et al.* (2017) provided evidence of reductions in the geographical range of *M. mustelus* in the Mediterranean Sea, with populations located along the coast of Spain and France near the Balearic Islands disappearing between the early 1960's and the present day, further restricting the BI population from interbreeding with other populations of *M. mustelus*.

A similar pattern of structuring was observed in the southern north-east Atlantic (SNEA), with pairwise F_{ST} estimates indicating that the CV population is isolated from SNEA populations (**Table 4.2**). Thus, similarly to what was observed in the MED, populations that occur at island locations are unable to migrate across the open ocean and instead display residency to these island locations. From an evolutionary perspective, this greatly affects the manner in which these populations will change over time, as they will likely not interbreed with other *M. mustelus* populations, leading to the fixation of alleles ultimately driving the divergence from the continental populations. This potentially explains the lack of correlation between genetic and geographic distance in the global dataset, as these island locations are geographically close to other sampling populations, but the open ocean limits the contact

between island and continental populations, driving genetic differentiation between said populations. Notably, when the island locations were excluded from the Mantel test, the correlation between genetic and geographic distance increased, although this correlation was still non-significant (**Figure 4.3**). Furthermore, there were instances where geographically close sampling populations were found to be genetically distinct from one another. For example, the sampling populations of Guinea Bissau (GB) and Guinea (GC) displayed a high pairwise F_{ST} estimate (0.289, $P < 0.01$), indicating a lack of gene flow between these areas. However, due to the movement of the Guinea Current from GB to GC along the coast of west Africa (Ukwe *et al.* 2006; Djakouré *et al.* 2017), a degree of connectivity was expected between these populations. Nevertheless, the clustering analyses of the present study illustrate genetic differentiation between these populations, as they assigned to separate clusters in both multivariate and Bayesian analyses. Therefore, the restricted gene flow between these regions may be attributed to loss of suitable habitats between GB and GC over time, or anthropogenic effects, such as pollution or overfishing, which was reported to occur for many marine species in GB and GC by Ukwe *et al.* (2006), although it is unlikely that such a high F_{ST} estimate would result due to human influences in a short time period. However, Φ_{ST} estimates were not statistically significant between these populations (Chapter III), thus indicating a lack of genetic structuring on a mitochondrial level. While there are various hypotheses that explain this mito-nuclear discordance, including differing modes of inheritance and mutation rates of either marker type, population size fluctuations, sampling bias, or sex-specific reproductive behaviour, the differing structuring patterns are more likely a consequence of incomplete lineage sorting, or the retention of ancestral polymorphisms in the present populations, leading to a lack of differentiation on a mitochondrial level (DeBiasse *et al.* 2014).

Interestingly the GC sampling population displayed similar allelic frequencies as the southern hemisphere (**Figure 4.5**), although it is more likely due to remnant gene flow between the northern and southern hemispheres, rather than contemporary gene flow. However, due to the sampling sites included in this study, which did not include locations between GC and AN, cryptic gene flow may be occurring between these regions and groups not included in this study, potentially aided by the

southward moving Guinea and Angolan currents (Ukwe *et al.* 2006). Several studies on coastal shark species have reported genetic connectivity over similarly large geographic distances, provided there are populations or regions that facilitate dispersal across the geographic range (*Sphyrna lewini*, Duncan *et al.* 2006; *Negaprion acutidens*, Schultz *et al.* 2008). Thus, these unsampled groups of *M. mustelus* would act as stepping-stones between GC and AN, and future studies should investigate this finer-scale structuring pattern on the coast of west Africa to validate this hypothesis.

In the southern hemisphere, the Angolan (AN) and South African (SA) sampling populations showed evidence of admixture based on shared alleles (**Figure 4.5**), despite F_{ST} estimates indicating a high level of genetic differentiation, similarly to what was observed between the regions in a previous study (Maduna *et al.* 2016). This high level of differentiation could be an indication of restricted gene flow between AN and SA, potentially due to the hydrodynamic barrier caused by the Angola-Benguela Front (ABF), where the warm Angolan and cold Benguela current meet just north of the border between Angola and Namibia, leading to the generation of a temperature gradient (Meeuwis and Lutjeharms 1990). This has been shown to influence migration patterns, and thus gene flow, in shark species, such as the blacktip shark, *Carcharhinus limbatus* (Keeney *et al.* 2005) and the tope shark, *Galeorhinus galeus* (although results based on mtDNA; Chabot and Allen 2009), and thus may be restricting contemporary connectivity of *M. mustelus* in the southern hemisphere. This is likely, given the results from a recent study showing that the movement of *M. mustelus*, specifically on the west coast of South Africa, was heavily influenced by temperature and that their movement was restricted by a shallow thermocline below 10 °C (da Silva 2018).

4.4.3 Demography of *Mustelus mustelus*

Several populations displayed signatures of recent population bottlenecks across multiple mutational models, based on the Wilcoxon signed-rank test as implemented in BOTTLENECK (**Table 4.4**). However, the TPM model is most likely the true probability estimate for microsatellite markers, as this model represents an intermediary of sorts between the IAM and SMM models, as it

incorporates the SMM mutational mechanism, where single repeats are added or removed during each mutational event while tolerating mutations of a larger extent (Piry *et al.* 1999). The results of this analysis paint a picture of global reductions in population size, due to recent bottleneck events that may have drastically reduced the size of the global population of *M. mustelus*. Furthermore, these results are in congruence with the neutrality tests in Chapter III, which found that the South African population underwent a historical expansion event, whereas the model of expansion was rejected in the remaining sampling populations.

However, the evaluation of recent bottleneck events may be undetected in demographic inference tests, as the loss of allelic diversity is not accompanied by an immediate reduction in heterozygosity, but rather by a transient heterozygosity excess (Cornuet and Luikart 1996; Luikart and Cornuet 1998). While there is evidence to suggest that the Wilcoxon signed-rank test outperforms other methods (e.g. interlocus *g*-tests) in detecting population expansions when the number of loci utilised is low (Luikart *et al.* 1998), future studies should investigate these ocean basins on a finer-scale to determine whether there are signatures of population bottlenecks, potentially with a greater number of markers and samples to increase the statistical support of the analyses performed.

Limited information is available on migration rates in sharks, and for *M. mustelus*, only one other study by Maduna *et al.* (2016) has investigated this. This chapter aimed to address this short-coming, and contributed baseline information on potential migration patterns in the three basins investigated in this study. The model of migration that was most likely in the MED population illustrated asymmetric gene flow between the sampling areas (**Table 4.5**). The results of this analysis were suggestive of asymmetric gene flow occurring from the AS to the SS, which supports the clustering analyses that indicated that these sampling populations assigned to a single genetic cluster (**Figure 4.4** and **Figure 4.5**). While these areas are geographically distant, the outflow from the Adriatic Sea to the Ionian Sea (Orlic *et al.* 1992) may be the driver of this gene flow, further supporting the effect of ocean currents on the dispersal potential of the species. Additionally, the migration rates from the

BI sampling population to the AS and SS sampling populations suggests asymmetric gene flow is occurring from the island location to the coastal areas.

A similar scenario was observed in the SNEA basin, with the most likely model of migration being suggestive of asymmetric gene flow from the CV sampling population to the GB and GC sampling populations (**Table 4.6**). However, this does not mean that migration is occurring from island locations to the coast, as pairwise F_{ST} estimates and clustering analyses are all indicative of island populations being genetically distinct from coastal populations (**Table 4.2**, **Figure 4.4** and **Figure 4.5**). Although limited work has been conducted in assessing migration rates from islands to coastal regions in demersal sharks, the likelihood of individuals moving from these island locations to the coast and contributing to subsequent generations is higher than the alternative explanation, as was observed in the MED and SNEA basins.

In the SAI basin, a previous study observed low levels of asymmetric gene flow from the Atlantic Ocean to Angola along the western coast of southern Africa (Maduna *et al.* 2016), which the authors attribute to the action of ocean currents influencing gene flow, particularly the strong northward movement of the Benguela current. The results of this chapter corroborate the results of Maduna *et al.* (2016), with the most likely model of migration indicating gene flow from South Africa to Angola (**Table 4.7**). As the analyses performed in MIGRATE-N are model based, and not indicative of actual migration rates as geographic distance and movement potential of the organism evaluated are not considered, the exact pattern of migration in these areas cannot be determined without verifying migration rate estimates with tagging or telemetry data for this species.

4.5 Conclusion

The microsatellite data indicates that present populations of the common smoothhound are characterised by low to moderate levels of genetic diversity based on number of alleles, allelic richness and heterozygosity. Furthermore, the results of the pairwise F_{ST} , hierarchical AMOVA, multivariate and Bayesian clustering analyses revealed elevated levels of differentiation between the

ocean basins investigated, as well as strong intra-oceanic structuring, highlighting the limited dispersal potential of the species. Beside distance, currents are the main oceanic features that appear to facilitate gene flow of this species, which was supported by the migration estimates in the MED and SAI basins, and in some cases can limit the connectivity between populations of *M. mustelus*. Furthermore, evidence of genetic bottlenecks in many of the global sampling populations may be indicative of recent reductions in population size, either driven by habitat destruction or fishing pressure, which has been documented in the MED and SNEA basins. Finally, comparisons between the nuclear data presented in this chapter, and the results of the mitochondrial data in Chapter III, may provide a more comprehensive assessment of global structuring patterns, and elucidate the degree of divergence between ocean basins. Overall, the lower diversity compared to other coastal sharks, coupled with declining biomass and limited genetic connectivity, warrants concern regarding the conservation status of this species.

CHAPTER V

Concluding remarks and future perspectives

5.1 Introduction

The harvesting of many species to sate a growing market for marine resources in numerous countries has led to the broad-scale overexploitation and habitat destruction of many organisms (Dulvy *et al.* 2014, 2017; Davidson *et al.* 2015). The species targeted include a range of invertebrates and teleost fish, generally characterised by shorter generation times and a multitude of offspring produced per mating event, as well as chondrichthyans that require many years to reach sexual maturity, and produce far fewer offspring in comparison (Compagno 1984; Jackson 2010; Ebert *et al.* 2013). The targeting of chondrichthyans, especially the species that play an integral role in the maintenance of ecosystems as keystone species, has severely affected marine diversity in all of the world's oceans. This has sparked concern on a global scale as to how these animals could be fished sustainably in the coming generations (Jackson 2010). Furthermore, the study of these changes in diversity is further limited to charismatic species, or those that are commercially important (Dulvy *et al.* 2014), particularly in countries located in the northern-hemisphere (Worm *et al.* 2009). Therefore, it has become essential to shift focus to the lesser studied species that have been affected by anthropogenic influences over time, either directly or indirectly.

The common smoothhound, *Mustelus mustelus*, is one of many species of shark that has experienced increasing levels of exploitation to satisfy a growing market for shark related products (Clarke *et al.* 2007; da Silva and Bürgener 2007; Serena *et al.* 2009; da Silva *et al.* 2013). Due to the growing economic interest in this species (Saidi *et al.* 2008; da Silva *et al.* 2015), *M. mustelus* and the genus as a whole have recently been the subject of numerous ecological and biological studies (Saidi *et al.* 2008; Boomer *et al.* 2012; Maduna *et al.* 2016; Colloca *et al.* 2017; Maduna and Bester-van der Merwe 2017; Marino *et al.* 2017), with the majority of these studies centred on a specific

oceanic region. Furthermore, the growing prevalence of molecular studies on marine organisms, and the accessibility of next-generation sequencing (NGS) technologies has enabled the transition from molecular ecology to ecological genomics, in order to assess a species on a genome-wide level (Tautz *et al.* 2010).

The over-arching aim of this study was two-fold: firstly, to assemble and annotate the complete mitochondrial genome of *M. mustelus* from next-generation sequencing (NGS) data. Subsequently, the phylogenetic placement of *M. mustelus* among numerous shark species spanning eight orders was determined, and the variable regions of the mitogenome were identified for future assessments of the Carcharhiniiformes order. Secondly, the widespread distribution pattern of the species, and subsequent lack of genetic data available in several oceanic regions, led to the investigation of mitochondrial and nuclear patterns of diversity and connectivity, both on historic and contemporary timescales. Ultimately, this thesis generated the complete sequence data of the mitochondrial genome of *M. mustelus*, and provides a baseline assessment of natural populations in three oceanic basins to aid in the management of the species, both from a fisheries and conservation perspective.

5.2 Summary of research results

To date, all molecular phylogenetic studies conducted on the *Mustelus* genus revealed that the genus is paraphyletic (López *et al.* 2006; Boomer *et al.* 2012; Naylor *et al.* 2012), with several authors suggesting that the genus can be divided into two groups or clades corresponding to reproductive mode (López *et al.* 2006; Boomer *et al.* 2012). Additionally, it is proposed that reproductive mode is correlated to the presence or absence of white spots on the body surface, with non-spotted species being placed in the placental clade, and spotted species being placed in the aplacental clade. However, several species, including the generally non-spotted *M. mustelus*, have been observed with sparse black spots on their dorsal surface (da Silva and Bürgener 2007; Farrell *et al.* 2009), meaning that the relationship between spots and reproductive mode may be more complicated than previously suggested. Thus, in chapter II the complete mitochondrial genome of the placental *M. mustelus* is

assembled and annotated, and used to validate the correlation between reproductive mode and phylogenetic placement of species in the *Mustelus* genus, as was suggested by López *et al.* (2006) and Boomer *et al.* (2012). Two mitogenomes were publicly available for the genus, including the placental *M. griseus* and the aplacental *M. manazo*, and thus it was expected that *M. mustelus* would be more closely related to *M. griseus*. Based on the phylogenetic analysis, *M. mustelus* and *M. griseus* were placed as sister taxa, confirming their close relation, in contrast to *M. manazo*, an aplacental species. This provides further evidence for the hypothesis of reproductive mode being correlated to phylogenetic positioning within either clade of the *Mustelus* genus.

Additionally, the analysis of sequence variation of the mitogenomes within the Carcharhiniformes order revealed that the *rRNA* genes were the most conserved regions, while the non-coding control region (mtCR) and the *NADH dehydrogenase* genes (*NADH1* – *NADH6*) were the most variable, and therefore are the most suitable markers for assessing macro- and micro-evolutionary processes within the Carcharhiniformes order.

Although the use of several mitochondrial genes or regions would improve the accuracy of the analyses performed in chapter III, the 571 bp mtCR dataset revealed high haplotype diversity across the distribution of *M. mustelus*, higher than what was observed in other *Mustelus* species (Boomer *et al.* 2012). The relatively high diversity was attributed to the accumulation of sequence variation through the process of genetic drift (a process that is accelerated by the uniparental mode of inheritance of mitochondria). due to the divergence of the sampling populations from one another as a result of the geographic separation of these locations, as well as the limited dispersal potential of the species (Mann and Bullen 2009). This was supported by the haplotype network and phylogenetic tree, with no haplotypes shared between populations in the Mediterranean Sea (MED) and the south-east Atlantic/south-west Indian (SAI) basin. This finding was also in accordance with a most likely northern hemisphere origin of the species inferred in a recent study (Maduna *et al.* in review).

The lowest mitochondrial diversity was observed within the MED region when compared to the other oceanic basins, with a lack of genetic structuring within the basin based on pairwise Φ_{ST} and D_{est} estimates. While suggestive of population connectivity propagated by females, this is unlikely based on a lack of pelagic movement potential of the species and the geographically distant location of the Balearic Islands (BI) population. The lack of differentiation and lower diversity could rather be attributed to large declines in species abundance in the region (Colloca *et al.* 2017) leading to the accelerated loss of unique female lineages, and subsequent “fixation” of the lineages or haplotypes observed in the present MED population. Alternatively, incomplete lineage sorting should not be ruled out, which could have led to the retention of ancestral polymorphisms and lack of divergence between the geographically representative populations assessed. In contrast to the low diversity observed in the MED, sampling populations in the southern north-east Atlantic (SNEA) basin displayed the greatest diversity of all basins. This high genetic diversity was mirrored in the number of private haplotypes in both northern and southern hemisphere haplogroups, which could potentially be a result of the west African coast being colonised independently from the Mediterranean Sea and southern African oceans, as was suggested by a recent study (Maduna *et al.* in review). The south-east Atlantic/south-west Indian (SAI) basin displayed no divergence between Angola (AN) and South Africa (SA), and was in contrast to a previous study based on the *NADH dehydrogenase 4 (ND4)* gene (Maduna *et al.* 2016), which could be indicative of the mtCR evolving at a slower rate than the *ND4* gene.

A more contemporary assessment using species-specific microsatellite markers was performed in chapter IV, to discern current patterns of diversity and connectivity in the global sampling population of *M. mustelus*. The global nuclear diversity of the species was low compared to other coastal shark species (Keeney *et al.* 2005; Schultz *et al.* 2008; Chabot *et al.* 2015); although small sample sizes should be taken into consideration and direct comparison between studies is probably not warranted given the different spatial scales assessed by previous studies, and the current investigation.

Analysis of the nuclear dataset gave strong signals of inter-oceanic structure, as well as high levels of intra-oceanic differentiation with gene flow most likely influenced by the respective ocean currents within these regions. Up to six genetic clusters were identified across the distribution range based on multivariate and Bayesian clustering analyses, largely corresponding to geographic location of the sampling populations. The estimation of migration rates further supported the influence of oceanic currents on the dispersal ability of this species, with asymmetric gene flow from the Adriatic Sea (AS) to the Strait of Sicily (SS) sampling population, potentially driven by the outflow from the Adriatic Sea to the Ionian Sea. Similarly, asymmetric gene flow from SA to AN was thought to be a result of the northward moving Benguela current, which was in accordance with a previous study (Maduna *et al.* 2016). Finally, several populations (especially within the MED) displayed signatures of recent population bottlenecks and was in congruence with neutrality tests performed in chapter III. However, the SA sampling population displayed signatures of population expansion with no evidence of a bottleneck, although this could be due to the pooling of samples from both the Atlantic and Indian Oceans to avoid over-representing a single region. The results of this chapter suggest that future conservation practices should consider the low diversity, limited connectivity, as well as the documented overfishing and habitat destruction of the species as indicators of an urgent need to increase efforts to conserve the diversity of this shark on a global scale.

5.3 Limitations and future prospects

This is the first study to report on the global population structure of *M. mustelus*, and as such serves as a baseline assessment of the species. However, it is noted that the study was limited by the small sample size and also lacked samples from the entire distribution range. While attempts were made to account for the latter by inference methods that account for uneven sample size (e.g. four estimates of Puechmaille 2016), future studies should aim to acquire additional sampling populations from areas not well represented in the current study.

The phylogenetic placement of species with similar reproductive modes, as was observed in the *Mustelus* genus in chapter II, points to a reliable method of elucidating the reproductive method of species in which it is currently unknown, potentially in other shark genera. Future studies should utilise more than one gene region, as improved statistical support was achieved in the studies by López *et al.* (2006) and Boomer *et al.* (2012) when five gene regions were used in their assessments. Furthermore, the near 100% accuracy of the phylogenetic analysis performed in chapter II illustrates the greater statistical power of using the complete mitochondrial genome. Coupling the higher statistical power of complete sequence information with the decrease in cost and improved accuracy of NGS technologies over the past few years (Tautz *et al.* 2010; Kumar and Kocour 2017) should allow for future research to generate this data for other species of interest.

Based on the level of diversity revealed using the mtCR, it appears that the region is variable across the distribution of this shark species. However, one cannot discount the degree to which the total length of the sequences used to assess these parameters influence the results of the current study. As the final alignment utilised was 571 bp in length, potential variation that exists in other parts of the region that were not sequenced may facilitate the identification of population stratification in the MED and SAI regions. Future studies could design species-specific primers to amplify a larger fragment of the mtCR, as complete sequence information is now available for the entire mitochondrial genome of *M. mustelus*.

Furthermore, the limited number of microsatellite markers hinders the degree to which the demographic parameters of the species can be assessed. While the number of markers used in the present study are comparable with studies in other shark species (Keeney *et al.* 2005; Barker *et al.* 2015; Bernard *et al.* 2016), the inclusion of additional markers could improve the accuracy of the inferences made in future works. However, with the advancements of sequencing technologies, and the accompanying shift from microsatellites to single nucleotide polymorphisms (SNPs) for the assessment of population genetic dynamics (Defaveri *et al.* 2013), future studies should aim to

develop a panel of SNP markers for the species. Although a higher number of SNPs relative to microsatellites are needed to detect lower levels of population differentiation (Morin *et al.* 2009; Helyar *et al.* 2011), the reproducibility of SNP genotyping is far superior to that of microsatellites (Seeb *et al.* 2011; Kraus *et al.* 2012). This will greatly improve the consistency of subsequent data analysis, both among research projects and between countries, which is crucial for the assessment of globally distributed species such as *M. mustelus*.

Finally, the lack of complete phenotypic data for many of the samples used in this study limits the degree to which many biological processes can be investigated, particularly sex-biased dispersal and philopatric behaviour. Future studies should investigate the species on a finer scale, as the mitochondrial discordance in terms of diversity and structure in these oceans is suggestive of underlying causes, such as sex-biased dispersal. The results of this study are suggestive of females being the drivers of gene flow, due to contradictory structuring patterns inferred from mitochondrial and nuclear markers in certain areas. Additionally, the greater size of females relative to males (Smale and Compagno 1997; Saidi *et al.* 2008) may be indicative of a greater movement potential of females, further supporting this form of gender-biased dispersal. This assumption is based off a previous study on *Mustelus lenticulatus*, which observed females (which are larger than males) travelling greater distances than males, with males displaying residency to specific sites (Francis 1988). Thus, the determination of whether gene flow is driven by either sex in *M. mustelus*, and whether the species displays philopatric behavior, requires validation through future telemetric or tagging studies. If this species is philopatric, the areas that mature adults return to should be investigated as potential areas for incorporation into existing Marine Protected Areas (MPAs) or additional MPAs should be established.

5.4 Final remarks

In conclusion, the complete mitochondrial genome for *M. mustelus* provides sequence information for all mitochondrial regions of this species, allowing future research to be based on

complete sequence information of any region investigated. Additionally, the strong genetic structure elucidated using both the nuclear and mitochondrial markers highlights the need for adjustments to be made to the conservation and management strategies of *M. mustelus* on a global scale, as the lack of connectivity between populations could lead to declines in genetic variation of the meta-population as a whole, an integral factor in the continued survival and adaptability of the species. There are numerous areas still lacking accurate fisheries data for the species, particularly along the coast of west Africa.

Generally, a cautious approach should be taken with regards to the management of a vulnerable species, such as *M. mustelus*. Populations that display low or non-significant F_{ST} , Φ_{ST} or D_{est} estimates may justify the management of these populations as a single stock (e.g. AS and SS) while genetically distinct populations that show no evidence of immigration from other populations should be managed separately, and require a management strategy tailored to the isolated population's specific needs (e.g. BI, CV). The results of this study suggest that the allelic divergence of island populations (across nuclear and mitochondrial data) from other coastal populations constitutes the definition of these populations as separate Management Units (MUs), which are important for short-term management strategies. Additionally, the reductions in abundance of the species in the Mediterranean (Colloca *et al.* 2017), driven by the fisheries in many areas, may further limit population connectivity in the future and should be closely monitored. Finally, the apparent success of the Langebaan Marine Protected Area (LMPA) along the west coast of South Africa (da Silva *et al.* 2013) in providing a haven for vulnerable species to recover from population declines warrants the expansion of other MPAs to include nursery sites, or the establishment of entirely new MPAs. Establishing a suitable management strategy for these sharks, with the inclusion of genetic data and successful protection of important nursery and/or aggregation sites, could contribute to the survival of future generations of this threatened marine resource.

References

- Abdul-Muneer PM. (2014) Application of microsatellite markers in conservation genetics and fisheries management: recent advances in population structure analysis and conservation strategies. *Genetics Research International* **2014**: 1–11.
- Adnet S, Cappetta H. (2008) New fossil traikid sharks from the early Eocene of Prémontré, France, and comments on fossil record of the family. *Acta Paleontologica Polonica* **55**: 433–448.
- Alam MT, Petit RA, Read TD, Dove ADM. (2014) The complete mitochondrial genome sequence of the world's largest fish, the whale shark (*Rhincodon typus*), and its comparison with those of related shark species. *Gene* **539**: 44–49.
- Andrews S. (2010) FASTQC: a quality control tool for high throughput sequence data. Retrieved from <http://www.bioinformatics.babraham.ac.uk/projects/fastqc/>.
- Arratia G, Wilson M, Cloutier R. (2005) Recent advances in the origin and early radiation of vertebrates. *Journal of Vertebrate Paleontology* **25**: 478.
- Avise JC, Neigel JE, Arnold J. (1984) Demographic influences on mitochondrial DNA lineage survivorship in animal populations. *Journal of Molecular Evolution* **20**: 99–105.
- Avise JC. (2012) Molecular Tools. In: Avise JC. (ed) *Molecular markers, natural history and evolution*. Springer Science and Business Media: New York, USA, pp. 44–91.
- Bailleul D, Mackenzie A, Sacchi O, Poisson F, Bierne N, Arnaud-Haond S. (2018) Large-scale genetic panmixia in the blue shark (*Prionace glauca*): a single worldwide population, or a genetic lag-time effect of the “grey zone” of differentiation? *Evolutionary Applications* **11**: 614–630.
- Bandelt HJ, Peter F, Röhl A. (1999) Median-Joining networks for inferring intraspecific phylogenies. *Molecular Biology* **16**: 37–48.

- Barbuto M, Galimberti A, Ferri E, Labra M, Malandra R, Galli P, Casiraghi M. (2010) DNA barcoding reveals fraudulent substitutions in shark seafood products: the Italian case of “palombo” (*Mustelus* spp.). *Food Research International* **43**: 376–381.
- Barker MJ, Schluessel V. (2005) Managing global shark fisheries: suggestions for prioritizing management strategies. *Aquatic Conservation: Marine and Freshwater Ecosystems* **15**: 325–347.
- Barker AM, Nosal AP, Lewallen EA, Burton RS. (2015) Genetic structure of leopard shark (*Triakis semifasciata*) populations along the Pacific coast of North America. *Journal of Experimental Marine Biology and Ecology* **472**: 151–157.
- Basson J, Petersen SL, Duarte A, Nel DC. (2007) The impact of longline fisheries on pelagic and demersal sharks in the Benguela Current Large Marine Ecosystem. In: Petersen S, Nel D, Omardien A. (eds) *Towards an ecosystem approach to longline fisheries in the Benguela: an assessment of impacts on seabirds, sea turtles and sharks*. WWF Report Series: pp. 49–67.
- Berli P, Palczewski M. (2010) Unified framework to evaluate panmixia and migration direction among multiple sampling locations. *Genetics* **185**: 313–326.
- Benavides MT, Feldheim KA, Duffy CA, Wintner S, Braccini JM, Boomer J, Huveneers C, Rogers P, Mangel JC, Alfaro-Shigueto J, *et al.* (2011) Phylogeography of the copper shark (*Carcharhinus brachyurus*) in the southern hemisphere: implications for the conservation of a coastal apex predator. *Marine and Freshwater Research* **62**: 861–869.
- Bernard AM, Feldheim KA, Heithaus MR, Wintner SP, Wetherbee BM, Shivji MS. (2016) Global population genetic dynamics of a highly migratory, apex predator shark. *Molecular Ecology* **25**: 5312–5329.
- Bester-van der Merwe AE, Bitalo D, Cuevas JM, Ovenden J, Hernández S, da Silva C, McCord M, Roodt-Wilding R. (2017) Population genetics of southern hemisphere tope shark (*Galeorhinus galeus*): intercontinental divergence and constrained gene flow at different geographical scales.

PLoS ONE **12**: e0184481.

- Bitalo DN, Maduna SN, da Silva C, Roodt-Wilding R, Bester-van der Merwe AE. (2015) Differential gene flow patterns for two commercially exploited shark species, tope (*Galeorhinus galeus*) and common smoothhound (*Mustelus mustelus*) along the south-west coast of South Africa. *Fisheries Research* **172**: 190–196.
- Bolger AM, Lohse M, Usadel B. (2014) TRIMMOMATIC: a flexible trimmer for Illumina sequence data. *Bioinformatics* **30**: 2114–2120.
- Bonfil R. (1994) World elasmobranch fisheries. In: Bonfil R. (ed) *Overview of world elasmobranch fisheries. FAO fisheries technical paper. No. 341*. FAO: Rome, Italy, pp. 4-62.
- Bonfil R. (2005) Fishery stock assessment models and their application to sharks. In: Musick J, Bonfil R. (eds) *Management techniques for elasmobranch fisheries. FAO fisheries technical paper. No. 474*. FAO: Rome, Italy, pp.154–181.
- Boomer JJ, Harcourt RG, Francis MP, Stow AJ. (2012) Genetic divergence, speciation and biogeography of *Mustelus* (sharks) in the central Indo-Pacific and Australasia. *Molecular Phylogenetics and Evolution* **64**: 697–703.
- Bustamante C, Bennett MB, Ovenden JR. (2016) Genotype and phylogenomic position of the frilled shark *Chlamydoselachus anguineus* inferred from the mitochondrial genome. *Mitochondrial DNA Part B* **1**: 18–20.
- Cao Y, Waddell PJ, Okada N, Hasegawa M. (1998) The complete mitochondrial DNA sequence of the shark *Mustelus manazo*: evaluating rooting contradictions to living bony vertebrates. *Molecular Biology and Evolution* **15**: 1637–1646.
- Carr AS, Bateman MD, Roberts DL, Murray-Wallace CV, Jacobs Z, Holmes PJ. (2010) The last interglacial sea-level high stand on the southern Cape coastline of South Africa. *Quaternary Research* **73**: 351–363.

- Carvalho GR, Hauser L. (1995) Molecular genetics and the stock concept in fisheries. *Molecular Genetics in Fisheries* **350**: 55–79.
- Cavanagh RD, Gibson C. (2007) *Overview of the conservation status of cartilaginous fishes (Chondrichthyans) in the Mediterranean Sea*. IUCN: Gland, Switzerland and Malaga, Spain, pp. 8-27.
- Cawthorn DM, Steinman HA, Witthuhn RC. (2012) DNA barcoding reveals a high incidence of fish species misrepresentation and substitution on the South African market. *Food Research International* **46**: 30–40.
- Chabot CL, Allen LG. (2009) Global population structure of the tope (*Galeorhinus galeus*) inferred by mitochondrial control region sequence data. *Molecular Ecology* **18**: 545–552.
- Chabot CL, Espinoza M, Mascareñas-Osorio I, Rocha-Olivares A. (2015) The effect of biogeographic and phylogeographic barriers on gene flow in the brown smoothhound shark, *Mustelus henlei*, in the northeastern Pacific. *Ecology and Evolution* **5**: 1585–1600.
- Chai A, Yamaguchi A, Furumitsu K, Zhang, J. (2016) Mitochondrial genome of Japanese angel shark *Squatina japonica* (Chondrichthyes: Squatinidae). *Mitochondrial DNA Part A* **27**: 832–833.
- Chang C-H, Shao K-T, Lin Y-S, Fang Y-C, Ho H-C. (2014) The complete mitochondrial genome of the great white shark, *Carcharodon carcharias* (Chondrichthyes, Lamnidae). *Mitochondrial DNA Part A* **25**: 357–358.
- Chang C-H, Jabado R, Lin Y-S, Shao K-T. (2015a) The complete mitochondrial genome of the sand tiger shark, *Carcharias taurus* (Chondrichthyes, Odontaspidae). *Mitochondrial DNA Part A* **26**: 728–729.
- Chang C-H, Shao K-T, Lin Y-S, Tsai A-Y, Su P-X, Ho H-C. (2015b) The complete mitochondrial genome of the shortfin mako, *Isurus oxyrinchus* (Chondrichthyes, Lamnidae) *Mitochondrial DNA Part A* **26**: 475–476.

- Chapman DD, Babcock EA, Gruber SH, Dibattista JD, Franks BR, Kessel SA, Guttridge T, Pikitch EK, Feldheim KA. (2005) Marine reserve design and evaluation using automated acoustic telemetry: a case-study involving coral reef-associated sharks in the Mesoamerican Caribbean. *Marine Technology Society* **39**: 42–55.
- Charif D, Lobry JR (2007) Seqin R 1.0-3: a contributed package to the R project for statistical computing devoted to biological sequences retrieval and analysis. In: *Structural approaches to sequence evolution*. Springer Berlin: Heidelberg, Germany, pp. 207–232.
- Chen H, Chen X, Gu X, Wan H, Chen X, Ai W. (2016) The phylogenomic position of the smooth lanternshark *Etmopterus pusillus* (Squaliformes: Etmopteridae) inferred from the mitochondrial genome. *Mitochondrial DNA Part B* **1**:341–342.
- Chen MH, Dorn S. (2010) Cross-amplification of microsatellites from the codling moth *Cydia pomonella* to three other species of the tribe Grapholitini (Lepidoptera: Tortricidae). *Molecular Ecology Resources* **10**: 1034–1037.
- Chen X, Peng X, Huang X, Xiang D. (2014) Complete mitochondrial genome of the Zebra bullhead shark *Heterodontus zebra* (Heterodontiformes: Heterodontidae). *Mitochondrial DNA Part A* **25**: 280–281.
- Chen X, Xiang D, Ai W, Shi X. (2015a) Complete mitochondrial genome of the blue shark *Prionace glauca* (Elasmobranchii: Carcharhiniformes). *Mitochondrial DNA Part A* **26**: 313–314.
- Chen X, Xiang D, Xu Y, Shi X. (2015b) Complete mitochondrial genome of the scalloped hammerhead *Sphyrna lewini* (Carcharhiniformes: Sphyrnidae). *Mitochondrial DNA Part A* **26**: 621–622.
- Chen X, Peng Z, Pan L, Shi X, Cai L. (2016) Mitochondrial genome of the spotless smooth-hound *Mustelus griseus* (Carcharhiniformes: Triakidae) *Mitochondrial DNA Part A* **27**: 78–79.
- Clarke SC, McAllister MK, Milner-Gulland EJ, Kirkwood GP, Michielsens CGJ, Agnew DJ, Pikitch

- EK, Nakano H, Shivji MS. (2006) Global estimates of shark catches using trade records from commercial markets. *Ecology Letters* **9**: 1115–1126.
- Clarke S, Milner-Gulland E, Bjørndal T. (2007) Social, economic, and regulatory drivers of the shark fin trade. *Marine Resource Economics* **22**: 305–327.
- Coates M, Friedman M. (2010) *Litoptychus bryanti* and characteristics of stem tetrapod neurocrania. In: Elliot DK, Maisey JG, Yu X, Miao D. (eds) *Morphology, phylogeny and paleobiogeography of fossil fishes*. Verlag Dr. Friedrich Pfeil: München, Germany, pp. 389–416.
- Colloca F, Enea M, Ragonese S, Di Lorenzo M. (2017) A century of fishery data documenting the collapse of smoothhounds (*Mustelus* spp.) in the Mediterranean Sea. *Aquatic Conservation: Marine and Freshwater Ecosystems* **27**: 1145–1155.
- Compagno LJV. (1984) An annotated and illustrated catalogue of shark species known to date. Carcharhiniformes. *FAO Fisheries Synopsis* **4**: 250-655.
- Compagno LJV. (2001) *Sharks of the world: an annotated and illustrated catalogue of shark species known to date*. FAO: Rome, Italy.
- Conesa A, Götz S, García-Gómez JM, Terol J, Talón M, Robles M. (2005) BLAST2GO: a universal tool for annotation, visualization and analysis in functional genomics research. *Bioinformatics* **21**: 3674–3676.
- Cornuet JM, Luikart G. (1996) Description and power analysis of two tests for detecting recent population bottlenecks from allele frequency data. *Genetics* **144**: 2001–2014.
- Corrigan S, Yang L, Cosmann PJ, Naylor GJP. (2016) A description of the mitogenome of the Endangered Taiwanese angelshark, *Squatina formosa*. *Mitochondrial DNA Part A* **27**: 1305–1306.
- Cortés E. (2000) Life history patterns and correlations in sharks. *Reviews in Fisheries Science* **8**: 299–344.

- Cross H. (2015) Elasmobranch capture by commercial small-scale fisheries in the Bijagós Archipelago, Guinea Bissau. *Fisheries Research* **168**: 105–108.
- Cunha RL, Coscia I, Madeira C, Mariani S, Stefanni S, Castilho R. (2012) Ancient divergence in the trans-oceanic deep-sea shark *Centroscyrnus crepidater*. *PLoS One* **7**: e49196.
- da Silva C, Bürgener M. (2007) South Africa's demersal shark meat harvest. *Traffic Bulletin* **21**: 55–56.
- da Silva C, Kerwath SE, Attwood CG, Thorstad EB, Cowley PD, Økland F, Wilke CG, Næsje TF. (2013) Quantifying the degree of protection afforded by a no-take marine reserve on an exploited shark. *African Journal of Marine Science* **35**: 57–66.
- da Silva C, Booth AJ, Dudley SFJ, Kerwath SE, Lamberth SJ, Leslie RW, McCord ME, Sauer WHH, Zweig T. (2015) The current status and management of South Africa's chondrichthyan fisheries. *African Journal of Marine Science* **37**: 233–248.
- da Silva C (2018) Biology, movement behaviour and spatial dynamics of an exploited population of smoothhound shark *Mustelus mustelus* around a coastal Marine Protected Area in South Africa. PhD Thesis, University of Cape Town.
- DAFF. (2013) *National Plan of Action for the Conservation and Management of Sharks (NPOA-Sharks)* Rogge Bay, Cape Town: Department of Agriculture, Forestry and Fisheries.
- Darriba D, Taboada GL, Doallo R, Posada D. (2012) JMODELTEST 2: more models, new heuristics and parallel computing. *Nature Methods* **9**: 772.
- Davidson LNK, Krawchuk MA, Dulvy NK. (2015) Why have global shark and ray landings declined: improved management or overfishing? *Fish and Fisheries* **17**: 438–458.
- DeBiasse MB, Nelson BJ, Hellberg ME. (2014) Evaluating summary statistics used to test for incomplete lineage sorting: mito-nuclear discordance in the reef sponge *Callyspongia vaginalis*. *Molecular Ecology* **23**: 225–238.

- Defaveri J, Viitaniemi H, Leder E, Merilä J. (2013) Characterizing genic and nongenic molecular markers: comparison of microsatellites and SNPs. *Molecular Ecology Resources* **13**: 377–392.
- Dieringer D, Schlötterer C. (2003) Two distinct modes of microsatellite mutation processes: evidence from the complete genomic sequences of nine species. *Genome Research* **13**: 2242–2251.
- Diop M, Dossa J. (2011) The SRPOA-Sharks project-inception, achievements and impacts. In: Diop M, Dossa J (eds) *30 years of shark fishing in west Africa*. FIBA Publications pp. 12–18.
- Djakouré S, Penven P, Bourlès B, Koné V, Veitch J. (2017) Respective roles of the Guinea Current and local winds on the coastal upwelling in the northern Gulf of Guinea. *Journal of Physical Oceanography* **47**: 1367–1387.
- Douady CJ, Dosay M, Shivji MS, Stanhope MJ. (2003) Molecular phylogenetic evidence refuting the hypothesis of Batoidea (rays and skates) as derived sharks. *Molecular Phylogenetics and Evolution* **26**: 215–221.
- Ducrocq M, Sidi MLO, Yarba LO. (2005). Comment le parc national du banc d’Arguin est devenu le plus grand sanctuaire d’Afrique pour les requins. FIBA/CSRP pp. 5.
- Dudgeon CL, Blower DC, Broderick D, Giles JL, Holmes BJ, Kashiwagi T, Krück NC, Morgan JAT, Tillett BJ, Ovenden JR. (2012) A review of the application of molecular genetics for fisheries management and conservation of sharks and rays. *Journal of Fish Biology* **80**: 1789–1843.
- Dudgeon CL, Ovenden JR. (2015) The relationship between abundance and genetic effective population size in elasmobranchs: an example from the globally threatened zebra shark *Stegostoma fasciatum* within its protected range. *Conservation Genetics* **16**: 1443–1454.
- Dulvy NK, Fowler SL, Musick JA, Cavanagh RD, Kyne PM, Harrison LR, Carlson JK, Davidson LNK, Fordham SV, Francis MP, *et al.* (2014) Extinction risk and conservation of the world’s sharks and rays. *eLife* **14**: e00590.
- Dulvy NK, Simpfendorfer CA, Davidson LNK, Fordham SV, Bräutigam A, Sant G, Welch DJ. (2017)

- Challenges and priorities in shark and ray conservation. *Current Biology* **27**: R565–R572.
- Duncan KM, Martin AP, Bowen BW, De Couet HG. (2006) Global phylogeography of the scalloped hammerhead shark (*Sphyrna lewini*). *Molecular Ecology* **15**: 2239–2251.
- Ebert D, Fowler S, Compagno LJV, Dando M. (2013) Carcharhiniformes: Ground Sharks. In: Ebert D, Fowler S, Compagno LJV. (eds) *Sharks of the world: a fully illustrated guide*. Wild Nature Press: Plymouth, England, pp. 406–430.
- Edwards AL, Civitello A, Hammond HA, Caskey CT. (1991) DNA typing and genetic mapping with trimeric and tetrameric tandem repeats. *American Journal of Human Genetics* **49**: 746–756.
- Ellegren H. (2004) Microsatellites: simple sequences with complex evolution. *Nature Reviews Genetics* **5**: 435–445.
- Evanno G, Regnaut S, Goudet J. (2005) Detecting the number of clusters of individuals using the software STRUCTURE: a simulation study. *Molecular Ecology* **14**: 2611–2620.
- Excoffier L, Lischer HEL. (2010) ARLEQUIN suite ver 3.5: a new series of programs to perform population genetics analyses under Linux and Windows. *Molecular Ecology Resources* **10**: 564–567.
- FAO. (2005) Review of the state of world marine fishery resources. FAO Fisheries Technical Paper No. 457. FAO: Rome, Italy.
- FAO. (2011) Review of the state of world marine fishery resources. FAO Fisheries Technical Paper No. 569. FAO: Rome, Italy.
- FAO. (2014) The state of world fisheries and aquaculture: opportunities and challenges. FAO: Rome, Italy.
- Farrell ED, Clarke MW, Mariani S. (2009) A simple genetic identification method for north-east Atlantic smoothhound sharks (*Mustelus spp.*). *ICES Journal of Marine Science* **66**: 561–565.
- Feitosa LM, Martins APB, Giarrizzo T, MacEdo W, Monteiro IL, Gemaque R, Nunes JLS, Gomes

- F, Schneider H, Sampaio I, *et al.* (2018) DNA-based identification reveals illegal trade of threatened shark species in a global elasmobranch conservation hotspot. *Scientific Reports* **8**: 3347.
- Feldheim KA, Gruber SH, Ashley MV. (2004) Reconstruction of parental microsatellite genotypes reveals female polyandry and philopatry in the lemon shark, *Negaprion brevirostris*. *Evolution* **58**: 2332–2342.
- Ferguson MM, Danzmann RG. (1998) Role of genetic markers in fisheries and aquaculture: useful tools or stamp collecting? *Canadian Journal of Fisheries and Aquatic Sciences* **55**: 1553–1563.
- Ferrer I, Bonanomi S, Colloca F, Di Lorenzo M, Marino IAM, Sala A, Zane L, Mazzoldi C. (2017) Genetic ID and preliminary population genetics of two threatened smoothhound sharks: insights for conservation. In: Euromarine Workshop, 23–25 May 2017, Venice, Italy.
- Feutry P, Pillans RD, Kyne PM, Chen X. (2016) Complete mitogenome of the Graceful Shark *Carcharhinus amblyrhynchoides* (Carcharhiniformes: Carcharhinidae). *Mitochondrial DNA Part A* **27**: 314–315.
- Francis MP. (1988) Movement patterns of rig (*Mustelus lenticulatus*) tagged in southern New Zealand. *New Zealand Journal of Marine and Freshwater Research* **22**: 259–272.
- Frankham R. (2005) Genetics and extinction. *Biological Conservation* **126**: 131–140.
- Frisk MG, Miller TJ, Fogarty MJ. (2001) Estimation and analysis of biological parameters in elasmobranch fishes: a comparative life history study. *Canadian Journal of Fisheries and Aquatic Sciences* **58**: 969–981.
- Fu YX. (1997) Statistical tests of neutrality of mutations against population growth, hitchhiking and background selection. *Genetics* **147**: 915–925.
- Funk WC, McKay JK, Hohenlohe PA, Allendorf FW. (2012) Harnessing genomics for delineating conservation units. *Trends in Ecology and Evolution* **27**: 489–496.

- Galtier N, Nabholz B, Glemin S, Hurst GDD. (2009) Mitochondrial DNA as a marker of molecular diversity: a reappraisal. *Molecular Ecology* **18**: 4541–4550.
- Gao Y, Liu T, Wei T, Geng X, Wang J, Ma H. (2016) Complete mitochondrial genome of clouded angelshark (*Squatina nebulosa*). *Mitochondrial DNA Part A* **27**: 1599–1600.
- Gardner MG, Ward RD. (2002) Taxonomic affinities within Australian and New Zealand *Mustelus* sharks (Chondrichthyes: Triakidae) inferred from allozymes, mitochondrial DNA and precaudal vertebrae counts. *Copeia* **2002**: 356–363.
- Grant WS, Bowen BW. (1998) Shallow population histories in deep evolutionary lineages of marine fishes: insights from sardines and anchovies and lessons for conservation. *Journal of Heredity* **89**: 415–426.
- Graves JE. (1998) Molecular insight into the population structure of cosmopolitan marine fishes. *Journal of Heredity* **89**: 427–437.
- Greig TW, Moore MK, Woodley CM, Quattro JM. (2001) Mitochondrial gene sequences useful for species identification of western North Atlantic Ocean sharks. *Fishery Bulletin* **103**: 516–523.
- Harpending HC. (1994) Signature of ancient population growth in a low-resolution mitochondrial DNA mismatch distribution. *Human Biology* **66**: 591–600.
- Hasegawa M, Kishino H, Yano T. (1985) Dating of the human-ape splitting by a molecular clock of mitochondrial DNA. *Journal of Molecular Evolution* **22**: 160–174.
- Hebert PDN, Cywinska A, Ball SL, DeWaard JR. (2003) Biological identifications through DNA barcodes. *Proceedings of the Royal Society* **270**: 313–321.
- Heemstra PC. (1973) A revision of the shark genus *Mustelus* (Squaliformes: Carcharhinidae). PhD thesis, University of Miami.
- Heemstra PC. (1997) A review of the smoothhound sharks (genus *Mustelus*, family Triakidae) of the western Atlantic Ocean, with descriptions of two new species and a new subspecies. *Bulletin of*

Marine Science **60**: 894–928.

Helyar SJ, Hemmer-Hansen J, Bekkevold D, Taylor MI, Ogden R, Limborg MT, Cariani A, Maes GE, Diopere E, Carvalho GR. (2011) Application of SNPs for population genetics of nonmodel organisms: new opportunities and challenges. *Molecular Ecology Resources* **11**: 123–136.

Ho SYW, Lanfear R, Bromham L, Phillips MJ, Soubrier J, Rodrigo AG, Cooper A. (2011) Time-dependent rates of molecular evolution. *Molecular Ecology* **20**: 3087–3101.

Hoelzel AR, Shivji MS, Magnussen J, Francis MP. (2006) Low worldwide genetic diversity in the basking shark (*Cetorhinus maximus*). *Biology Letters* **2**: 639–642.

Hoffman JI, Nichols HJ. (2011) A novel approach for mining polymorphic microsatellite markers *in silico*. *PLoS ONE* **6**: e23283.

Hueter RE, Heupel MR, Heist EJ, Keeney DB. (2005) Evidence of philopatry in sharks and implications for the management of shark fisheries. *Journal of Northwest Atlantic Fishery Science* **35**: 239–247.

Iwasaki W, Fukunaga T, Isagozawa R, Yamada K, Maeda Y, Satoh TP, Sado T, Mabuchi K, Takeshima H, Miya M, *et al.* (2013) MITOFISH and MITOANNOTATOR: a mitochondrial genome database of fish with an accurate and automatic annotation pipeline. *Molecular Biology and Evolution* **30**: 2531–2540.

Jackson JBC. (2010) The future of the oceans past. *Philosophical Transactions of the Royal Society B: Biological Sciences* **365**: 3765–3778.

Jamieson A. (1974) Genetic "tags" for marine fish stocks. In: Hardin JFR. (ed.) *Sea Fisheries Research*. Elek Science: London, England, pp. 91–99.

Jombart T. (2008) ADEGENET: a R package for the multivariate analysis of genetic markers. *Bioinformatics* **24**: 1403–1405.

Jombart T, Devillard S, Balloux F. (2010) Discriminant analysis of principal components: a new

- method for the analysis of genetically structured populations. *BMC Genetics* **11**: 94–108.
- Jost L (2008) G_{ST} and its relatives do not measure differentiation. *Molecular Ecology* **17**: 4015–4026.
- Kalinowski ST. (2005) HP-RARE 1.0: a computer program for performing rarefaction on measures of allelic richness. *Molecular Ecology Notes* **5**: 187–189.
- Karl SA, Castro ALF, Lopez JA, Charvet P, Burgess GH. (2011) Phylogeography and conservation of the bull shark (*Carcharhinus leucas*) inferred from mitochondrial and microsatellite DNA. *Conservation Genetics* **12**: 371–382.
- Katoh K, Standley DM. (2013) MAFFT multiple sequence alignment software version 7: improvements in performance and usability. *Molecular Biology and Evolution* **30**: 772–780.
- Kearse M, Moir R, Wilson A, Stones-Havas S, Cheung M, Sturrock S, Buxton S, Cooper A, Markowitz S, Duran C, *et al.* (2012). GENEIOUS Basic: an integrated and extendable desktop software platform for the organization and analysis of sequence data. *Bioinformatics* **28**: 1647–1649.
- Keeney DB, Heupel M, Hueter RE, Heist EJ. (2003) Genetic heterogeneity among blacktip shark, *Carcharhinus limbatus*, continental nurseries along the U.S. Atlantic and Gulf of Mexico. *Marine Biology* **143**: 1039–1046.
- Keeney DB, Heupel MR, Hueter RE, Heist EJ. (2005) Microsatellite and mitochondrial DNA analyses of the genetic structure of blacktip shark (*Carcharhinus limbatus*) nurseries in the northwestern Atlantic, Gulf of Mexico, and Caribbean Sea. *Molecular Ecology* **14**: 1911–1923.
- Keeney DB, Heist EJ. (2006) Worldwide phylogeography of the blacktip shark (*Carcharhinus limbatus*) inferred from mitochondrial DNA reveals isolation of western Atlantic populations coupled with recent Pacific dispersal. *Molecular Ecology* **15**: 3669–3679.
- Kemper JM, Naylor GJP. (2016) The complete mitochondrial genome and phylogenetic position of

- the Philippines spurdog, *Squalus montalbani*. Mitochondrial DNA Part A **27**: 4522–4523.
- Kimura M. (1968) Evolutionary rate at the molecular level. *Nature* **217**: 624–626.
- Kopelman NM, Mayzel J, Jakobsson M, Rosenberg NA, Mayrose I. (2015) CLUMPAK: a program for identifying clustering modes and packaging population structure inferences across *K*. *Molecular Ecology Resources* **15**: 1179–1191.
- Kousteni V, Kasapidis P, Kotoulas G, Megalofonou P. (2015) Strong population genetic structure and contrasting demographic histories for the small-spotted catshark (*Scyliorhinus canicula*) in the Mediterranean Sea. *Heredity* **114**: 333–343.
- Kraus RHS, Kerstens HHD, Hooft PV, Megens HJ, Elmberg J, Tsvey A, Sartakov D, Soloviev SA, Crooijmans RPMA, Groenen MAM. (2012) Widespread horizontal genomic exchange does not erode species barriers among sympatric ducks. *BMC Evolutionary Biology* **12**: 45.
- Kriwet J, Kiessling W, Klug S. (2012) Diversification trajectories and evolutionary life-history traits in early sharks and batoids. *Proceedings of the Royal Society B: Biological Sciences* **276**: 945–951.
- Kroese M, Sauer W. (1998) Elasmobranch exploitation in Africa. *Marine Freshwater Research* **49**: 573–577.
- Kumar G, Kocour M. (2017) Applications of next-generation sequencing in fisheries research: a review. *Fisheries Research* **186**: 11–22.
- Kumar S, Stecher G, Tamura K. (2016) MEGA7: Molecular evolutionary genetics analysis version 7.0 for bigger datasets. *Molecular Biology and Evolution* **33**: 1870–1874.
- Li YL, Liu JX. (2018) STRUCTURESELECTOR: a web-based software to select and visualize the optimal number of clusters using multiple methods. *Molecular Ecology Resources* **18**: 176–177.
- Librado P, Rozas J. (2009) DNASP v5: a software for comprehensive analysis of DNA polymorphism data. *Bioinformatics* **25**: 1451–1452.

- Liu N, Chen L, Wang S, Oh C, Zhao H. (2005) Comparison of single-nucleotide polymorphisms and microsatellites in inference of population structure. *BMC Genetics* **6**: S26.
- Liu ZJ, Cordes JF. (2004) DNA marker technologies and their applications in aquaculture genetics. *Aquaculture* **238**: 1–37.
- Loget N, Van Den Driessche J. (2006) On the origin of the Strait of Gibraltar. *Sedimentary Geology* **188–189**: 341–356.
- López JA, Ryburn JA, Fedrigo O, Naylor GJP. (2006) Phylogeny of sharks of the family Triakidae (Carcharhiniformes) and its implications for the evolution of carcharhiniform placental viviparity. *Molecular Phylogenetics and Evolution* **40**: 50–60.
- Luikart G, Allendorf FW, Cornuet JM, Sherwin WB. (1998) Distortion of allele frequency distributions provides a test for recent population bottlenecks. *Journal of Heredity* **89**: 238–247.
- Luikart G, Cornuet J. (1998) Empirical evaluation of a test for identifying recently bottlenecked populations from allele frequency data. *Conservation Biology* **12**: 228–237.
- Maduna SN, Rossouw C, Roodt-Wilding, R, Bester-van der Merwe, AE. (2014) Microsatellite cross-species amplification and utility in southern African elasmobranchs: a valuable resource for fisheries management and conservation. *BMC Research Notes* **7**: 352.
- Maduna SN, da Silva C, Wintner SP, Roodt-Wilding R, Bester-van der Merwe AE. (2016) When two oceans meet: regional population genetics of an exploited coastal shark, *Mustelus mustelus*. *Marine Ecology Progress Series* **544**: 183–196.
- Maduna SN, Rossouw C, da Silva C, Bester-van der Merwe AE. (2017) Species identification and comparative population genetics of four coastal houndsharks based on novel NGS-mined microsatellites. *Wiley Ecology and Evolution* **7**: 1462–1486.
- Maduna SN, Bester-van der Merwe AE. (2017) Molecular research on the systematically challenging smoothhound shark genus *Mustelus*: a synthesis of the past 30 years. *African Journal of Marine*

Science **39**: 373–387.

Mann BQ, Bullen EM (2009) ORI/WWF-SA Tagging Project: summary of tag and recapture data for smoothhoundsharks (*Mustelus mustelus*) caught along the southern African coast from 1984–2008. Durban, South Africa: Oceanographic Research Institute.

Mantel N. (1967) The detection of disease clustering and a generalized regression approach. Cancer Research **27**: 1183–1185.

Marino IAM, Finotto L, Colloca F, Di Lorenzo M, Gristina M, Farrell ED, Zane L, Mazzoldi C. (2014) New molecular tools for the identification of 2 endangered smooth-hound sharks, *Mustelus mustelus* and *Mustelus punctulatus*. Journal of Heredity **106**: 123–130.

Marino IAM, Finotto L, Colloca F, Di Lorenzo M, Gristina M, Farrell ED, Zane L, Mazzoldi C. (2017) Resolving the ambiguities in the identification of two smooth-hound sharks (*Mustelus mustelus* and *Mustelus punctulatus*) using genetics and morphology. Marine Biodiversity **3**: 1551–1562.

Mazzoldi C, Sambo A, Riginella E. (2014) The Clodia database: A long time series of fishery data from the Adriatic Sea. Scientific Data **1**: 140018.

McCord ME, Lamberth SJ. (2009) Catching and tracking the world’s largest Zambezi (bull) shark *Carcharhinus leucas* in the Breede Estuary, South Africa: the first 43 hours. African Journal of Marine Science **31**: 107–111.

Meeuwis JM, Lutjeharms JRE. (1990) Surface thermal characteristics of the Angola-Benguela front. South African Journal of Marine Science **9**: 261–279.

Mendonça FF, Oliveira C, Gadig OBF, Foresti F. (2013) Diversity and genetic population structure of the Brazilian sharpnose shark *Rhizoprionodon lalandii*. Aquatic Conservation: Marine and Freshwater Ecosystems **23**: 850–857.

Miller MA, Pfeiffer W, Schwartz T. (2010) Creating the CIPRES Science Gateway for inference of

- large phylogenetic trees. In: Proceedings of the Gateway Computation and Environment Workshop (GCE): 1–8.
- Mooi RD, Gill AC. (2002) Historical biogeography of fishes. In: Hart P, Reynolds J. (eds.) *Handbook of fish biology and fisheries*. Blackwell Science: Oxford, England, pp. 43–68.
- Morin PA, Martien KK, Taylor BL. (2009) Assessing statistical power of SNPs for population structure and conservation studies. *Molecular Ecology Resources* **9**: 66–73.
- Morin PA, Martien KK, Archer FI, Cipriano F, Steel D, Jackson J, Taylor BL. (2010) Applied conservation genetics and the need for quality control and reporting of genetic data used in fisheries and wildlife management. *Journal of Heredity* **101**: 1–10.
- Moritz C. (1994) Defining "Evolutionary Significant Units" for conservation. *Trends in Ecology and Evolution* **9**: 373–375.
- Musick JA, Harbin MM, Compagno LJV. (2004) Historical zoogeography of the Selachii. In: Carrier J, Musick JA, Heithaus M. (eds.) *Biology of sharks and their relatives* CRC press: Boca Raton, Florida, pp. 33–78.
- Naylor GJP, Caira JN, Jensen K, Rosana KAM. (2012) A DNA sequence-based approach to the identification of shark and ray species and its implications for global elasmobranch diversity and parasitology. *Bulletin of the American Museum of Natural History* pp. 8–31.
- Noller HF, Hoffarth V, Zimniak L. (1992) Unusual resistance of peptidyl transferase to protein extraction procedures. *Science* **256**: 1416–1419.
- O'Brien SJ. (1991) Mammalian genome mapping: lessons and prospects. *Current Opinion in Genetics and Development* **1**: 105–111.
- Ohta T. (1973) Slightly deleterious mutant substitutions in evolution. *Nature* **246**: 96–98.
- Oliver S, Braccini M, Newman SJ, Harvey ES. (2015) Global patterns in the bycatch of sharks and rays. *Marine Policy* **54**: 86–97.

- Orlic M, Gacic M, Laviolette P. (1992) The currents and circulation of the Adriatic Sea. *Oceanologica Acta* **15**: 109–124.
- Ovenden JR. (1990) Mitochondrial DNA and marine stock assessment: a review. *Marine and Freshwater Research* **41**: 835–853.
- Ovenden JR, Kashiwagi T, Broderick D, Giles J, Salini J. (2009) The extent of population genetic subdivision differs among four co-distributed shark species in the Indo-Australian archipelago. *BMC Evolutionary Biology* **9**: 40.
- Ovenden JR. (2013) Crinkles in connectivity: combining genetics and other types of biological data to estimate movement and interbreeding between populations. *Marine and Freshwater Research*. **64**: 201–207.
- Paradis E, Claude J, Strimmer K (2004) APE: analyses of phylogenetics and evolution in R language. *Bioinformatics* **20**: 289–290.
- Park S. (2001) The Excel Microsatellite toolkit (version 3.1.1). Animal Genomics Laboratory: University College, Dublin, Ireland.
- Peakall R, Smouse PE. (2006) GENALEX 6: genetic analysis in Excel. Population genetic software for teaching and research. *Molecular Ecology Notes* **6**: 288–295.
- Pennings PS, Achenbach A, Foitzik S (2011) Similar evolutionary potentials in an obligate ant parasite and its two host species. *Journal of Evolutionary Biology* **24**: 871–886.
- Pereyra S, García G, Miller P, Oviedo S, Domingo A. (2010) Low genetic diversity and population structure of the narrownose shark (*Mustelus schmitti*). *Fisheries Research* **106**: 468–473.
- Piry S, Luikart G, Cornuet JM. (1999) BOTTLENECK: a computer program for detecting recent reduction in the effective population size using allele frequency data. *Journal of Heredity* **90**: 502–503.
- Predtechenskyj N, Karatajute-Talimaa V. (1995) The distribution of the vertebrates in the Late

- Ordovician and Early Silurian palaeobasins of the Siberian Platform. *Bulletin of the National Museum of Natural History* **17**: 39–55.
- Pritchard JK, Stephens M, Donnelly P. (2000) Inference of population structure using multilocus genotype data. *Genetics* **155**: 945–959.
- Puechmaille SJ. (2016) The program STRUCTURE does not reliably recover the correct population structure when sampling is uneven: subsampling and new estimators alleviate the problem. *Molecular Ecology Resources* **16**: 608–627.
- Quraishia SF, Panneerchelvam S, Zainuddin Z, Haslindawaty Abd Rashid N. (2015) Molecular characterization of Malaysian marine fish species using partial sequence of mitochondrial DNA *12S* and *16S rRNA* markers. *Sains Malaysiana* **44**: 1119–1123.
- Rasmussen AS and Arnason U. (1999) Molecular studies suggest that cartilaginous fishes have a terminal position in the piscine tree. *Proceedings of the National Academy of Sciences* **96**: 2177–2182.
- Ronquist F, Teslenko M, Van Der Mark P, Ayres DL, Darling A, Höhna S, Larget B, Liu L, Suchard MA, Huelsenbeck JP. (2012) MRBAYES 3.2: efficient bayesian phylogenetic inference and model choice across a large model space. *Systematic Biology* **61**: 539–542.
- Rousset F. (2008) ‘GENEPOP’007: a complete re-implementation of the genepop software for Windows and Linux. *Molecular Ecology Resources* **8**: 103–106.
- Saidi B, Bradaï MN, Bouaïn A. (2008) Reproductive biology of the smoothhound shark *Mustelus mustelus* (L.) in the Gulf of Gabès (south-central Mediterranean Sea). *Journal of Fish Biology* **72**: 1343–1354.
- Sambrook J, Russell DW. (2001) *Molecular cloning: A laboratory manual*. Cold Spring Harbour Laboratory Press: New York, USA.
- Santaquiteria A, Nielsen J, Klemetsen T, Willassen NP, Præbel K. (2017) The complete

- mitochondrial genome of the long-lived Greenland shark (*Somniosus microcephalus*): characterization and phylogenetic position. *Conservation Genetics Resources* **9**: 351–355.
- Schmidt JV, Schmidt CL, Ozer F, Ernst RE, Feldheim KA, Ashley MV, Levine M. (2009) Low genetic differentiation across three major ocean populations of the whale shark, *Rhincodon typus*. *PLoS ONE* **4**: e4988.
- Schmieder R, Edwards R. (2011) Quality control and preprocessing of metagenomic datasets. *Bioinformatics* **27**: 863–864.
- Schultz JK, Feldheim KA, Gruber SH, Ashley MV, McGovern TM, Bowen BW. (2008) Global phylogeography and seascape genetics of the lemon sharks (genus *Negaprion*). *Molecular Ecology* **17**: 5336–5348.
- Schwarz G. (1978) Estimating the dimension of a model. *The Annals of Statistics* **6**: 461–464.
- Seeb JE, Carvalho G, Hauser L, Naish K, Roberts S, Seeb LW. (2011) Single nucleotide polymorphism (SNP) discovery and applications of SNP genotyping in non-model organisms. *Molecular Ecology Resources* **11**: 1–8.
- Serena F, Mancusi C, Clò S, Ellis J, Valenti SV. (2009) *Mustelus mustelus*. The IUCN Red List of Threatened Species 2009: e.T39358A10214694. <http://dx.doi.org/10.2305/IUCN.UK.2009-2.RLTS.T39358A10214694.en>
- Simpfendorfer C, Heupel M. (2004) Assessing habitat use and movement. In: Carrier JC, Musick JA, Heithaus MR. (eds.) *Biology of sharks and their relatives*. CRC Press: Boca Raton, USA. pp 553–572.
- Smale MJ, Compagno LJV. (1997) Life history and diet of two southern African smoothhound sharks, *Mustelus mustelus* (Linnaeus, 1758) and *Mustelus palumbes* Smith, 1957 (Pisces: Triakidae). *South African Journal of Marine Science* **18**: 229–248.
- Smale MJ, Booth AJ, Farquhar MR, Meyer, MR, Rochat L. (2012) Migration and habitat use of

- formerly captive and wild raggedtooth sharks (*Carcharias taurus*) on the southeast coast of South Africa. *Marine Biology Research* **8**: 115–128.
- Smith PJ. (1990) Protein Electrophoresis for identification of Australasian fish stocks. *Marine and Freshwater Research* **41**: 823–833.
- Springer MS, DeBry RW, Douady C, Amrine HM, Madsen O, De Jong WW, Stanhope MJ. (2001) Mitochondrial versus nuclear gene sequences in deep-level mammalian phylogeny reconstruction. *Molecular Biology and Evolution* **18**: 132–143.
- Stevens JD, Bonfil R, Dulvy NK, Walker PA. (2000) The effects of fishing on sharks, rays, and chimaeras (chondrichthyans), and the implications for marine ecosystems. *ICES Journal of Marine Science* **57**: 476–494.
- Tajima F. (1989) Statistical method for testing the neutral mutation hypothesis by DNA polymorphism. *Genetics* **123**: 585–595.
- Tanaka K, Shiina T, Tomita T, Suzuki S, Hosomichi K, Sano K, Doi H, Kono A, Komiyama T, Inoko H, *et al.* (2013) Evolutionary relations of hexanchiformes deep-sea sharks elucidated by whole mitochondrial genome sequences. *BioMed Research International* **2013**.
- Tautz D. (1989) Hypervariability of simple sequences as a general source for polymorphic DNA markers. *Nucleic Acids Research* **17**: 6463–6471.
- Tautz D, Ellegren H, Weigel D. (2010) Next generation molecular ecology. *Molecular Ecology* **19**: 1–3.
- Teshima K, Koga S. (1973) Studies on sharks. V. Taxonomic characteristics of reproductive organs in Japanese *Mustelus*. *Marine Biology* **23**: 337–341.
- Teske PR, Golla TR, Sandoval-Castillo J, Emami-Khoyi A, van der Lingen CD, von der Heyden S, Chiazzari B, Jansen van Vuuren B, Beheregaray LB. (2018) Mitochondrial DNA is unsuitable to test for isolation by distance. *Scientific Reports* **8**: 8448.

- Tillett BJ, Meekan MG, Field IC, Thorburn DC, Ovenden JR. (2012) Evidence for reproductive philopatry in the bull shark *Carcharhinus leucas*. *Journal of Fish Biology* **80**: 2140–2158.
- Towner AV, Wcisel MA, Reisinger RR, Edwards D, Jewell OJD. (2013) Gauging the threat: the first population estimate for white sharks in South Africa using photo identification and automated software. *PLoS ONE* **8**: e66035.
- Ukwe CN, Ibe CA, Sherman K. (2006) A sixteen-country mobilization for sustainable fisheries in the Guinea Current Large Marine Ecosystem. *Ocean and Coastal Management* **49**: 385–412.
- Van Oosterhout C, Hutchinson WF, Will DPM, Shipley P. (2004) MICROCHECKER: software for identifying and correcting genotyping errors in microsatellite data. *Molecular Ecology Notes* **4**: 535–538.
- van Zyl K. (1993) *Marine products: die eerste 50 jaar*. Cape Town: Nasionale Boekdrukkery
- Velez-Zuazo X, Alfaro-Shigueto J, Mangel J, Papa R, Agnarsson I. (2015) What barcode sequencing reveals about the shark fishery in Peru. *Fisheries Research* **161**: 34–41.
- Vella N, Vella A. (2017) Population genetics of the deep-sea bluntnose sixgill shark, *Hexanchus griseus*, revealing spatial genetic heterogeneity. *Marine Genomics* **36**: 25–32.
- Veríssimo A, Sampaio Í, McDowell, JR, Alexandrino P, Mucientes G, Queiroz, N, da Silva C, Jones CS, Noble LR. (2017) World without borders—genetic population structure of a highly migratory marine predator, the blue shark (*Prionace glauca*). *Ecology and Evolution* **7**: 4768–4781
- Vignaud T, Clua E, Mourier J, Maynard J, Planes S. (2013) Microsatellite analyses of blacktip reef sharks (*Carcharhinus melanopterus*) in a fragmented environment show structured clusters. *PLoS ONE* **8**: e61067.
- von Bonde C. (1934) Shark fishing as an industry. *Fisheries and Marine Biology Division, Union of South Africa, Investigational Report 2*: pp. 1–19.

- Walker P, Cavanagh RD, Ducrocq M, Fowler SL. (2005) Regional overviews: north-east Atlantic (including Mediterranean and Black Sea). In: Fowler SL, Cavanagh RD, Camhi M, Burgess GH, Cailliet GM, Fordham SV, Simpfendorfer CA, Musick JA. (eds.). *Sharks, Rays and Chimaeras: The Status of the Chondrichthyan Fishes*. IUCN/SSC Shark Specialist Group: Gland, Switzerland and Cambridge, UK, pp. 86.
- Waples RS, Gaggiotti O. (2006) What is a population? An empirical evaluation of some genetic methods for identifying the number of gene pools and their degree of connectivity. *Molecular Ecology* **15**: 1419–1439.
- Ward RD, Zemlak TS, Innes BH, Last PR, Hebert PDN. (2005) DNA barcoding Australia's fish species. *Philosophical Transactions of the Royal Society* **360**: 1847–1857.
- Weigmann S. (2016) Annotated checklist of the living sharks, batoids and chimaeras (Chondrichthyes) of the world, with a focus on biogeographical diversity. *Journal of Fish Biology* **88**: 837–1037.
- Weigmann S. (2017) Reply to Borsa (2017): Comment on ‘Annotated checklist of the living sharks, batoids and chimaeras (Chondrichthyes) of the world, with a focus on biogeographical diversity by Weigmann (2016)’. *Journal of Fish Biology* **90**: 1176–1181.
- Weiss H, Friedrich T, Hofhaus G, Preis D (1991) The respiratory-chain *NADH dehydrogenase* (complex I) of mitochondria. In: Christen P, Hofmann E. (eds.) *EJB Reviews 1991*. Springer: Heidelberg, Germany. pp. 55–68.
- Worm B, Hilborn R, Baum JK, Branch TA, Collie JS, Costello C, Fogarty MJ, Fulton EA, Hutchings JA, Jennings S, *et al.* (2009) Rebuilding global fisheries. *Science* **325**: 578–585
- Wright S. (1943) Isolation by distance. *Genetics* **28**: 114–138

Yang L, Matthes-Rosana KA, Naylor GJP. (2016). Determination of complete mitochondrial genome sequence from the holotype of the southern Mandarin dogfish *Cirrhigaleus australis* (Elasmobranchii: Squalidae). *Mitochondrial DNA Part A* **27**: 593–594.

Zenetos A, Sioku-Frangou I, Gotsis-Skretas O, Groom S. (2002) The Mediterranean Sea – blue oxygen rich, nutrient poor waters. In: Condé S, Richard D. (eds.) *Europe's biodiversity, biogeographical regions and seas. Seas around Europe*. European Environment Agency: Copenhagen, Denmark.

Appendix A

Supplementary information for Chapter II

Table S2.1 BLAST results for *Mustelus mustelus* sequence comparison of mitochondrial regions with six species within the Carcharhiniformes order.

<i>Mustelus mustelus</i> sequences								<i>Carcharhinus amblyrhynchoides</i> mitogenome			<i>Galeocerdo cuvier</i> mitogenome			<i>Mustelus griseus</i> mitogenome			<i>Mustelus manazo</i> mitogenome			<i>Prionace glauca</i> mitogenome			<i>Sphyrna lewini</i> mitogenome		
COIII	NADH3	NADH4L	NADH4	NADH5	NADH6	Cyt b	CR	Alignment length (bp)	E-value	Similarity (%)	Alignment length (bp)	E-value	Similarity (%)	Alignment length (bp)	E-value	Similarity (%)	Alignment length (bp)	E-value	Similarity (%)	Alignment length (bp)	E-value	Similarity (%)	Alignment length (bp)	E-value	Similarity (%)
786	349	297	1,381	1,830	522	1,145	1,118																		
0.00E+00	2.76E-123	1.87E-99	0.00E+00	0.00E+00	6.67E-156	0.00E+00	0.00E+00																		
89.8	88.8	87.9	84.4	86.3	85.3	88.6	84.3																		
786	349	297	1,381	1,834	522	1,147	1,084																		
0.00E+00	1.74E-103	1.91E-84	0.00E+00	0.00E+00	2.31E-167	0.00E+00	0.00E+00																		
89.6	83.1	84.8	86.2	84.9	84.5	84.9	86.8																		
786	349	297	1,381	1,830	522	1,145	1,119																		
0.00E+00	1.20E-171	3.80E-141	0.00E+00	0.00E+00	0.00E+00	0.00E+00	0.00E+00																		
98.5	87.1	96.3	95.3	95.5	95.4	96.1	97.2																		
786	349	297	1,381	1,830	522	1,145	1,073																		
0.00E+00	5.77E-145	8.21E-138	0.00E+00	0.00E+00	0.00E+00	0.00E+00	0.00E+00																		
94.1	92.6	95.6	92.3	91.4	91.6	91.4	93.4																		
786	349	297	1,381	1,830	522	1,145	1,118																		
0.00E+00	2.80E-113	4.07E-91	0.00E+00	0.00E+00	6.62E-161	0.00E+00	3.12E-157																		
90.0	87.1	86.2	84.4	85.8	85.9	85.9	83.1																		
786	349	297	1,381	1,830	522	1,145	1,118																		
0.00E+00	2.90E-88	4.13E-81	0.00E+00	0.00E+00	5.24E-147	0.00E+00	7.10E-119																		
89.4	82.8	84.2	85.1	85.1	84.3	86.1	81.1																		

		<i>Mustelus mustelus</i> sequences						
		12S rRNA	16S rRNA	NADH1	NADH2	COI	COII	ATPase 8
<i>Carcharias amblyrhynchoides</i> mitogenome	Alignment length (bp)	951	1,669	975	1,045	1,557	691	168
	E-value	0.00E+00	0.00E+00	0.00E+00	0.00E+00	0.00E+00	0.00E+00	2.33E-56
	Similarity (%)	92.1	92.3	82.9	86.2	88.1	91.0	88.7
<i>Galeocerdo cuvier</i> mitogenome	Alignment length (bp)	951	1,670	975	1,029	1,556	691	168
	E-value	0.00E+00	0.00E+00	0.00E+00	0.00E+00	0.00E+00	0.00E+00	2.30E-66
	Similarity (%)	90.3	91.5	85.7	84.5	87.6	88.9	92.3
<i>Mustelus griseus</i> mitogenome	Alignment length (bp)	951	1,669	975	1,045	1,557	691	168
	E-value	0.00E+00	0.00E+00	0.00E+00	0.00E+00	0.00E+00	0.00E+00	4.86E-83
	Similarity (%)	98.1	98.6	97.1	95.8	97.0	97.7	98.2
<i>Mustelus manazo</i> mitogenome	Alignment length (bp)	953	1,671	965	1,045	1,557	691	168
	E-value	0.00E+00	0.00E+00	0.00E+00	0.00E+00	0.00E+00	0.00E+00	4.95E-86
	Similarity (%)	95.5	96.8	91.5	92.1	92.4	95.2	92.9
<i>Prionace glauca</i> mitogenome	Alignment length (bp)	951	1,669	957	1,045	1,557	691	168
	E-value	0.00E+00	0.00E+00	0.00E+00	0.00E+00	0.00E+00	0.00E+00	1.09E-49
	Similarity (%)	91.2	92.4	85.5	83.1	88.3	89.4	86.3
<i>Sphyrna lewini</i> mitogenome	Alignment length (bp)	951	1,669	975	1,045	1,557	691	168
	E-value	0.00E+00	0.00E+00	0.00E+00	0.00E+00	0.00E+00	0.00E+00	2.37E-46
	Similarity (%)	90.6	91.5	85.6	84.0	87.0	88.4	85.1

Appendix B

Supplementary Information for Chapter III

Table S3.1 Mean pairwise genetic distance between global sampling populations of *Mustelus mustelus*.

	AS	SS	BI	CV	GB	GC	AN	SA
AS								
SS	0.001							
BI	0.001	0.001						
CV	0.010	0.010	0.009					
GB	0.004	0.004	0.004	0.008				
GC	0.005	0.005	0.005	0.006	0.004			
AN	0.004	0.004	0.004	0.006	0.004	0.004		
SA	0.001	0.005	0.004	0.007	0.005	0.005	0.001	

Table S3.2 Pairwise D_{est} estimates between global sampling populations of *Mustelus mustelus*. D_{est} values below the diagonal, corresponding P -value above the diagonal.

	AS	SS	BI	CV	GB	GC	AN	SA
AS		0.925	0.069	0.000	0.000	0.005	0.000	0.000
SS	0.000		0.201	0.001	0.000	0.004	0.000	0.000
BI	0.138	0.103		0.000	0.000	0.000	0.000	0.000
CV	1.000*	1.000*	1.000*		0.000	0.002	0.000	0.000
GB	1.000*	1.000*	1.000*	1.000*		0.015	0.000	0.028
GC	1.000*	1.000*	1.000*	1.000*	0.748		0.000	0.003
AN	1.000*	1.000*	1.000*	1.000*	0.813*	1.000*		0.011
SA	1.000*	1.000*	1.000*	1.000*	0.682	1.000*	0.300	

* statistical significance at a 0.01 level; **bold values** indicate statistical significance after B-H correction

Table S3.3 Genetic differentiation between sampling populations grouped into broad oceanic regions. Φ_{ST} estimates below the diagonal, P -values above the diagonal. MED – Mediterranean Sea; SNEA – southern north-east Atlantic; SAI – south-east Atlantic/south-west Indian

	<i>MED</i>	<i>SNEA</i>	<i>SAI</i>
<i>MED</i>		0.000	0.000
<i>SNEA</i>	0.554*		0.000
<i>SAI</i>	0.742*	0.343*	

* statistical significance at a 0.01 level; **bold values indicate statistical significance after B-H correction**

Appendix C

Supplementary information for Chapter IV

Table S4.1 Multiplex assay characterisation. MP – multiplex number; SSR – repeat motif; T_A – annealing temperature.

MP	Marker	SSR	Dye	Size range (bp)	T _A (°C)	Reference
1	Mmu1	(AT) ₇	VIC	200 - 219	57	Maduna <i>et al.</i> 2017
	Mmu5	(CTC) ₆	FAM	265 - 285		
	Mmu7	(GCT) ₅	NED	200 - 217		
	Mmu14	(AGC) ₆	FAM	160 - 190		
2	Mmu2	(AC) ₆	FAM	150 - 175	56	
	Mmu3	(TC) ₇	NED	200 - 245		
	Mmu4	(TG) ₇	VIC	150 - 180		
	Mmu8	(CAG) ₅	VIC	410 - 440		
	Mmu13	(GCA) ₅	NED	90 - 120		

Table S4.2 Genetic diversity indices per microsatellite marker for *Mustelus mustelus* sampling populations at eight collection sites along its global distribution: polymorphic information content (PIC); average number of alleles (A_N); effective number of alleles (A_E); Shannon's information index (I); observed heterozygosity (H_o); fixation index (F) and null allele frequencies ($Fr_{(Null)}$), as well as the standard error (SE) for each mean estimate. An asterisk (*) indicates deviation from Hardy-Weinberg equilibrium ($P < 0.01$).

Population	Locus	PIC	A_N	A_E	I	H_o	F	$Fr_{(Null)}$
Adriatic Sea	Mmu1	0.73	8.00	4.21	1.69	0.60	0.21	0.09
	Mmu5	0.00	1.00	1.00	0.00	0.00	n.d.	0.00
	Mmu7	0.00	1.00	1.00	0.00	0.00	n.d.	0.00
	Mmu14	0.37	2.00	1.99	0.69	0.27	0.46	0.15
	Mmu2	0.55	3.00	2.63	1.03	0.47	0.25	0.09
	Mmu3	0.41	4.00	1.77	0.86	0.00	1.00*	0.30
	Mmu4	0.00	1.00	1.00	0.00	0.00	n.d.	0.00
	Mmu8	0.42	5.00	1.79	0.93	0.27	0.40*	0.12
	Mmu13	0.00	1.00	1.00	0.00	0.00	n.d.	0.00
Mean (SE)		0.28 (0.07)	2.90 (0.81)	1.82 (0.36)	0.58 (0.20)	0.18 (0.08)	0.46 (0.11)	0.09 (0.03)
Strait of Sicily	Mmu1	0.68	6.00	3.63	1.46	0.80	-0.10	0.00
	Mmu5	0.37	3.00	1.72	0.73	0.00	1.00*	0.29
	Mmu7	0.18	3.00	1.23	0.39	0.07	0.64	0.10
	Mmu14	0.57	5.00	2.57	1.20	0.47	0.24	0.09
	Mmu2	0.73	7.00	4.29	1.62	0.67	0.13	0.06
	Mmu3	0.43	4.00	2.03	0.88	0.67	-0.32	0.00
	Mmu4	0.56	5.00	2.47	1.20	0.27	0.55*	0.21
	Mmu8	0.49	5.00	2.09	1.06	0.47	0.11	0.04
	Mmu13	0.06	2.00	1.07	0.15	0.07	-0.03	0.00
Mean (SE)		0.45 (0.06)	4.44 (0.53)	2.34 (0.35)	0.97 (0.16)	0.39 (0.10)	0.245 (0.138)	0.09 (0.03)
Balearic Islands	Mmu1	0.73	7.00	4.33	1.63	0.87	-0.13	0.00
	Mmu5	0.20	2.00	1.30	0.39	0.00	1.00*	0.19

	Mmu7	0.27	3.00	1.41	0.56	0.07	0.77*	0.17
	Mmu14	0.37	4.00	1.64	0.78	0.27	0.32	0.09
	Mmu2	0.38	3.00	1.74	0.76	0.20	0.53*	0.16
	Mmu3	0.51	5.00	2.45	1.06	1.00	-0.69	0.00
	Mmu4	0.00	1.00	1.00	0.00	0.00	n.d.	0.00
	Mmu8	0.22	3.00	1.31	0.47	0.27	-0.12	0.00
	Mmu13	0.00	1.00	1.00	0.00	0.00	n.d.	0.00
Mean (SE)		0.30 (0.06)	3.22 (0.53)	1.80 (0.35)	0.63 (0.17)	0.30 (0.126)	0.24 (0.2)	0.07 (0.02)
Cape Verde	Mmu1	0.61	5.00	3.08	1.26	1.00	-0.480	0.00
	Mmu5	0.00	1.00	1.00	0.00	0.00	n.d.	0.00
	Mmu7	0.00	1.00	1.00	0.00	0.00	n.d.	0.00
	Mmu14	0.12	2.00	1.14	0.24	0.13	-0.071	0.00
	Mmu2	0.12	3.00	1.15	0.29	0.13	-0.053	0.00
	Mmu3	0.47	4.00	2.28	0.94	1.00	-0.779	0.00
	Mmu4	0.00	1.00	1.00	0.00	0.00	n.d.	0.00
	Mmu8	0.37	3.00	1.78	0.72	0.33	0.239	0.07
	Mmu13	0.00	1.00	1.00	0.00	0.00	n.d.	0.00
Mean (SE)		0.19 (0.06)	2.33 (0.50)	1.49 (0.25)	0.38 (0.16)	0.29 (0.13)	-0.23 (0.13)	0.01 (0.01)
Guinea Bissau	Mmu1	0.56	3.00	2.74	1.05	0.92	-0.44	0
	Mmu5	0.00	1.00	1.00	0.00	0.00	n.d.	0.29
	Mmu7	0.34	3.00	1.65	0.67	0.08	0.79*	0.22
	Mmu14	0.38	2.00	2.00	0.69	0.50	0.00	0.00
	Mmu2	0.28	4.00	1.42	0.62	0.33	-0.13	0.00
	Mmu3	0.68	6.00	3.60	1.47	1.00	-0.38	0.00
	Mmu4	0.44	4.00	1.88	0.92	0.42	0.11	0.04
	Mmu8	0.56	5.00	2.50	1.18	0.83	-0.39	0.00
	Mmu13	0.14	2.00	1.18	0.29	0.17	-0.09	0.00
Mean (SE)		0.37 (0.06)	3.33 (0.53)	2.00 (0.28)	0.77 (0.15)	0.47 (0.12)	-0.07 (0.13)	0.07 (0.03)
Guinea	Mmu1	0.58	5.00	2.57	1.23	0.67	-0.09	0.00
	Mmu5	0.00	1.00	1.00	0.00	0.00	n.d.	0.00
	Mmu7	0.14	2.00	1.18	0.29	0.17	-0.09	0.00

	Mmu14	0.48	4.00	2.06	0.98	0.50	0.03	0.01
	Mmu2	0.30	2.00	1.60	0.56	0.50	-0.33	0.00
	Mmu3	0.64	5.00	3.27	1.35	1.00	-0.44	0.00
	Mmu4	0.27	3.00	1.41	0.57	0.17	0.43	0.10
	Mmu8	0.24	2.00	1.38	0.45	0.33	-0.20	0.00
	Mmu13	0.14	2.00	1.18	0.29	0.17	-0.09	0.00
Mean (SE)		0.31 (0.09)	2.90 (0.48)	1.74 (0.25)	0.64 (0.15)	0.39 (0.08)	-0.10 (0.08)	0.01 (0.01)
Angola	Mmu1	0.59	5.00	2.82	1.23	1.00	-0.55	0.00
	Mmu5	0.00	1.00	1.00	0.00	0.00	n.d.	0.00
	Mmu7	0.08	2.00	1.09	0.17	0.08	-0.04	0.00
	Mmu14	0.73	6.00	4.24	1.59	0.75	0.02	0.01
	Mmu2	0.19	2.00	1.28	0.38	0.25	-0.14	0.00
	Mmu3	0.43	3.00	2.17	0.84	1.00	-0.86	0.00
	Mmu4	0.14	2.00	1.18	0.29	0.17	-0.09	0.00
	Mmu8	0.66	10.00	3.13	1.67	0.58	0.14	0.06
	Mmu13	0.00	1.00	1.00	0.00	0.00	n.d.	0.00
Mean (SE)		0.31 (0.08)	3.56 (0.99)	1.99 (0.39)	0.69 (0.22)	0.426 (0.138)	-0.22 (0.12)	0.01 (0.01)
South Africa	Mmu1	0.58	4.00	2.76	1.13	1.00	-0.57	0.00
	Mmu5	0.12	2.00	1.14	0.24	0.00	1.00	0.11
	Mmu7	0.12	2.00	1.14	0.24	0.13	-0.07	0.00
	Mmu14	0.79	7.00	5.36	1.76	0.53	0.34*	0.15
	Mmu2	0.59	4.00	2.87	1.18	0.87	-0.33	0.00
	Mmu3	0.63	5.00	3.17	1.31	1.00	-0.46	0.00
	Mmu4	0.57	3.00	2.76	1.06	0.87	-0.36	0.00
	Mmu8	0.62	6.00	2.96	1.34	0.60	0.09	0.04
	Mmu13	0.71	5.00	3.98	1.45	0.93	-0.25	0.00
Mean (SE)		0.52 (0.06)	4.22 (0.57)	2.91 (0.43)	1.08 (0.17)	0.66 (0.13)	-0.07 (0.16)	0.03 (0.02)
Overall mean (SE)		0.34 (0.02)	3.36 (0.23)	2.01 (0.12)	0.72 (0.06)	0.39 (0.04)	0.028 (0.05)	0.05 (0.01)

n.d. – not determined as loci was monomorphic

Table S4.3 Pairwise F_{ST} estimates between oceanic regions. F_{ST} estimates below diagonal, corresponding P value above diagonal. MED – Mediterranean Sea; SNEA – southern north-east Atlantic; SAI – south-east Atlantic/south-west Indian.

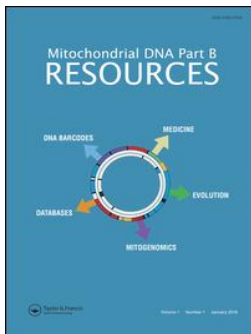
	<i>MED</i>	<i>SNEA</i>	<i>SAI</i>
<i>MED</i>		0.001	0.001
<i>SNEA</i>	0.182*		0.001
<i>SAI</i>	0.235*	0.231*	

* statistical significance at a 0.01 level; **bold values** indicate statistical significance after B-H correction

Appendix D

Published papers

Hull KL, Maduna SN, Bester-van der Merwe AE. (2018) Characterization of the complete mitochondrial genome of the common smoothhound shark, *Mustelus mustelus* (Carcharhiniformes: Triakidae). Mitochondrial DNA Part B **3**: 964–965.



Mitochondrial DNA Part B Resources

ISSN: (Print) 2380-2359 (Online) Journal homepage: <http://www.tandfonline.com/loi/tmdn20>

Characterization of the complete mitochondrial genome of the common smoothhound shark, *Mustelus mustelus* (Carcharhiniformes: Triakidae)

Kelvin L. Hull, Simo N. Maduna & Aletta E. Bester-van der Merwe

To cite this article: Kelvin L. Hull, Simo N. Maduna & Aletta E. Bester-van der Merwe (2018) Characterization of the complete mitochondrial genome of the common smoothhound shark, *Mustelus mustelus* (Carcharhiniformes: Triakidae), Mitochondrial DNA Part B, 3:2, 964-965, DOI: 10.1080/23802359.2018.1507642

To link to this article: <https://doi.org/10.1080/23802359.2018.1507642>



© 2018 The Author(s). Published by Informa UK Limited, trading as Taylor & Francis Group.



Published online: 28 Aug 2018.



Submit your article to this journal [↗](#)



View Crossmark data [↗](#)

MITOGENOME ANNOUNCEMENT



Characterization of the complete mitochondrial genome of the common smoothhound shark, *Mustelus mustelus* (Carcharhiniformes: Triakidae)

Kelvin L. Hull , Simo N. Maduna  and Aletta E. Bester-van der Merwe

Molecular Breeding and Biodiversity Group, Department of Genetics, Stellenbosch University, Stellenbosch, Western Cape, South Africa

ABSTRACT

We present the complete mitochondrial genome of the common smoothhound, *Mustelus mustelus*, which is 16,755 bp long, contains 13 protein-coding genes, 22 tRNA genes, 2 rRNA genes, and non-coding control region. All protein-coding genes begin with the ATG codon, except for the *COI* gene, which begins with GTG. Six protein-coding genes terminated with the TAA codon, and six with incomplete codons, T or TA. The phylogenetic reconstruction places *M. mustelus* within the genus *Mustelus*, with the closest relationship to the placental species, *M. griseus*. This mitogenome provides valuable information to further unravel the evolution of alternate reproductive modes within the genus.

ARTICLE HISTORY

Received 5 July 2018

Accepted 29 July 2018

KEYWORDS

Carcharhiniformes; smoothhound; mitogenome; *Mustelus mustelus*; phylogenetic analysis



The common smoothhound, *Mustelus mustelus* (Linnaeus 1758), is a medium-sized epibenthic shark, distributed from the Mediterranean and eastern Atlantic to the south-west Indian Ocean (Weigmann 2016), with the reproduction mode being placental viviparity (Saidi et al. 2008).

In this study, a specimen was collected by the Department of Agriculture, Forestry and Fisheries, South Africa during tagging surveys off the south-west coast of South Africa (Langebaan Lagoon, Western Cape, latitude: 33°06' S, longitude: 18°01' E). Total genomic DNA was extracted (Elasmobranch Genetics, Lab 242, SU) from a fin clip sample (LL5MM) using a cetyltrimethylammonium bromide extraction protocol of Sambrook and Russell (2001) and sent to the Agricultural Research Council Biotechnology Platform, South Africa for high throughput sequencing. One microgram of genomic DNA was used for 2 × 250 bp paired-end library preparation with a mean insert size of 400 bp using the Illumina TruSeq[®] DNA library preparation kit (Illumina). The library was sequenced on two lanes of an Illumina HiSeq[™] 2000 sequencer.

The generated reads were submitted to quality control as per Maduna et al. (2017). Mitochondrial sequences were filtered from the data set by conducting a BLASTn search (maximum E-value 1.0 E−20) against the mitogenome of *M. griseus* (Genbank accession NC_023527.1, Chen et al. 2016) in Geneious v10.1 (Kearse et al. 2012). These putative mitochondrial sequences were mapped against the mitogenome of *M. griseus* using the Geneious Read Mapper algorithm, with default parameters. The mitogenome was then annotated using the MitoFish and MitoAnnotator web service (Iwasaki et al. 2013).

To infer the phylogenetic placement of *M. mustelus*, the mitogenome of the species (Genbank Accession MH559351) was aligned against 31 complete mitogenomes representing the eight orders of sharks (Figure 1) using MAFFT (Katoh and Standley 2013), with default parameters. The nucleotide substitution model that best fit the alignment was determined in JMODELTEST v2.0 (Darriba et al. 2012) according to the Bayesian Information Criterion, with the GTR+I+G model being the best fit. Bayesian inference of the phylogenetic relationships among mitogenomes was performed in MRBAYES v3.2.6 (Ronquist et al. 2012) with 2,000,000 MCMC generations and the first 500,000 generations discarded as burn-in, performed through the CIPRES Science Gateway (Miller et al. 2010). The consensus tree (Figure 1) was visualized in FIGTREE v1.4.3 (<http://tree.bio.ed.ac.uk/software/figtree>).

The assembled mitogenome of *M. mustelus* is 16,755 bases in length and displayed synteny with other shark and broader vertebrate mitogenomes. The overall base composition of the genome was: A: 31%, T: 30%, C: 25%, and G: 14%. The phylogenetic reconstruction shows the phylogenetic placement of *M. mustelus* within the genus *Mustelus* with the closest relationship to the placental species, *M. griseus*. The positioning of the species could be explained by reproductive mode, as *M. mustelus* and *M. griseus* are viviparous placental, in contrast to *M. manazo*, which is aplacental (Teshima and Koga 1973; Smale and Compagno 1997). Therefore, the mitogenome for *M. mustelus* is an important resource for future conservation and evolutionary biology research such as in-depth phylogenetic placement of species of *Mustelus* with alternate modes of reproduction.

CONTACT Kelvin L. Hull  17507537@sun.ac.za  Molecular Breeding and Biodiversity Group, Department of Genetics, Stellenbosch University, Private Bag X1, Stellenbosch, Western Cape, 7602, South Africa.

© 2018 The Author(s). Published by Informa UK Limited, trading as Taylor & Francis Group.

This is an Open Access article distributed under the terms of the Creative Commons Attribution License (<http://creativecommons.org/licenses/by/4.0/>), which permits unrestricted use, distribution, and reproduction in any medium, provided the original work is properly cited.

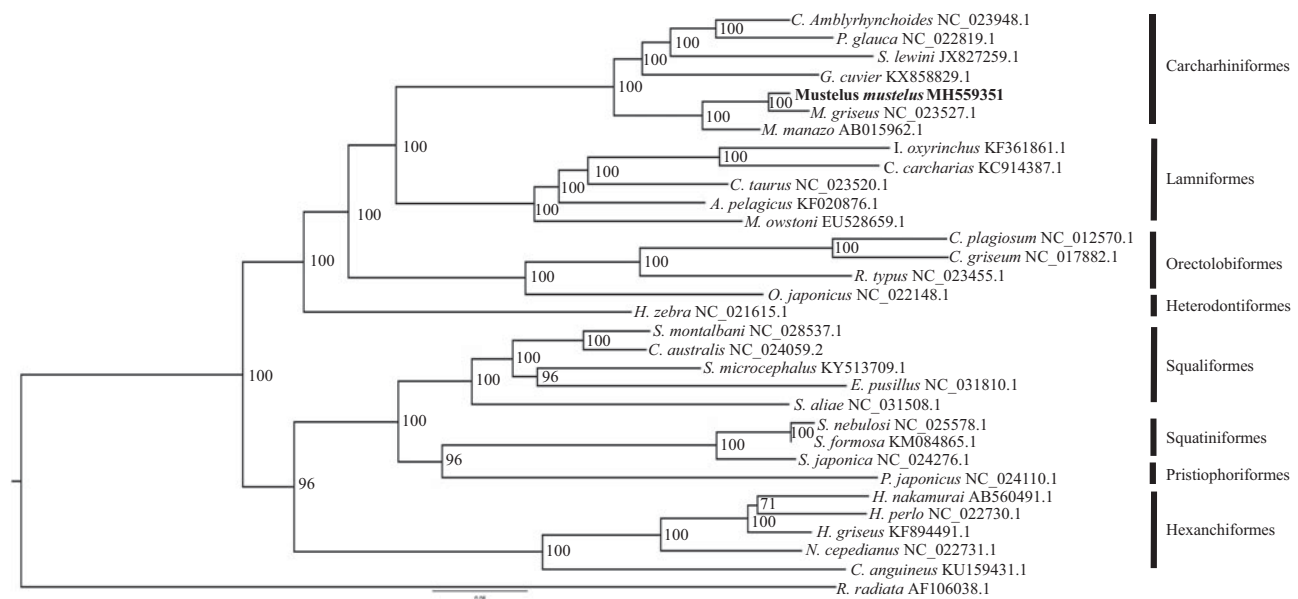


Figure 1. Phylogenetic relationships between the eight orders of shark constructed using Bayesian inference from 31 whole mitogenome sequences, with the thorny skate (*Raja radiata*) mitogenome included as an outgroup. Numbers at nodes indicate posterior probabilities. Genbank accession numbers are given adjacent to the species name, and scale bar indicates groupings of species into orders.

Acknowledgments

This research did not receive any specific grant but was partly funded by the National Research Foundation of South Africa. The authors would like to acknowledge the field work of the Department of Agriculture, Forestry and Fisheries, South Africa for the provision and identification of the sample utilized in the present study.

Disclosure statement

The authors declare no conflict of interest and were solely responsible for the content and writing of this paper.

ORCID

Kelvin L. Hull  <http://orcid.org/0000-0001-9865-5790>

Simo N. Maduna  <http://orcid.org/0000-0002-9372-4360>

References

- Chen X, Peng Z, Pan L, Shi X, Cai L. 2016. Mitochondrial genome of the spotless smooth-hound *Mustelus griseus* (Carcharhiniformes: Triakidae). *Mitochondrial DNA A DNA Mapp Seq Anal.* 27:78–79.
- Darriba D, Taboada GL, Doallo R, Posada D. 2012. jModelTest 2: more models, new heuristics and parallel computing. *Nat Methods.* 9:772
- Iwasaki W, Fukunaga T, Isagozawa R, Yamada K, Maeda Y, Satoh TP, Sado T, Mabuchi K, Takeshima H, Miya M, et al. 2013. Mitofish and mitoan-notator: a mitochondrial genome database of fish with an accurate and automatic annotation pipeline. *Mol Biol Evol.* 30:2531–2540.

- Katoh K, Standley DM. 2013. MAFFT multiple sequence alignment software version 7: improvements in performance and usability. *Mol Biol Evol.* 30:772–780.
- Kearse M, Moir R, Wilson A, Stones-Havas S, Cheung M, Sturrock S, Buxton S, Cooper A, Markowitz S, Duran C, et al. 2012. Geneious Basic: an integrated and extendable desktop software platform for the organization and analysis of sequence data. *Bioinformatics.* 28:1647–1649.
- Maduna SN, Rossouw C, da Silva C, Soekoe M, Bester-van der Merwe AE. 2017. Species identification and comparative population genetics of four coastal houndsharks based on novel NGS-mined microsatellites. *Ecol Evol.* 7:1462–1425.
- Miller MA, Pfeiffer W, Schwartz T. 2010. Creating the CIPRES Science Gateway for inference of large phylogenetic trees. In *Proceedings of the Gateway Computation and Environment Workshop (GCE)*. Nov 14; New Orleans, LA. p. 1–8.
- Ronquist F, Teslenko M, Van Der Mark P, Ayres DL, Darling A, Höhna S, Larget B, Liu L, Suchard MA, Huelsenbeck JP. 2012. Mrbayes 3.2: efficient Bayesian phylogenetic inference and model choice across a large model space. *Syst Biol.* 61:539–542.
- Saidi B, Bradai MN, Bouaïn A. 2008. Reproductive biology of the smooth-hound shark *Mustelus mustelus* (L.) in the Gulf of Gabès (south-central Mediterranean Sea). *J Fish Biol.* 72:1343–1354.
- Sambrook J, Russell DW. 2001. *Molecular cloning: a laboratory manual*. New York (NY): Cold Spring Harbor Laboratory Press.
- Smale MJ, Compagno LJV. 1997. Life history and diet of two southern African smoothhound sharks, *Mustelus mustelus* (Linnaeus, 1758) and *Mustelus palumbes* Smith, 1957 (Pisces: Triakidae). *South Afr J Mar Sci.* 18:229–248.
- Teshima K, Koga S. 1973. Studies on sharks. V. Taxonomic characteristics of reproductive organs in Japanese *Mustelus*. *Mar Biol.* 23:337–341.
- Weigmann S. 2016. Annotated checklist of the living sharks, batoids and chimaeras (Chondrichthyes) of the world, with a focus on biogeographical diversity. *J Fish Biol.* 88:837–1037.